USGS
science for a changing world

Prepared in cooperation with the U.S. Department of Agriculture (USDA) Forest Service

Earth Science Studies in Support of Public Policy Development and Land Stewardship—Headwaters Province, Idaho and Montana

Circular 1305

U.S. Department of the Interior
U.S. Geological Survey

Earth Science Studies in Support of Public Policy Development and Land Stewardship—Headwaters Province, Idaho and Montana

By U.S. Geological Survey Headwaters Province Project Team

Karen Lund, Scientific Editor

Prepared in cooperation with the U.S. Department of Agriculture (USDA) Forest Service

USGS Contributors
John N. Aleinikoff
Robert R. Carlson
Robert G. Eppinger
Karl V. Evans
Gregory N. Green
Jane M. Hammarstrom
Terry L. Klein
Michael J. Kunk
Gregory K. Lee
Karen Lund
J. Michael O'Neill
P.K. Sims
Cliff D. Taylor
Russell G. Tysdal
Daniel M. Unruh
Bradley S. Van Gosen
Jeffrey A. Winick

USDA Forest Service Contributors
G.L. Jackson
D.W. Peters
Betsy Rieffenberger

Circular 1305

U.S. Department of the Interior
U.S. Geological Survey

U.S. Department of the Interior
DIRK KEMPTHORNE, Secretary

U.S. Geological Survey
Mark D. Myers, Director

U.S. Geological Survey, Reston, Virginia: 2007

For product and ordering information:
World Wide Web: http://www.usgs.gov/pubprod
Telephone: 1-888-ASK-USGS

For more information on the USGS--the Federal source for science about the Earth, its natural and living resources, natural hazards, and the environment:
World Wide Web: http://www.usgs.gov
Telephone: 1-888-ASK-USGS

Suggested citation:
U.S. Geological Survey Headwaters Province Project Team (Karen Lund, scientific ed.), 2007, Earth science studies in support of public policy development and land stewardship—Headwaters province, Idaho and Montana: U.S. Geological Survey Circular 1305, 92 p.

Cover photographs. *Front upper:* Color Creek falls, tributary to Middle Fork Salmon River. Flowing across Mesoproterozoic muscovite-biotite schist. (R.G. Eppinger, 2001.) *Front lower:* Stoddard packbridge, main Salmon River. Prominent north-dipping metamorphic layering in Mesoproterozoic biotite metasandstone on skyline. (K. Lund, 2005.) *Back:* Rattlesnake Camp, Middle Fork Salmon River. Outcrops of Mesoproterozoic biotite metasandstone are prominent. Boat in mid-foreground is part of USGS–USDA Forest Service baseline geochemical characterization study of the river basin. (K. Lund, 2001.)

Contents

Figures

Tables

Conversions, Abbreviations, and Acronyms

[Both metric and non-metric units were used in these studies, and some studies report older data using non-metric units; those data are not converted to metric herein]

To convert	To	Multiply by
2,000 lb tons	Metric tons (t)	0.91
Ounces (oz)	Grams (g)	28.35
Miles (mi)	Kilometers (km)	1.60
Square miles (mi^2)	Square kilometers (km^2)	2.60
Feet (ft)	Meters (m)	0.3048
Kilograms (kg)	Pounds (lb)	2.21
Grams (g)	Ounces (oz)	0.035
Metric tons (t)	2,000 lb tons	1.10

FLMA	Federal Land Management Agencies
MRDS	Mineral Resources Data System
MAS	Mineral Availability System
CUSMAP	Conterminous United States Mineral Assessment Program
NURE	National Uranium Resource Evaluation
HSSR	Hydrogeochemical and Stream Sediment Reconnaissance
MILS	Minerals Industry Location System
RASS	Rock Analysis Storage System

Earth Science Studies in Support of Public Policy Development and Land Stewardship—Headwaters Province, Idaho and Montana

By U.S. Geological Survey Headwaters Province Project Team

Introduction

The development and institution of sound Public Land policy and stewardship practices for a region require the accumulation and integration of earth science and biologic data. The U.S. Geological Survey Headwaters Province project covering western Montana and northern and central Idaho was designed to provide geoscience data and interpretations to Federal Land Management Agencies (FLMA). Managers in USDA Forest Service Regions 1 and 4 made national priority requests for the U.S. Geological Survey Mineral Resources Program (1) to provide interim products that help them meet their planning cycles and (2) to provide topical studies to meet longer range goals of integrating geoscience data into decision making. Toward this end, the Headwaters Province project team have emphasized development of digital geoscience data, GIS analyses, topical studies, and critical new geologic interpretation to ensure that geoscience data are available for GIS-based science integration and land-use planning. The interrelated products of the project are at complementary scales.

A major goal of the project was to provide consistent background and baseline geoscience information for the Headwaters Province. Studies were designed to more completely map lithologic units and determine controls of deformation, magmatism, and mineralizing processes. These studies were initiated at localities determined to have the most application to regional issues. Topical studies addressed several aspects of geologic basement control on these processes within the region. These include studies of

1. Regional metallogenic patterns and their relationship to the composition and architecture of underlying, unexposed basement. A study of the Idaho-Montana porphyry belt was designed to determine whether igneous processes in the upper crust or basement metals endowment was critical to formation of these deposits.

2. Timing of igneous and hydrothermal systems, to identify regionally important metallogenic magmatism. Study of the Boulder batholith and associated mineral deposits at Butte, Mont., revealed much about an important set of systems.

3. The geologic setting of Proterozoic strata, to better understand how their sedimentary basins developed and to define the origin of sediment-hosted mineral deposits. This work includes proxy studies of the structural setting of the Blackbird mining district and identification of sedimentary successions that bear on Snowball Earth models.

Digital GIS-Based Geoscience Databases

The project developed internally consistent digital geoscience map databases using previously published sources, augmented by new studies at scales of 1:100,000 and 1:250,000. Derivative and interpretive digital products developed from these base data were used in all aspects of the project. Digital data utilization was emphasized (1) to enhance FLMA's ability to integrate geoscience data and (2) to provide geoscience data in a flexible format that enhanced their applicability to a large and evolving variety of uses. As a result, geoscience information will more likely be used in FLMA decision-making processes.

Preparation of the Digital Geologic Map for the Headwaters Province Project

By Gregory N. Green

Planning

For most earth science-based evaluations, a geologic map is required. At the start of this project, digital geologic

maps at the appropriate scale and detail were available for only selected parts of the Headwaters Province study area. The quickest and least expensive way to create a comprehensive geologic database required that various published maps or maps-in-progress be mosaiced. Available geologic maps were evaluated for scale, areal extent, quality, and original purpose. Unfortunately, some gaps in coverage exist where mapping at the appropriate scale or detail was not available or where available maps did not contain sufficient detail.

Forty-five maps were finally selected for mosaicing (fig. 1; table 1). These maps varied in scale from 1:100,000 to 1:250,000, covering areas from 122 square miles (3.15×10^8 m^2) to 9,537 square miles ($2.47 \times 1{,}010$ m^2). As noted, some available maps were not sufficiently detailed and were not used. Conversely, the content of some detailed or topical maps was not applicable to the mineral resource survey.

Existing digital formats varied from nonexistent to various fully attributed Arc/Info formats. Geologic data sets were simultaneously assembled at the Montana Bureau of Mines and Geology, at the Idaho Geological Survey, and at the U.S. Geological Survey (USGS) offices in Denver, Colo., Spokane, Wash., and Sioux Falls, S. Dak. After initial data collection, data conversion work was completed in USGS offices in Denver and Spokane.

In order to mosaic the maps using Arc/Info, digital versions of the 45 maps needed consistent internal formatting; each data set needed to contain the same items in the same sequence. Geologic features had to be consistently coded and stored in the same manner before joining. Digital data sources had slightly different standard format interpretations and required final revision before assembly was completed in Spokane.

Several map overlap problems had to be solved. Detailed but irregularly shaped geologic maps of national forests overlapped regular-shaped quadrangle maps. Project geologists decided which maps were the most accurate and current. A standard sequence of clipping, erasing, and joining of map data sets was used to create both geologic graphic decorations and geologic formation polygons. The sequence was used to create seamless geologic and graphic layers, both of which were required to create the digital geologic map.

Database Design

Arc/Info was chosen as the vector-based spatial database system. Raster-based or illustrator-style systems do not work as well as Arc/Info with geologic maps made of points, lines, and polygons (formations). All maps were converted to the same Albers Equal Area projection, and original map scale for each was preserved. Original data sets were archived at the U.S. Geological Survey, Denver.

To ensure consistent coding, a common data dictionary was created for line layers, whether contacts, folds, or faults. The dictionary contains a line description and specifies a standard color and width and whether dashes and (or) dots are needed. Each line type, in conjunction with the definition table, when used to plot a map yields graphical output that includes the standard linear components of a geologic map.

Polygon layers for formations, overprints, or graphical layers are specified in another common data dictionary. The dictionary contains polygon labels, age, description, color, and patterns as appropriate. Each type of polygon, in conjunction with this translation table, produces graphical output that looks like the polygonal components of a geologic map.

On geologic maps, contacts depict the boundary between two types or ages of rocks, so contacts denote the color boundaries between formations. Thus, in the database, the lines that define polygon perimeters are contacts. In this database, shorelines and map edges are included with the contacts because they are color boundaries as well. Because contacts define the spatial limits of formations, they are stored as an integral part of the formation layer. Each formation is also identified by a text label, and the database includes an attribute for the associated text label.

Faults can be contacts and thus may be color boundaries. In some data sets, faults are stored in the formation part of the database and so are part of the contact data. However, in many geologic data sets, the fault data are stored in a way similar to that for folds, as a separate layer. In most cases, this results from how the data were captured. Scanners can be set to recognize faults because they are graphically portrayed using thicker lines, and consequently these features can be saved in a separate database layer. Data subsets are easily created but much harder to integrate. Consequently, in this study the faults were stored in a separate database layer.

A separate graphic decoration layer was created for each map. For geologic mineral resource assessment work, the surface area of each formation must be accurate. In traditional single-layer geologic databases, graphic symbols disrupt areal geologic formation definitions. By keeping graphic symbols in a separate layer, the symbols did not impact these formation definitions.

Folds or warps in formations are represented on a geologic map by a line that traces the fold axis. Because almost no folds are color boundaries, graphical representations for folds are usually stored as a separate database layer. Regional zones, such as metamorphic grade, shear zones, or extent of glaciation, are similar in that few or none are coincident with geologic formation polygons; rather, they are depicted by some sort of pattern. These zones are considered overlays and are stored in separate graphical layers.

The graphical representation of faults often includes special symbols to indicate fault orientation and movement. These include teeth on thrust faults, bar-and-ball symbols on normal faults, and other markings. These asymmetrical lines can be generated in a variety of ways in Arc/Info. As all lines must have the same internal format in order to seamlessly join, lines for these faults were converted to a standard style. Issues arise when one data set decorates faults on their left whereas an adjacent data set decorates lines on the right; this requires line data to be converted, as well. One distinct disadvantage to using database-generated asymmetrical linesets is that finished

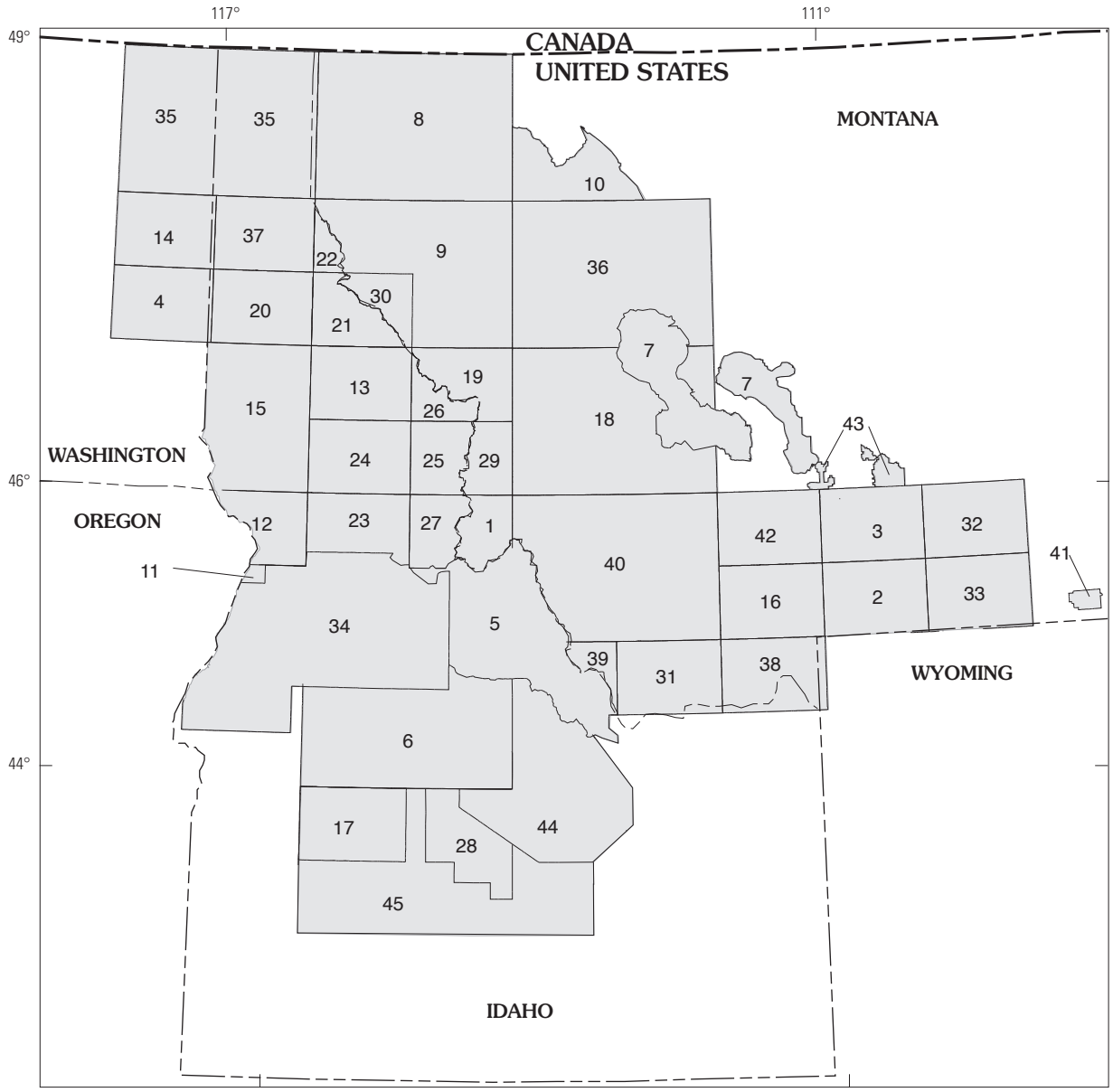

Figure 1. Sources of data (gray shade) used to compile digital geologic map database for Headwaters Province project study area. References for sources are in table 1.

Table 1. Geologic map data sets used to construct Headwaters Province geologic map database.

1. Berg, R.B., and Lonn, J.D., 1996, Preliminary geologic map of the Nez Perce Pass 30- by 60-minute quadrangle, Montana: Montana Bureau of Mines and Geology Open-File Report MBMG 339, 7 p., 1 plate, scale 1:100,000.
2. Berg, R.B., Lonn, J.D., and Locke, W.W., 1999, Geologic map of the Gardiner 30′×60′ quadrangle, south-central Montana: Montana Bureau of Mines and Geology Open-File Report MBMG 387, 2 plates, scale 1:100,000.
3. Berg, R.B., Lopez, D.A., and Lonn, J.D., 2000, Geologic map of the Livingston 30′×60′ quadrangle, south-central Montana: Montana Bureau of Mines and Geology Open-File Report MBMG 406, scale 1:100,000.
4. Derkey, P.D., Johnson, B.R., Lackaff, B.B., and Derkey, R.E., 1998, Digital geologic map of the Rosalia 1:100,000 quadrangle, Washington and Idaho; a digital database for the 1990 S.Z. Waggoner map: U.S. Geological Survey Open-File Report 98-357, 27 p., scale 1:100,000.
5. Evans, K.V., and Green, G.N., compilers, 2003, Geologic map of Salmon National Forest and vicinity, east-central Idaho: U.S. Geological Survey Geologic Investigations Series Map I–2765, scale 1:100,000.
6. Fisher, F.S., McIntyre, D.H., and Johnson, K.M., 1992, Geologic map of the Challis 1°×2° quadrangle, Idaho: U.S. Geological Survey Miscellaneous Investigations Series Map I–1819, scale 1:250,000, 39 p. pamphlet.
7. Green, G.N., and Tysdal, R.G., 1996, Digital maps and figures on CD-ROM for mineral and energy resource assessment of the Helena National Forest, west-central Montana: U.S. Geological Survey Open-File Report 96-683-B, CD-ROM, scale 1:126,720.
8. Harrison, J.E., Cressman, E.R., and Whipple, J.W., 1992, Geologic and structure maps of the Kalispell 1°×2° quadrangle, Montana, and Alberta and British Columbia: U.S. Geological Survey Miscellaneous Investigations Map I–2267, scale 1:250,000.
9. Harrison, J.E., Griggs, A.B., Wells, J.D., Kelley, W.N., Derkey, P.D., and EROS Data Center, 2000, Geologic and structure maps of the Wallace 1°×2° quadrangle, Montana and Idaho—A digital database: U.S. Geological Survey Miscellaneous Investigations Series Map I–1509–A, version 1.0, 21 p., scale 1:250,000.
10. Harrison, J.E., Whipple, J.W., and Lidke, D.J., 1998, Geologic map of the western part of the Cut Bank 1°×2° quadrangle, Montana: U.S. Geological Survey Geologic Investigations Series Map I–2593, 1 sheet, scale 1:250,000.
11. Idaho Geological Survey, 1996, Digital geology of the Riggins 1:100,000-scale quadrangle, Idaho, *in* Digital geologic map compilation for the Nez Perce and Clearwater National Forests: Idaho Geological Survey CD-ROM, produced under contract to USDA Forest Service [unpublished], scale 1:100,000.
12. Idaho Geological Survey, 1996, Digital geology of the Grangeville 1:100,000-scale quadrangle, Idaho, *in* Digital geologic map compilation for the Nez Perce and Clearwater National Forests: Idaho Geological Survey CD-ROM, produced under contract to USDA Forest Service [unpublished], scale 1:100,000.
13. Idaho Geological Survey, 1996, Digital geology of the Headquarters 1:100,000-scale quadrangle, Idaho, *in* Digital geologic map compilation for the Nez Perce and Clearwater National Forests: Idaho Geological Survey CD-ROM, produced under contract to USDA Forest Service [unpublished], scale 1:100,000.
14. Johnson, B.R., and Derkey, P.D., 1998, Digital geologic map of the Spokane 1:100,000 quadrangle, Washington and Idaho; a digital database for the 1990 N.L. Joseph map: U.S. Geological Survey Open-File Report 98-115, 13 p. and 1 digital plate, scale 1:100,000.
15. Kayser, H.Z., 2001, Digital geologic map of the east half of the Pullman 1°×2° quadrangle, Idaho; a digital database for the 1979 Rember and Bennett map: U.S. Geological Survey Open-File Report 01-262, 29 p., 1 sheet, scale 1:250,000.
16. Kellogg, K.S., and Williams, V.S., 2000, Geologic map of the Ennis 30′×60′ quadrangle, Madison and Gallatin Counties, Montana, and Park County, Wyoming: U.S. Geological Survey Geologic Investigations Series I–2690, scale 1:100,000.
17. Kiilsgaard, T.H., Stanford, L.R., and Lewis, R.S., 2001, Geologic map of the Idaho City 30×60 minute quadrangle, Idaho: Idaho Geological Survey Geologic Map Series 29, scale 1:100,000.

Table 1. Geologic map data sets used to construct Headwaters Province geologic map database.—Continued

18. Lewis, R.S., 1998, Geologic map of the Butte 1°×2° quadrangle, Montana: Montana Bureau of Mines and Geology Open-File Report MBMG 363, 16 p., 1 plate, scale 1:250,000.

19. Lewis, R.S., 1998, Geologic map of the Montana part of the Missoula West 30- by 60-minute quadrangle: Montana Bureau of Mines and Geology Open-File Report MBMG 373, 20 p., 2 plates, scale 1:100,000.

20. Lewis, R.S., Burmester, R.F., Kauffman, J.D., and Frost, T.P., 2000, Geologic map of the St. Maries 30×60 minute quadrangle, Idaho: Idaho Geological Survey Digital Geologic Map DGM–1, scale 1:100,000.

21. Lewis, R.S., Burmester, R.F., McFadden, M.D., Derkey, P.D., and Oblad, J.R., 1999, Digital geologic map of the Wallace quadrangle, Idaho: U.S. Geological Survey Open-File Report 99-390, 46 p., scale 1:100,000.

22. Lewis, R.S., and Derkey, P.D., 1999, Digital geologic map of part of the Thompson Falls 1:100,000 quadrangle, Idaho: U.S. Geological Survey Open-File Report 99-438, 32 p., 1 digital plate.

23. Lewis, R.S., and Stanford, L.R., 2002, Digital geologic map of the Elk City 30×60 minute quadrangle, Idaho: Idaho Geological Survey Digital Geologic Map Series DGM–05, 1 CD-ROM, scale 1:100,000.

24. Lewis, R.S., and Stanford, L.R., 2002, Digital geologic map of the Kooskia 30×60 minute quadrangle, Idaho: Idaho Geological Survey Digital Geologic Map Series DGM–06, 1 CD-ROM, scale 1:100,000.

25. Lewis, R.S., and Stanford, L.R., 2002, Digital geologic map of the Hamilton 30×60 minute quadrangle, Idaho: Idaho Geological Survey Digital Geologic Map Series DGM–03, 1 CD-ROM, scale 1:100,000.

26. Lewis, R.S., and Stanford, L.R., 2002, Digital geologic map of the Missoula West 30×60 minute quadrangle, Idaho: Idaho Geological Survey Digital Geologic Map Series DGM–02, 1 CD-ROM, scale 1:100,000.

27. Lewis, R.S., and Stanford, L.R., 2002, Digital geologic map of the Nez Perce Pass 30×60 minute quadrangle, Idaho: Idaho Geological Survey Digital Geologic Map Series DGM–04, 1 CD-ROM, scale 1:100,000.

28. Link, P.K., Mahoney, J.B., Bruner, D.J., Batatian, L.D., Wilson, Eric, and Williams, F.J.C., 1995, Geologic map of outcrop areas of sedimentary units in the eastern part of the Hailey 1°×2° quadrangle and the southern part of the Challis 1°×2° quadrangle, south-central Idaho: U.S. Geological Survey Bulletin 2064–C, plate 1, scale 1:100,000.

29. Lonn, J.D., and Berg, R.B., 1996, Preliminary geologic map of the Hamilton 30- by 60-minute quadrangle, Montana: Montana Bureau of Mines and Geology Open-File Report MBMG 340, 9 p., 1 plate, scale 1:100,000.

30. Lonn, J.D., and McFaddan, M.D., 1999, Geologic map of the Montana part of the Wallace 30- by 60-minute quadrangle: Montana Bureau of Mines and Geology Open-File Report MBMG 388, 15 p., 2 plates, scale 1:100,000.

31. Lonn, J.D., Skipp, Betty, Ruppel, E.T., Janecke, S.U., Perry, W.J., Jr., Sears, J.W., Bartholomew, M.J., Stickney, M.C., Fritz, W.J., Hurlow, H.A., and Thomas, R.C., 2000, Geologic map of the Lima quadrangle, southwest Montana: Montana Bureau of Mines and Geology Open-File Report MBMG 408, 3 sheets, parts A, B, and C, scale 1:100,000.

32. Lopez, D.A., 2000, Geologic map of the Big Timber 30′×60′ quadrangle, south-central Montana: Montana Bureau of Mines and Geology Open-File Report MBMG 405, scale 1:100,000.

33. Lopez, D.A., 2001, Preliminary geologic map of the Red Lodge 30′×60′ quadrangle, south-central Montana: Montana Bureau of Mines and Geology Open-File Report MBMG 423, 1 plate, scale 1:100,000.

34. Lund, Karen, Derkey, P.D., Brandt, T.R., and Oblad, Jon, 1999, Digital geologic map database of the Payette National Forest and vicinity, Idaho: U.S. Geological Survey Open-File Report 98-219–B, 45 p., scale 1:100,000.

35. Miller, F.K., Burmester, R.F., Miller, D.M., Powell, R.E., and Derkey, P.D., 1998, Digital geologic map of the Sandpoint 1°×2° quadrangle, Washington, Idaho, and Montana: U.S. Geological Survey Open-File Report 99-144, 72 p., 1 digital plate, scale 1:250,000.

36. Mudge, M.R., Earhart, R.L., Whipple, J.W., and Harrison, J.E., 1982, Geologic and structure map of the Choteau 1°×2° quadrangle, western Montana: U.S. Geological Survey Miscellaneous Investigations Series Map I–1300, 2 sheets, scale 1:250,000.

Table 1. Geologic map data sets used to construct Headwaters Province geologic map database.—Continued

37. Munts, S.R., 2000, Digital geologic map of the Coeur d'Alene 1:100,000 quadrangle, Idaho and Montana: U.S. Geological Survey Open-File Report 00-135, version 1.0, 30 p., 1 digital plate, scale 1:100,000.

38. O'Neill, J.M., and Christiansen, R.L., 2002, Geologic map of the Hebgen Lake quadrangle, Beaverhead, Madison, and Gallatin Counties, Montana, Park and Teton Counties, Wyoming, and Clark and Fremont Counties, Idaho: Montana Bureau of Mines and Geology Open-File Report MBMG 464, 1 plate, scale 1:100,000.

39. Ruppel, E.T., 1998, Geologic map of the eastern part of the Leadore 30′×60′ quadrangle, Montana and Idaho: Montana Bureau of Mines and Geology Open-File Report MBMG 372, scale 1:100,000.

40. Ruppel, E.T., O'Neill, J.M., and Lopez, D.A., 1993, Geologic map of the Dillon 1°×2° quadrangle, Idaho and Montana: U.S. Geological Survey Miscellaneous Investigations Series Map I–1803–H, scale 1:250,000.

41. Van Gosen, B.S., Wilson, A.B., Hammarstrom, J.M., and Kulik, D.M., 1996, Mineral resource assessment of the Custer National Forest in the Pryor Mountains, Carbon County, south-central Montana: U.S. Geological Survey Open-File Report 96-256, scale 1:126,720.

42. Vuke, S.M., Berg, R.B., Lonn, J.D., and Kellogg, K.S., 1995, Geologic map of the Bozeman 30′×60′ quadrangle, Montana: Montana Bureau of Mines and Geology Open-File Report MBMG 334, scale 1:100,000.

43. Wilson, A.B., and Elliott, J.E., 1997, Geologic maps of western and northern parts of Gallatin National Forest, south-central Montana: U.S. Geological Survey Geologic Investigation Series I–2584, scale 1:126,720.

44. Wilson, A.B., and Skipp, Betty, 1994, Geologic map of the eastern part of the Challis National Forest and vicinity, Idaho: U.S. Geological Survey Miscellaneous Investigations Series Map I–2395, scale 1:250,000.

45. Worl, R.G., and Johnson, K.M., 1995, Map showing geologic terranes of the Hailey 1°×2° quadrangle and the western part of the Idaho Falls 1°×2° quadrangle, south-central Idaho: U.S. Geological Survey Bulletin 2064–A, plate 1, scale 1:250,000.

products seldom look like the originals. Authors generally place one bar-and-ball symbol near the center of the fault, or at some place that clearly shows known fault movement, whereas automatic asymmetrical decorations, placed by software, are added every inch or so. Inconsistency in identifying the start and end of a digital fault can cause associated decorations to switch sides along multi-segmented faults.

Manual and automatic placement of graphic teeth, ticks, boxes, bar-and-ball symbols, strike-slip symbols, and fold symbols, along with correction and simplification of symbols, was required to create digital geologic data sets. The decoration symbols for each feature were drawn in Arc/Info for Adobe Illustrator and then converted back to Arc/Info using the Adobe plug-in, Avenza MAPublisher. Consequently, symbols and decorations became isolated in a separate Arc/Info layer that was no longer dependent upon associated line orientation. Regardless of how the original geologic symbol was depicted, the final separate graphic decoration layer was consistent. Geologic symbols were easily corrected or deleted without altering the areal geologic formation database.

Stroked or crosshatched graphic symbols were converted to filled-polygon symbols. Filled polygons draw faster, and associated graphic files are more compact. Paper versions of original maps were used to assure accurate symbol placement.

Conclusions

A new seamless spatial database was created for the Headwaters Province project area. The database is available for USGS resource assessments, for many needs of the FLMA, and is a critical resource for future geologic investigations; this single geologic database is available for local to regional studies and can be queried to create derivative maps.

Compilation and Interpretation for New Geologic Maps

By Karl V. Evans and Gary L. Jackson[1]

Background

A key goal of the Headwaters Province project was completion of new geologic maps of areas where existing maps were incomplete or inadequate. A number of new maps at intermediate regional scale were completed or updated as part of this project. An example is the new map of the Salmon National Forest and vicinity (Evans and Green, compilers, 2003) at 1:100,000 scale—a scale useful for making land-use decisions, especially by FLMA.

Geologic investigations in the Salmon National Forest and vicinity have a long history, extending as far back as the Lewis and Clark expedition, but they began in earnest with studies at the turn of the 19th–20th century. (See, for example, Lindgren, 1904; Umpleby, 1913.) Through the years, much of this interest was prompted by the search for mineral resources such as gold, copper, cobalt, lead, and thorium (Umpleby, 1913; Ross, 1925; Anderson, 1947; Vhay, 1948; Sharp and Cavender, 1962; Cater and others, 1973; Lund and others, 1983; Ruppel and Lopez, 1988; Nash and Hahn, 1989; Moye, 1990). Nevertheless, compared to many parts of the western United States, this area remained poorly studied, probably because of the inaccessibility of large parts of it. Considerable areas of the Salmon National Forest and of the adjacent Payette National Forest now are incorporated in the Frank Church–River of No Return Wilderness.

The new geologic map compilation of the Salmon National Forest (fig. 2) utilizes more than 50 sources of data. Because recent work resulted in significant revisions concerning regional structure and stratigraphy, older maps were directly incorporated only in areas for which no other coverage was available, or where these maps could be reinterpreted in light of more recent work. The scale of new mapping varied from reconnaissance at 1:100,000 to local studies done at 1:24,000; however, even the reconnaissance work incorporates insights gained by topical mapping at larger scales.

Use of Geologic Map Data Set in Producing a National Forest Soils Map

As an example of derivative uses for the Headwaters Province geologic maps, the geologic map of the Salmon National Forest is being used as the basis for a forest soils map by USDA Forest Service personnel. Chemical, weathering, and other characteristics of geologic units can be used to infer soil characteristics known as Land Type Association (LTA) for large areas not covered by detailed soil studies (Soil Resource Inventories). In this process, all lithologic units are assigned to one of four broad categories determined by the type of soil they weather to produce: granitic, volcanic, quartzitic, and sedimentary (mostly calcareous). Once this information is converted to a spatial database, it becomes possible to conduct rapid evaluation of landscapes for forest planning and management in support of decisions regarding construction of roads or building sites associated with timber sales, mineral exploration, mining, grazing, or public recreation. In addition, if a forest fire occurs in the forest, this LTA information is especially useful for evaluating the erodability of denuded hillslopes associated with precipitation runoff or mass wastage processes (such as landslides). In either a hillwash or a landslide

[1]USDA Forest Service, Salmon-Challis National Forest, Rural Route 2, Box 600, Salmon, ID 83467.

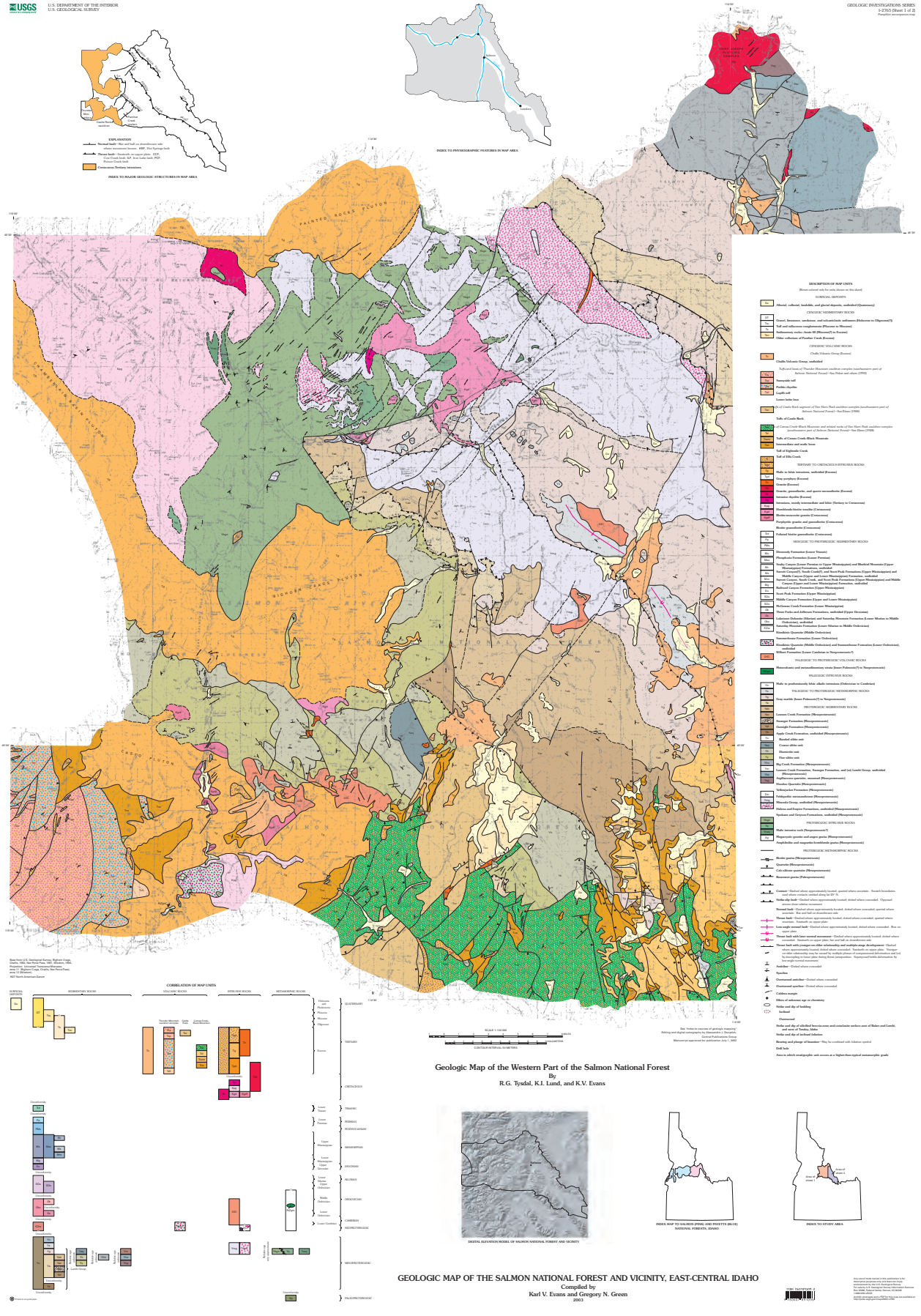
U.S. DEPARTMENT OF THE INTERIOR
U.S. GEOLOGICAL SURVEY
GEOLOGIC INVESTIGATIONS SERIES
I-2765 (Sheet 1 of 2)
INDEX TO MAJOR GEOLOGIC STRUCTURES IN MAP AREA
INDEX TO PHYSIOGRAPHIC FEATURES IN MAP AREA
DESCRIPTION OF MAP UNITS
CORRELATION OF MAP UNITS
Geologic Map of the Western Part of the Salmon National Forest
By
R.G. Tysdal, K.I. Lund, and K.V. Evans
DIGITAL ELEVATION MODEL OF SALMON NATIONAL FOREST AND VICINITY
INDEX MAP TO SALMON (PINE) AND PIOGETTE (BLUE) NATIONAL FORESTS, IDAHO
INDEX TO STUDY AREA
GEOLOGIC MAP OF THE SALMON NATIONAL FOREST AND VICINITY, EAST-CENTRAL IDAHO
Compiled by
Karl V. Evans and Gregory N. Green
2003

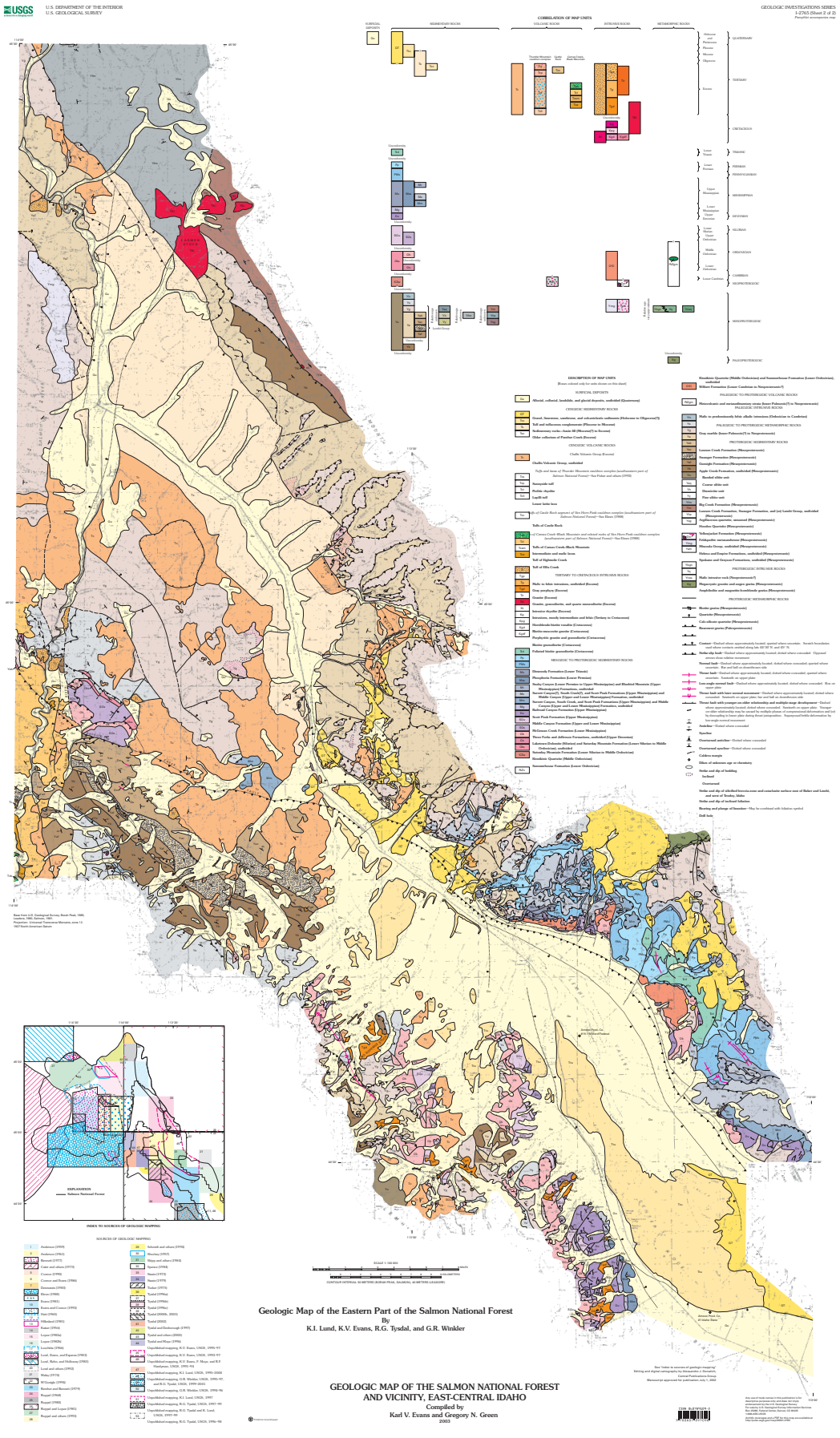

Figure 2. Reduced view of geologic map of Salmon National Forest and vicinity. See U.S. Geological Survey Geologic Investigations Series Map I–2765; published on paper as well as posted online at URL http://pubs.usgs.gov/imap/i-2765/.

situation, large influxes of clastic debris can adversely affect populations of anadromous fish (seagoing–fresh-water-breeding species such as salmon, steelhead, bull trout) and other fish in rivers draining the burned region.

Statistical Integration and Geochemical Surface Modeling of the NURE and USGS Geochemical Databases

By Robert R. Carlson and Gregory K. Lee

The geochemical data used in this report derive from chemical analyses performed on the 51,411 stream-sediment samples collected under the auspices of the National Uranium Resource Evaluation (NURE) Hydrogeochemical and Stream Sediment Reconnaissance (HSSR). Within the Headwaters Province project area, NURE data are available for the rectangle bounded by lat 42°–49°N., long 108°–118°W. (example (cadmium), figs. 3, 4). This area contains thirty-five 1°×2° quadrangles, of which thirty-one were fully sampled, two partially sampled, and two not sampled by the NURE program. The areas not sampled are the Pullman and Grangeville quadrangles and the west halves of the Driggs and Preston quadrangles. The number of the NURE analyses performed by the HSSR program varies by element and ranges from a low of 17,338 samples analyzed for selenium to a high of 50,251 samples analyzed for uranium. In addition, various USGS investigations reanalyzed NURE samples relevant to specific study areas. In these cases also, the number of analyses varies by element and ranges from a low of 264 samples analyzed for tungsten to a high of 8,926 samples analyzed for arsenic.

Methods of Study

Analysis

The NURE samples were analyzed by a wide variety of analytical methods and in many laboratories (table 2). Four U.S. Department of Energy (DOE) laboratories were charged with analyzing NURE stream-sediment samples under the HSSR program: Lawrence Livermore Laboratory, Los Alamos Scientific Laboratory, Oak Ridge Gaseous Diffusion Plant, and Savannah River Laboratory. Each DOE laboratory developed its own sample collection, analytical, and data management methodologies and used contractors to do much of the work. NURE samples reexamined by the USGS were analyzed using USGS methods (table 2).

Each of the many analytical methods–laboratory combinations just mentioned has its own lower and upper determination limits and different levels of accuracy, precision, and analytical interferences. Sampling and analysis protocols for the NURE program were specific to individual 1°×2° quadrangles. Consequently, artificial anomalies are present along quadrangle boundaries (fig. 3), whether analytical results are plotted for the entire study area as original chemical values or as normalized values (derived from the entire data set). Normalizing analytical data on a quadrangle-by-quadrangle basis (to reduce or eliminate boundary anomalies) for all element-method combinations would produce more than 1,800 normalized data sets. Instead, all quadrangles for which the contained samples share common laboratory and analytical methods are treated as one data set for each element. This reduced the number of data sets to be normalized to 197. The NURE samples reanalyzed for the USGS were treated similarly, resulting in an additional 55 data sets to be normalized.

Surface Modeling and Geographic Information Systems (GIS)

Each of the elements was modeled using Dynamic Graphics, Inc., EarthVision software. Erdas, Inc., IMAGINE image-processing/GIS software was used to interpret the geochemical surface models and drape the surfaces over digital shaded-relief topography to provide geographic reference.

Results

Standardizing concentration values on an element-by-element, method-by-method, and laboratory-by-laboratory basis resulted in three categories. These categories are those with (1) relatively little difference between anomalies on the element-concentration and the standardized-values surfaces; (2) significant positive differences between the two surfaces; and (3) significant negative differences between the two surfaces. Positive differences are those that suppress areas of artificial anomalies or enhance areas of artificially suppressed anomalies (or both). The accompanying figures for cadmium (figs. 3, 4), as an example of significant positive differences, show the suppression of artificial, low-level anomalies and the resulting enhancement of suppressed real anomalies.

Normalization of data sets based on laboratory, analytical method, and element groupings appears to be a viable methodology and reduces the amount of work involved in equating disparate geochemical data in the Headwaters Province study area. Artificial geochemical anomalies that remain, or are created, after normalizing indicate areas that require further subsetting prior to standardization.

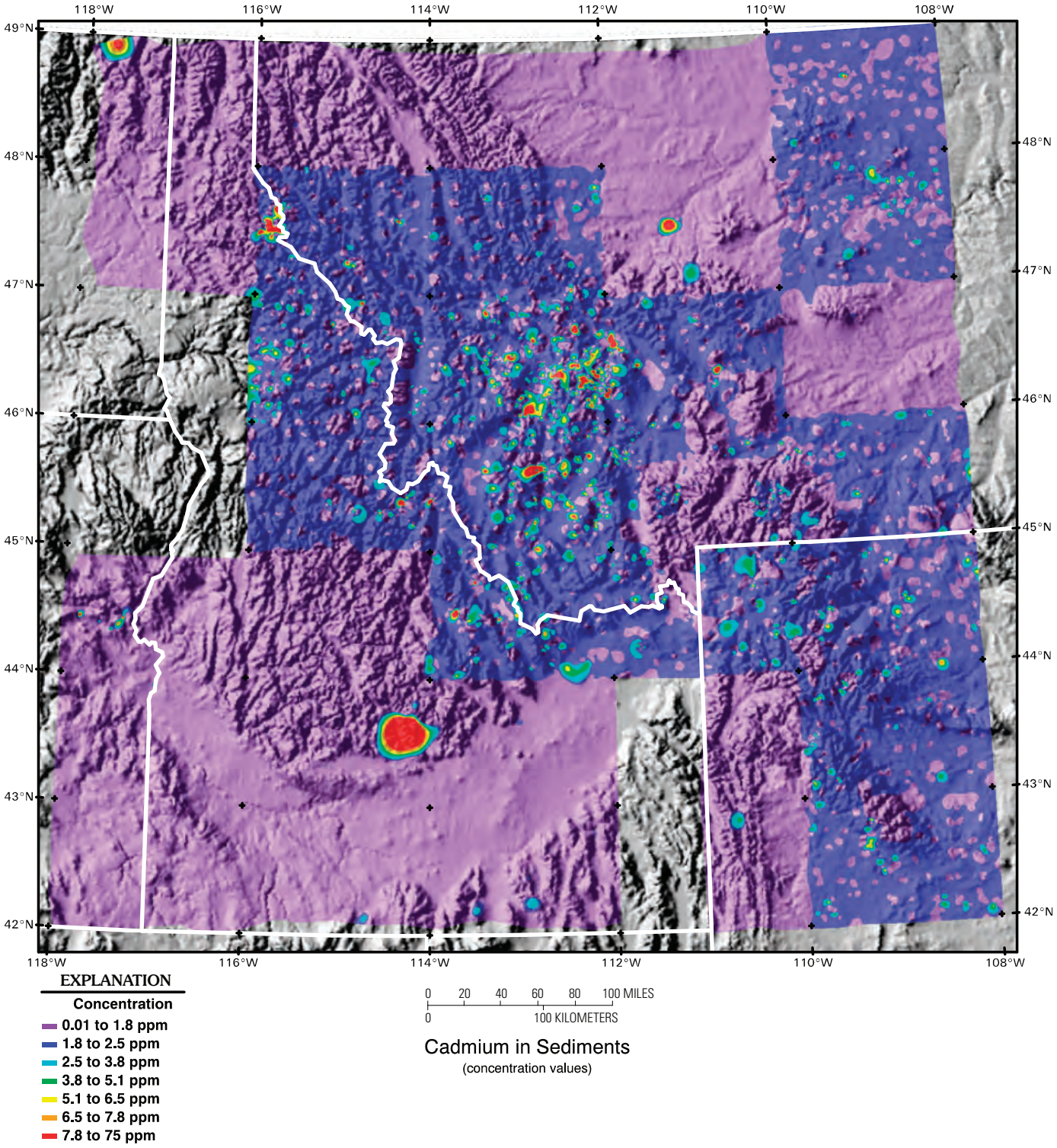

Figure 3. Original (non-normalized) NURE data showing geochemical distribution of cadmium in stream sediments, for comparison to normalized data in figure 4. Shown as concentrations in parts per million.

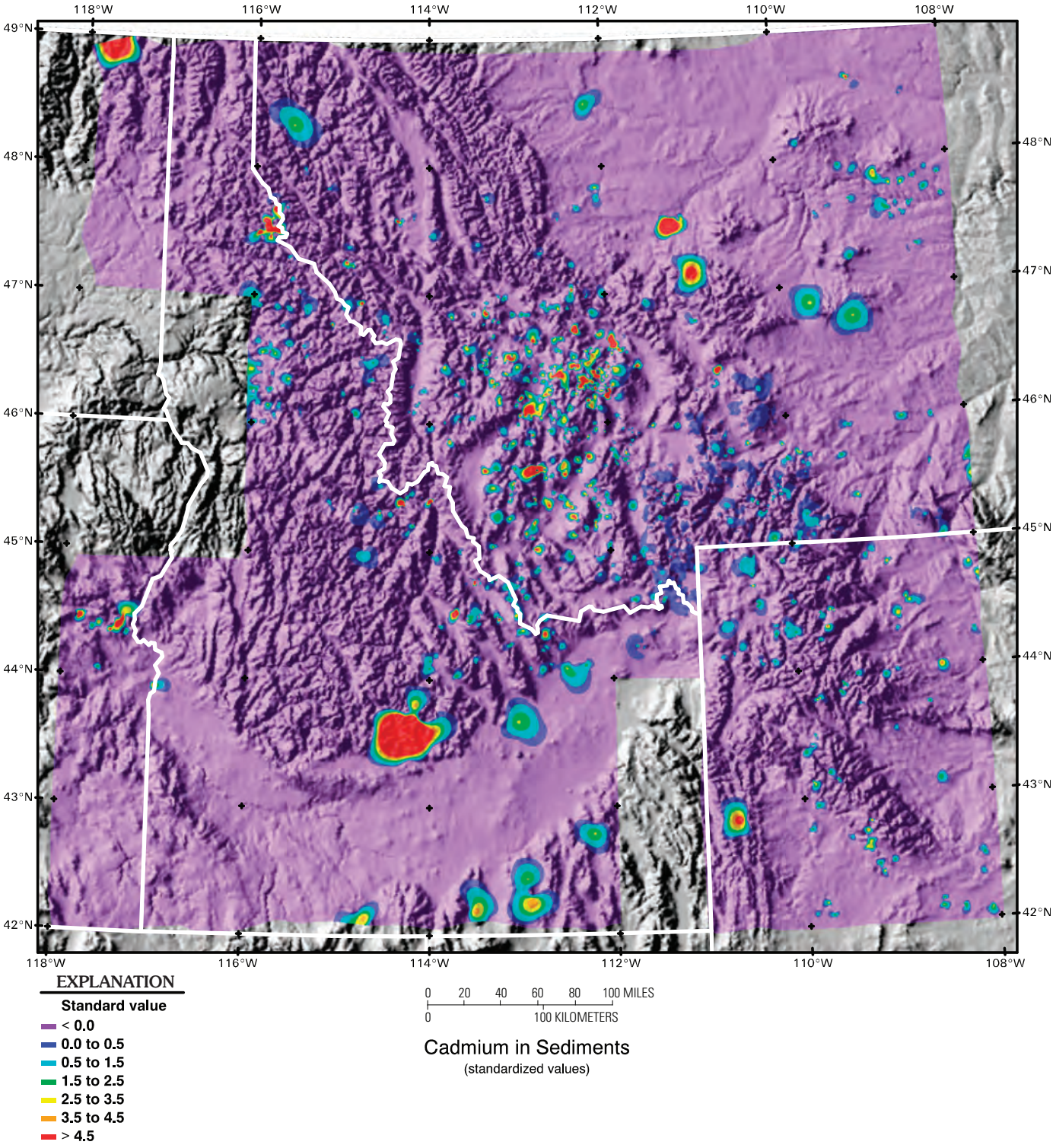

Figure 4. Normalized NURE data showing geochemical distribution of cadmium in stream sediments. Shown as standardized concentrations.

Table 2. Inventory for the Headwaters Province project showing number of NURE samples analyzed for the indicated elements by each laboratory and analytical method used.

[NURE data subsetted for this report]

	LA2	LA3	LA5	LL1	OR7	SR2	SR3A	SR3B	ICP10	ICP40A	ICP40B	AA1	AA2	INAA
Ag	12,167	14,343		2,055	14,497		2,991		1,481	3,221	2,046			
As		14,343		2,055				2,749 (**SR3XX**)	1,481	3,221	2,046	2,046	132	
Au			26,834			5,946			1,479	3,221	2,004	43	3,193	264
Ba			26,867	2,055	14,497					3,221	2,045			
Bi	12,167	14,343							1,481	3,221	2,046			
Cd	12,167	14,343							1,481	3,221	2,046			
Co			26,825	2,055	14,497		2,993			3,221	2,046			
Cr			26,853	2,055	14,497		2,994			3,221	2,046			
Cu	12,167	14,343			14,497		2,993		1,481	3,221	2,046			
Li			20,303 (**LA4**)		14,497			2,982 (**SR3FE**)		3,221	2,046			
Mo		1,269			14,497		2,994		1,481	3,221	2,046			
Ni	12,167	14,343			14,497		2,992			3,221	2,046			
Pb	12,167	14,343			11,974		2,981		1,481	3,221	2,046			
Sb			26,712	2,055					1,479					264
Se		14,343						2,995 (**SR3XX**)				2,046	132	
Sn	12,167	14,343					2,980			3,221	2,046			
Th			26,854	2,055	14,497	6,079				3,221	2,046			
V			26,865	2,055	14,497	6,129				3,221	2,046			
W	12,167	14,343		2,055				2,989 (**SR3CA**)						264
Zn			26,437	2,055	14,497		2,993		1,481	3,221	2,046			
	UDN-LA1	**UDN-LL1**	**UDN-OR2**	**UDN-SR1**	**UFL**					**ICP40A**	**ICP40B**			
U	30,966	2,058	8,569	6,149	2,509					3,221	2,046			

NURE-HSSR program analytical methods:

LA2 - Los Alamos Energy dispersive X-ray fluorescence analysis of sediments for Ag, Bi, Cd, Cu, Nb, Ni, Pb, Sn, and W.

LA3 - Los Alamos Energy dispersive X-ray fluorescence analysis of sediments for Ag, As, Bi, Cd, Cu, Nb, Ni, Pb, Se, Sn, W, and Zr.

(Note: Some LA3 analyses may include Mo—noted only in Special Studies.)

LA4 - Los Alamos arc-source emission spectrography analysis of sediments for Be and Li.

LA5 - Los Alamos neutron activation analysis of sediments for Al, Au, Ba, Ca, Ce, Cl, Co, Cr, Cs, Dy, Eu, Fe, Hf, K, La, Lu, Mg, Mn, Na, Rb, Sb, Sc, Sm, Sr, Ta, Tb, Th, Ti, V, Yb, and Zn.

LL1 - Lawrence Livermore neutron activation analysis of sediments for Ag, Al, As, Ba, Br, Ca, Ce, Cl, Co, Cr, Cs, Dy, Eu, Fe, Hf, Hg, K, La, Lu, Mg, Mn, Na, Rb, Sb, Sc, Sm, Sr, Ta, Tb, Th, Ti, U, V, W, Yb, and Zn.

OR7 - Oak Ridge emission spectrochemical analysis of sediments for Ag, Al, B, Ba, Be, Ca, Ce, Co, Cr, Cu, Fe, Hf, K, La, Li, Mg, Mn, Mo, Na, Nb, Ni, P, Pb, Sc, Sr, Th, Ti, V, Y, Zn, and Zr.

SR2 - Savannah River neutron activation analysis of sediments for Al, Ce, Dy, Eu, Fe, Hf, La, Lu, Mn, Na, Sc, Sm, Th, Ti, V, and Yb.

(Note: Detectable Au values for samples analyzed by SR2 reported in GJBX-135(82).)

SR3A - Savannah River (supplemental analysis by contract laboratory) Atomic Absorption Spectroscopy Analysis of sediments for Ag, Ba, Be, Co, Cr, Cu, Mg, Mo, Ni, Pb, Sn, Sr, Y, and Zn.

Table 2. Inventory for the Headwaters Province project showing number of NURE samples analyzed for the indicated elements by each laboratory and analytical method used.—*Continued.*

SR3B:
SR3CA - Savannah River (supplemental analysis by unnamed contract laboratory) colorimetric analysis of sediments for Nb, P, and W.
SR3FE - Savannah River (supplemental analysis by unnamed contract laboratory) flame emission analysis of sediments for K, and Li.
SR3XX - Savannah River (supplemental analysis by unnamed contract laboratory) analysis (analytical method not recorded) of sediments for As, Se, and Ca.
UDN-LA1 - Los Alamos delayed-neutron counting analysis of sediments for U.
UDN-LL1 - Lawrence Livermore neutron activation analysis of sediments for Ag, Al, As, Ba, Br, Ca, Ce, Cl, Co, Cr, Cs, Dy, Eu, Fe, Hf, Hg, K, La, Lu, Mg, Mn, Na, Rb, Sb, Sc, Sm, Sr, Ta, Tb, Th, Ti, U, V, W, Yb, and Zn.
UDN-OR2 - Oak Ridge neutron activation analysis—neutron counting of sediments for U.
UDN-SR1 - Savannah River neutron activation analysis—neutron counting of sediments for U.
UFL - Oak Ridge fluorescence spectroscopy analysis of sediments for U.
UNA-LL1 - Lawrence Livermore neutron activation analysis of sediments for Ag, Al, As, Ba, Br, Ca, Ce, Cl, Co, Cr, Cs, Dy, Eu, Fe, Hf, Hg, K, La, Lu, Mg, Mn, Na, Rb, Sb, Sc, Sm, Sr, Ta, Tb, Th, Ti, U, V, W, Yb, and Zn.
UNA-OR2 - Oak Ridge neutron activation analysis—neutron counting of sediments for U.
UXX-SR3 - Savannah River (supplemental analysis by unnamed contract laboratory) analysis (analytical method not recorded) of sediments for extractable U.

USGS analytical methods:
ICP10 - ICP-AES (inductively coupled plasma–atomic emission spectroscopy) performed in USGS laboratories using a method described by Motooka (1988).
ICP40A - ICP-AES performed in USGS laboratories using a method described by Crock and others (1983).
ICP40B - ICP-AES performed in USGS-contracted laboratories using a method described by Briggs (1990).
AA1 - (**Au**) - GF-AA (graphite furnace atomic absorption) performed in USGS-contracted laboratories using a method described by O'Leary and Meier (1986).
- (**As, & Se**) - Hydride generation atomic absorption spectrophotometry performed in USGS-contracted laboratories using a method described by Welsch and others (1990).
AA2 - (**Au**) - GF-AA (graphite furnace atomic absorption) performed in USGS laboratories using a method described by O'Leary and Meier (1986).
- (**As & Se**) - Hydride generation atomic absorption spectrophotometry performed in USGS laboratories using a method described by Welsch and others (1990).
INAA - (**Au, Sb & W**) neutron activation analysis in private sector laboratory.

Integrative Geologic Framework of the Headwaters Province

Ancient Laurentian (pre-Mesozoic continental core of North America) basement rocks underlie thick younger Proterozoic and Paleozoic sedimentary rocks and Proterozoic to Tertiary magmatic rocks in the eastern, central, and northern Headwaters Province but are only locally exposed at the surface. In western Idaho, oceanic rocks were accreted to the Laurentian continental core during Cretaceous time. The fabrics of the continental basement and of the western accretionary belt control many of the younger geologic features, depositional basins, composition and chemistry of magmatic rocks, location and type of epithermal mineral deposits, and multiple-times-reactivated structures. Study and better understanding of this architecture knits together the studies in the Headwaters Province.

Architecture of the Geologic Basement

By J. Michael O'Neill, P.K. Sims, and Karen Lund

The age and configuration of Precambrian crystalline (pre-Belt Supergroup) basement rocks in northwestern United States have been problematical because of sparse, widely dispersed exposures, a generally thick cover of Mesoproterozoic and younger sedimentary rocks, and the complexity of younger superposed tectonism and magmatism. Because direct observations of basement rocks are scarce, except in the mountains of southwestern Montana, knowledge of these rocks is strongly dependent on geophysical data and geochemical heritage gained from isotopic studies of younger igneous rocks.

Recent compilations of Precambrian basement maps of the States of Idaho (Sims and others, 2005), Montana (Sims and others, 2004), and Wyoming (Sims, Finn, and Rystrom, 2001) utilized updated aeromagnetic data (NAMAG, 2002) and available geologic and geochemical data (Rhodes and Hyndman, 1988; Mueller and others, 1995; O'Neill, 1999; Doughty and others, 1998; Mueller and others, 2002). These data provide a means to decipher the basement terranes and integrate them with the Precambrian geology of the western margin of Laurentia in adjacent Canada (Cook, 1995; Ross, 2002; Gorman and others, 2002).

Our study confirms and extends the postulate of O'Neill (1999), which has been further substantiated by new age data (Mueller and others, 2002), that the Archean Medicine Hat block was attached to the northwest margin of the Archean Wyoming province (fig. 5) by convergent deformation in Paleoproterozoic time. The long, broad disturbed zone in the basement was first delineated by reactivation features in overlying Phanerozoic rocks and named the Great Falls tectonic zone (O'Neill and Lopez, 1985; this report, see figs. 5, 6), and subsequently, the features of the underlying Paleoproterozoic suture were defined (O'Neill, 1999).

Conclusions reached during study of the geologic architecture and tectonic framework of the Precambrian basement of the Headwaters Province and adjacent regions are as follows. The Precambrian crystalline basement of the northern Rocky Mountains consists of the Archean Wyoming province in the southeastern part and an accreted composite terrane, the Trans-Montana orogen, composed of the Paleoproterozoic Wallace ocean-arc terrane and two accompanying minicontinents(?), the Pend Oreille domain and the Medicine Hat block in the northwestern part (fig. 5). The amalgamated terranes of the Trans-Montana orogen were accreted to the northern margin of the Wyoming province at about 1.9–1.8 Ga as a result of late Paleoproterozoic convergence (O'Neill, 1999; Brady and others, 2004). The accretionary events produced a zone of juvenile crust and a metamorphic-plutonic belt between the Great Falls and Dillon shear zones (fig. 5). Southeast of the Dillon shear zone is a 125-km-wide fold-and-thrust belt along the convergent margin of the Wyoming province, characterized by imbricate juxtaposition of thrust wedges composed of Archean and Paleoproterozoic rocks. Farther southeast, this Paleoproterozoic orogenic belt is interpreted to include a north-facing passive continental assemblage overlying the Archean Wyoming basement province, which is overstepped southward by a synorogenic foredeep succession (O'Neill, 1999).

Suturing of the Precambrian terranes and their incorporation into what was to become the Laurentian continent were followed at about 1.5 Ga (only about 200 m.y. after) by a major, continent-wide episode of strike-slip shearing. These Mesoproterozoic shear zones are generally oriented northwestward and segmented the crust into fault-bounded blocks of varying dimensions (fig. 5).

All of these basement structural features influenced and provided centers for subsequent deformation, sedimentation, magmatism, and mineral deposits in the Great Falls tectonic zone. Northeast-trending ductile shears within the Great Falls tectonic zone controlled the emplacement of major late Mesozoic-Eocene magmatic systems and the formation of related mineral deposits, extending from central Idaho to north-central Montana. Reactivation of the northwest-trending Mesoproterozoic strike-slip fault system provided depocenters for the Belt Supergroup (U.S.) and equivalent Purcell Supergroup (Canada). Reactivation of the northwest-trending structures in the late Mesozoic influenced tectonic activity along the western margin of the continent possibly by controlling orientation of the Sevier thrust faults.

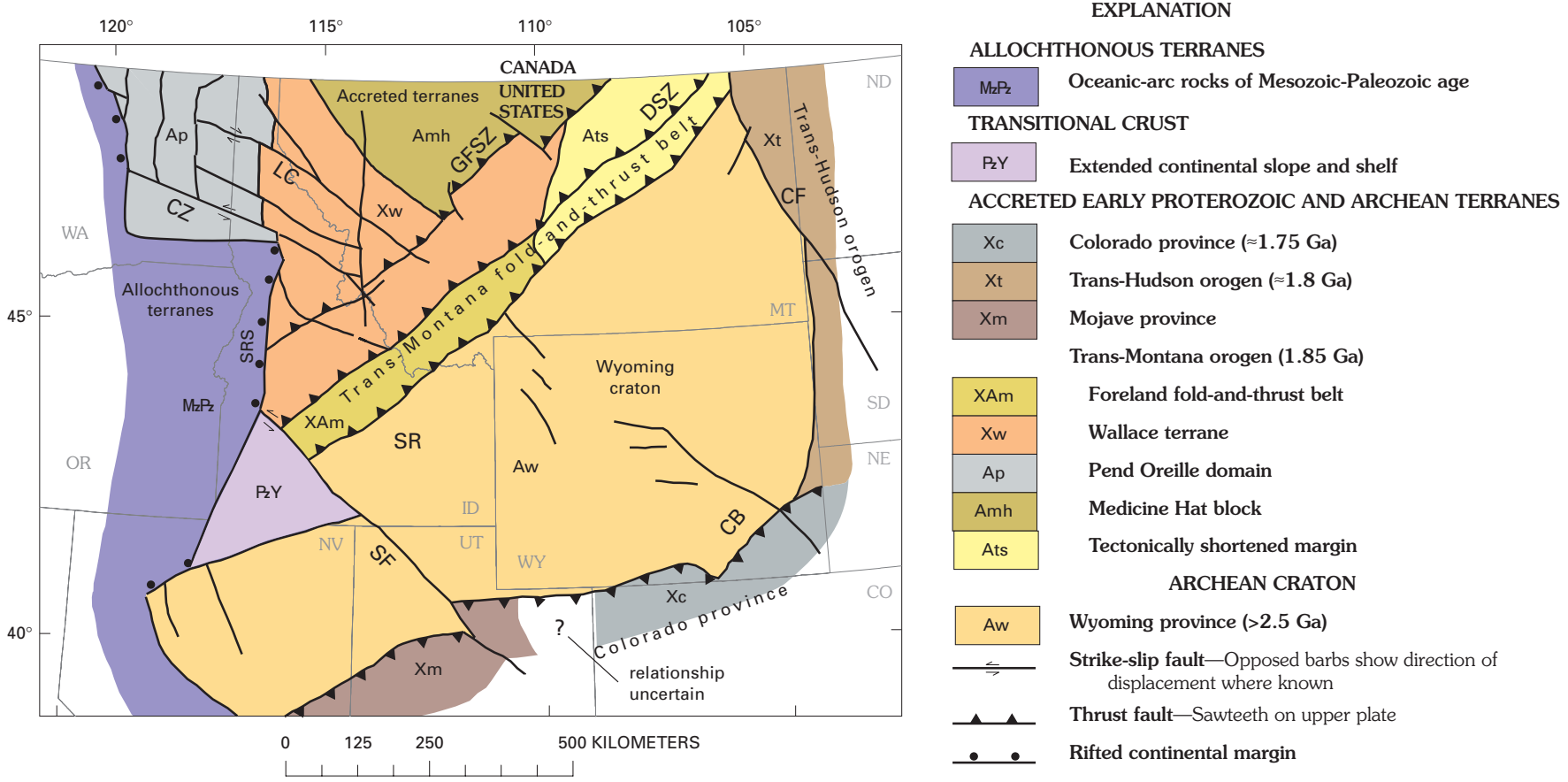

Figure 5. Generalized Precambrian basement map of part of northwestern United States, showing major geologic terranes assembled in the Paleoproterozoic. Major northwest-trending strike-slip shear zones recurrently active since the Mesoproterozoic are superimposed on the basement map. The faults are confined to Precambrian continental rocks. Barbs indicate relative horizontal displacement, where known. Compiled from Sims, Bankey, and Finn (2001); Sims, Finn, and Rystrom (2001); Sims and others (2004); Sims and others (2005). CB, Cheyenne belt suture; CF, Cedar Creek fault; CZ, Clearwater zone; DSZ, Dillon shear (suture) zone; GFSZ, Great Falls shear zone; LC, Lewis and Clark fault zone; SF, Snake River fault zone; SR, Snake River Plain volcanic field; SRS, Salmon River suture.

Metallogeny in the Context of the Great Falls Tectonic Zone

Major mineral deposit trends in the Headwaters Province include the northwest-trending Coeur d'Alene, a less well defined northwest-trending zone of cobalt-copper deposits, and the northeast-trending Idaho-Montana porphyry belt. (See the report by Taylor and others, p. 26.) The Idaho-Montana porphyry belt was originally named for elongated Eocene porphyry intrusions and dike swarms that are coincident with lode deposits in the Boise Basin (Ross, 1934a) and Casto (Ross, 1934b) areas. The belt was later identified across the entire province (Armstrong and others, 1978; Rostad, 1978) after many along-trend porphyry molybdenum deposits had been identified. The Montana-Idaho porphyry belt was one of the features originally used to define the Great Falls tectonic zone (O'Neill and Lopez, 1985). The basement architecture framework and particularly our understanding of its significant impact on subsequent regional mineralization trends were significantly improved as a consequence of geologic map compilations and metallogenic tectonic syntheses produced by the Headwaters Province project. (See the report by Klein and Sims, this page.)

Additionally, at the more local scale, determination of the magmatic systems responsible for particular hydrothermal mineralization events is considered crucial for development of mineral exploration models that include age, source, geochemical, tectonic, and emplacement characteristics of deposit types of interest. Assessment of mineral resource potential and potential geoenvironmental impacts of mineralizing systems requires similar data and models. Comparing and contrasting different mineralizing systems hosted by a single pluton can provide important constraints for predictive models. The Boulder batholith (Lund, Aleinikoff, Kunk, and Unruh, p. 39) lies at a critical junction between the basement structures that influenced mineralization in the Coeur d'Alene district and the Great Falls tectonic zone that controlled the Montana-Idaho porphyry belt and other types of epigenetic deposits. Topical studies in the Boulder batholith and its mineral deposits provide detailed data on timing, source, and emplacement characteristics for one of the regionally most important deposit systems.

As part of the Headwaters Province study, information on epigenetic mineral deposits was acquired by three studies at different scales within the Idaho-Montana porphyry belt. The results determine that the Great Falls tectonic zone is the fundamental structural and possibly geochemical control for mineral accumulations across the Headwaters Province. Future mineral resource and geoenvironmental assessments as well as future minerals exploration programs will be significantly enhanced by the results of these studies.

Control of Epigenetic Metal Deposits by Paleoproterozoic Basement Architecture

By Terry L. Klein and P.K. Sims

Large quantities of metals (gold, silver, copper, molybdenum, lead, and zinc) have been produced from mineral deposits in central and western Montana and central Idaho from the early 1860s to the present. The majority of these deposits are epigenetic and are associated with granitoid rocks of the Late Cretaceous Idaho and Boulder batholiths as well as felsic volcanic rocks of the Eocene Challis Volcanic Group and related subvolcanic intrusions in central and western Montana and central Idaho. Most of the deposits are in a 200-km-wide northeast-trending belt that extends from southwestern Idaho to the Little Rocky Mountains of north-central Montana, a distance of more than 1,000 km (figs. 5, 6). This belt contains the world-class copper deposits of the Butte district and more than 80 deposits designated as economically significant (Long and others, 1998; Spanski, 2004).

The deposits chiefly coincide with the northeast-trending Great Falls tectonic zone (O'Neill and Lopez, 1985), the multiple-times-reactivated and poorly exposed northeast-trending Paleoproterozoic suture complex in the basement between previously amalgamated Paleoproterozoic and Archean terranes of the Trans-Montana orogen (to the northwest) and the Archean Wyoming province to the southeast (Sims and others, 2004; Sims and others, 2005). A Paleoproterozoic magmatic arc, which extends between the Great Falls and Dillon shear zones, formed at 1.9–1.8 Ga (Mueller and others, 2002) during collision and continued convergence of the amalgamated Paleoproterozoic and Archean terranes of the Trans-Montana orogen with the Archean Wyoming province. A Paleoproterozoic fold-and-thrust belt affects Paleoproterozoic marginal basin sediments, as well as the edge of the Wyoming province, and extends from the Dillon shear zone southeastward to the Madison mylonite zone (fig. 6). This belt predominantly consists of Archean gneisses but includes thrust slices of early Paleoproterozoic quartzite and metadolomite (O'Neill, 1999).

The location and the economic significance of the Cretaceous and Eocene mineralized belt are associated with two fundamental aspects of the Precambrian geology. The northeast-striking shear zones (thrust faults) that formed during collision along the Paleoproterozoic Dillon shear zone provided the primary structural control for intrusion of the metal-bearing Cretaceous and Eocene magmas. The Paleoproterozoic magmatic arc that developed within the suture complex likely was a major source of metals. Reactivation of the preexisting

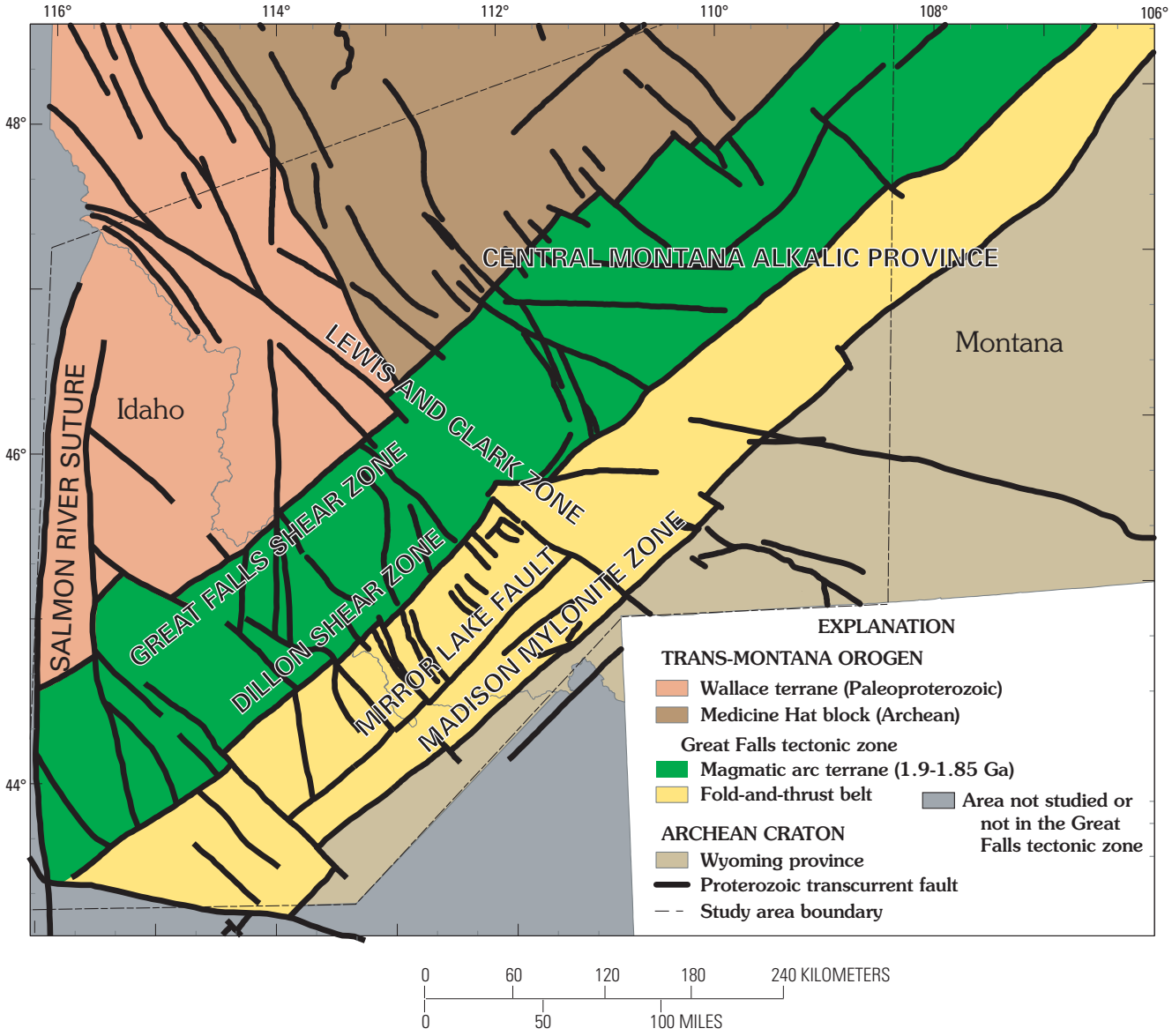

Figure 6. Basement map of west-central Montana and east-central Idaho, showing location of Great Falls tectonic zone and crosscutting northwest-trending faults.

fractures in the suture zone by recurrent regional tectonism in the Late Cretaceous and Tertiary provided openings for magma emplacement and conduits for ore-bearing fluids; it also facilitated concentration of the metals by convection in hydrothermal systems. A secondary but important control in localizing epigenetic metal deposits is the northwest-trending Mesoproterozoic fault system that traverses the region and overlaps with the northeast-striking shears formed during earlier suturing.

Updated aeromagnetic data (McCafferty and others, 1998) were critical to identification of Precambrian basement geology and the ore-controlling structures (Sims and others, 2004; Sims and others, 2005). Mineral deposit data were compiled and classified from information in the U.S. Geological Survey MRDS and MAS mineral occurrences databases. Information from U.S. Geological Survey CUSMAP and national forest studies and published reports from the Idaho Geological Survey and the Montana Bureau of Mines and Geology were used to supplement information gleaned from the databases and to upgrade location and production data (Klein, 2004).

Epigenetic metal deposits of probable Cretaceous age within this northeast-trending mineralized belt include (1) polymetallic veins (gold, silver, copper, lead, antimony, and zinc), (2) polymetallic carbonate replacement deposits, (3) epithermal gold veins, (4) distal disseminated gold deposits, (5) base- and precious-metal and tungsten skarn and contact metamorphic deposits, (6) disseminated, stockwork and breccia-hosted porphyry copper and molybdenum deposits, (7) Butte district silver veins, (8) high-sulfidation copper veins (Butte district copper vein deposits), and (9) tungsten veins (figs. 7, 8). Deposits related to Eocene magmatism include (1) epithermal vein, disseminated, and breccia-pipe controlled precious-metal deposits, (2) porphyry copper and molybdenum deposits, (3) polymetallic veins, and (4) alkaline intrusion-related precious-metal deposits. Alkaline intrusion-related deposits are concentrated in the northeastern part of the mineralized belt and are associated with Eocene intrusions that make up the Montana alkalic province (Larsen, 1940). Both temporal groups of deposits are spatially related to a pronounced gravity low (shown in fig. 8) that encompasses the Late Cretaceous Idaho and Boulder batholiths and also the Eocene Challis volcanic and subvolcanic intrusive rocks.

Many mineral districts and individual deposits are located at fault intersections between a northwest-trending, Mesoproterozoic set and a northeast-trending, Paleoproterozoic set that were both reactivated during the Late Cretaceous Sevier orogeny and Neogene extensional deformation. The northwest-striking Lewis and Clark zone (fig. 6), in particular, controlled the location of many deposits in the northern part of the study area. Perhaps significantly, this zone marks the transition from calc-alkaline magmatism in the southwestern part of the mineralized belt to alkaline magmatism to the northeast. Detailed structural studies have shown that the Boulder and adjacent Pioneer batholiths were localized by reactivation of preexisting Proterozoic structures during the Sevier orogeny (Kalakey and others, 2001). These intrusions lie in the northeasternmost part of the area of calc-alkaline magmatism.

Most of the large porphyry copper, porphyry molybdenum, and epithermal gold deposits are confined to the Paleoproterozoic juvenile magmatic arc and metamorphic-plutonic belt in the Paleoproterozoic suture complex directly northwest of the Dillon shear zone (fig. 6). These deposits lie within the –180 mGal (milligal) Bouguer anomaly of the central Idaho gravity low (Bankey and Kleinkopf, 1988; this report, fig. 8), or in the directly adjacent low-density area in the Medicine Hat block. Most of the large polymetallic vein and carbonate replacement deposits are confined to the belt of juvenile magmatic arc rocks in the Paleoproterozoic suture complex but extend southward into the foreland fold-and-thrust belt (figs. 5, 6). These epithermal deposits are coincident with a major zone of Eocene magmatism, as is depicted by mapped exposures and inferred from aeromagnetic data (fig. 8).

Gold production and resources, primarily from epithermal and gold-rich polymetallic vein deposits, are overwhelmingly concentrated in the part of the Great Falls tectonic zone underlain by juvenile magmatic arc rocks of the Paleoproterozoic suture zone and directly adjacent areas underlain by basement rocks of the Archean Medicine Hat block and Paleoproterozoic Wallace terrane. The most productive deposits, for all deposit types, in the Great Falls tectonic zone overlie the area thought to be composed of Paleoproterozoic juvenile crust (fig. 9*A*). The distribution of silver deposits is similar to that of gold (fig. 9*B*). The areal distribution of significant copper production and resources also is similar to that of gold; note that significant copper production is coincident spatially with the area underlain by the Boulder batholith (fig. 9*C*). Deposits with the greatest lead (fig. 9*D*) resources are more widely distributed areally than deposits containing gold and copper; these lead-rich deposits are present in all basement sectors of the Great Falls tectonic zone and are most abundant in the southern part of the Idaho batholith and the northern part of the Boulder batholith. The metal distribution of zinc is similar to that of lead.

An estimate of production from lode deposits (current to 1999) is based on available USGS MRDS and MAS databases and data from the CUSMAP (Butte, Dillon, Challis, Hailey–Idaho Falls) and national forest mineral resource assessments (Helena, Salmon, Payette), significant deposits databases (Long and others, 1998), and recent data compiled by Spanski (2004) and Klein (2004). These data indicate that epigenetic deposits in this area have produced more than 21 million troy ounces of gold, nearly 1 billion troy ounces of silver, 11 million tons of copper, nearly 0.5 million tons of molybdenum, 1 million tons of lead, and more than 2.5 million tons of zinc (all 2,000-pound tons). This amount of metal production is similar to that for the Colorado mineral belt of central and southwestern Colorado. The Colorado mineral belt and the Idaho-Montana porphyry belt are geologically similar. In particular, the Colorado mineral belt includes Cretaceous and

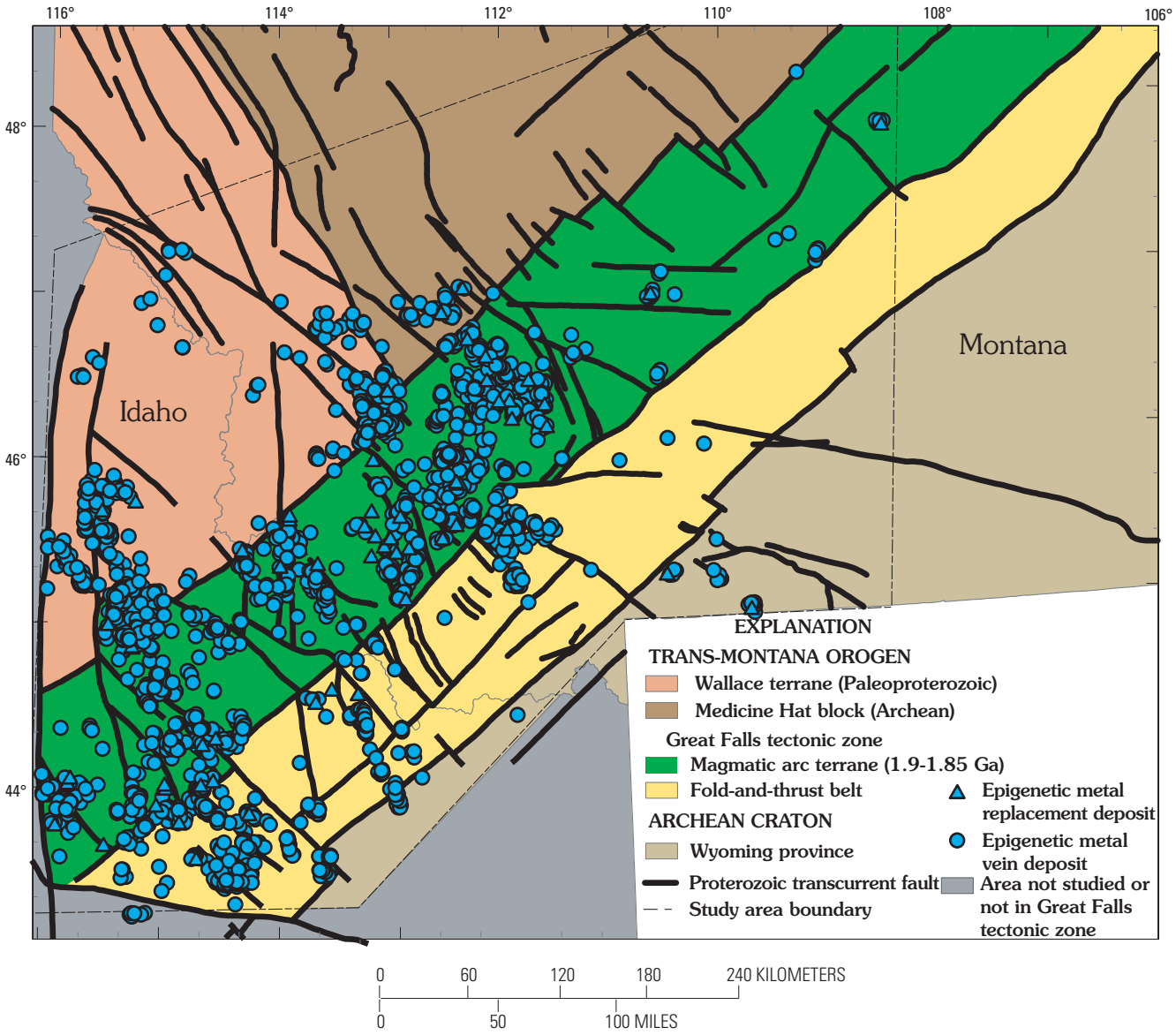

Figure 7. Location of studied epigenetic mineral deposits and outline of area for which mineral deposit data were compiled (Klein, 2004).

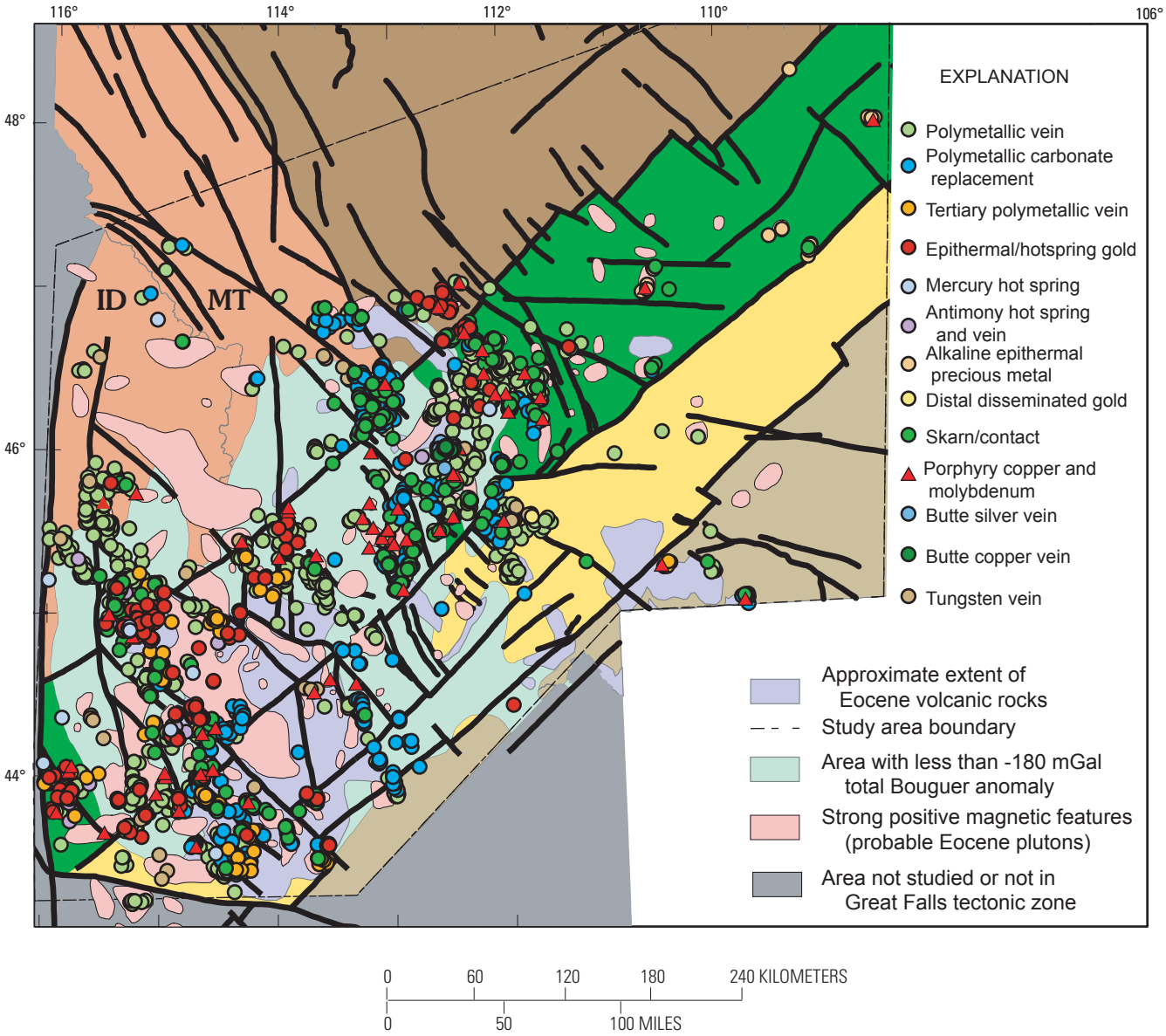

Figure 8. Location of epigenetic mineral deposits, shown by deposit type, relative to basement geology. Principal areas of Tertiary volcanism and intrusions and a regional negative Bouguer gravity anomaly (related to Late Cretaceous and Tertiary granitic intrusions) shown. Basement units and structure are same as in figure 6.

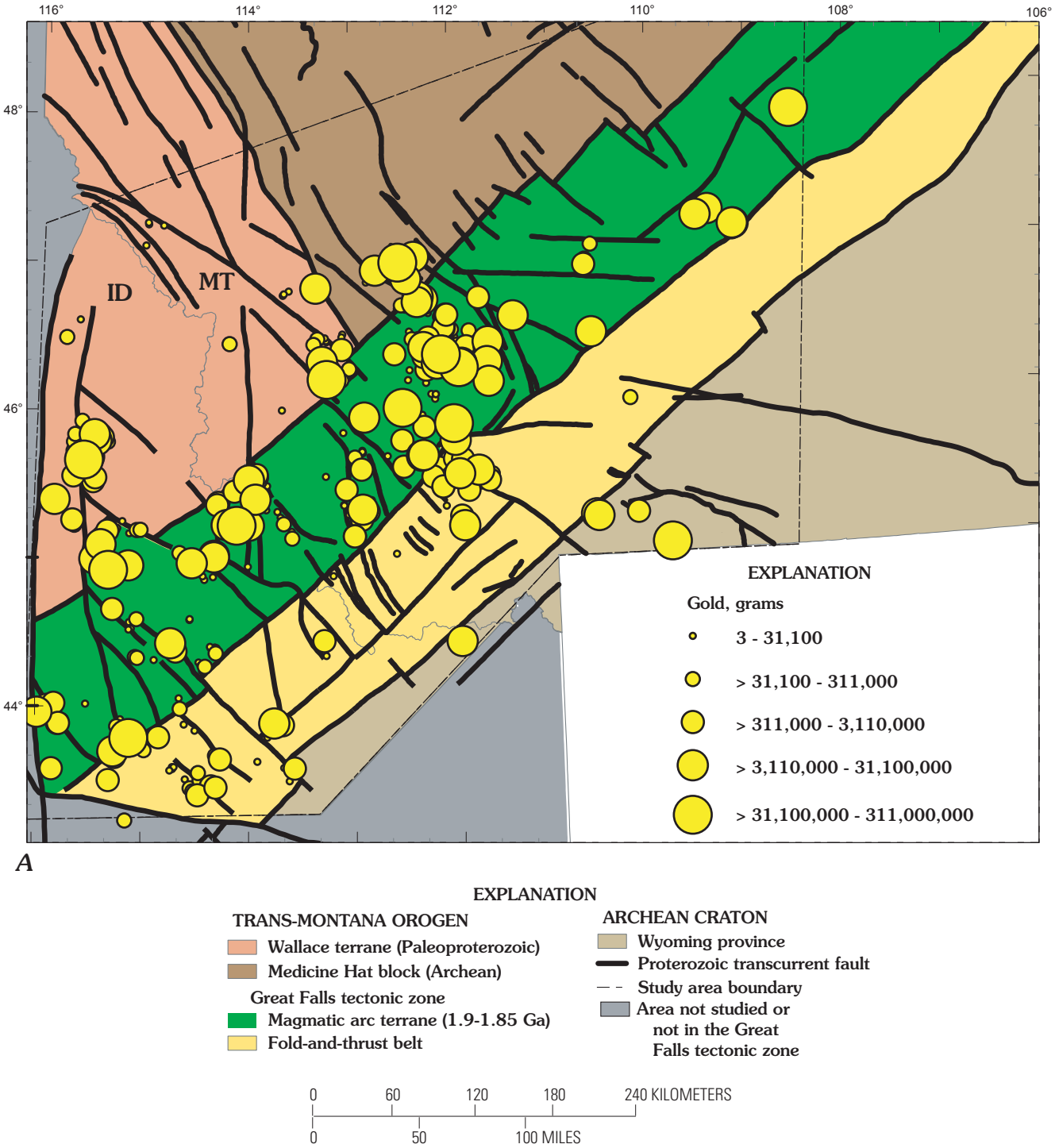

Figure 9 (above and following three pages). Location and quantity of metals produced from deposits with greater than 100 tons ore production and prospects with identified resources. Basement units and structure are same as in figure 6. *A*, gold; *B*, silver; *C*, copper; *D*, lead.

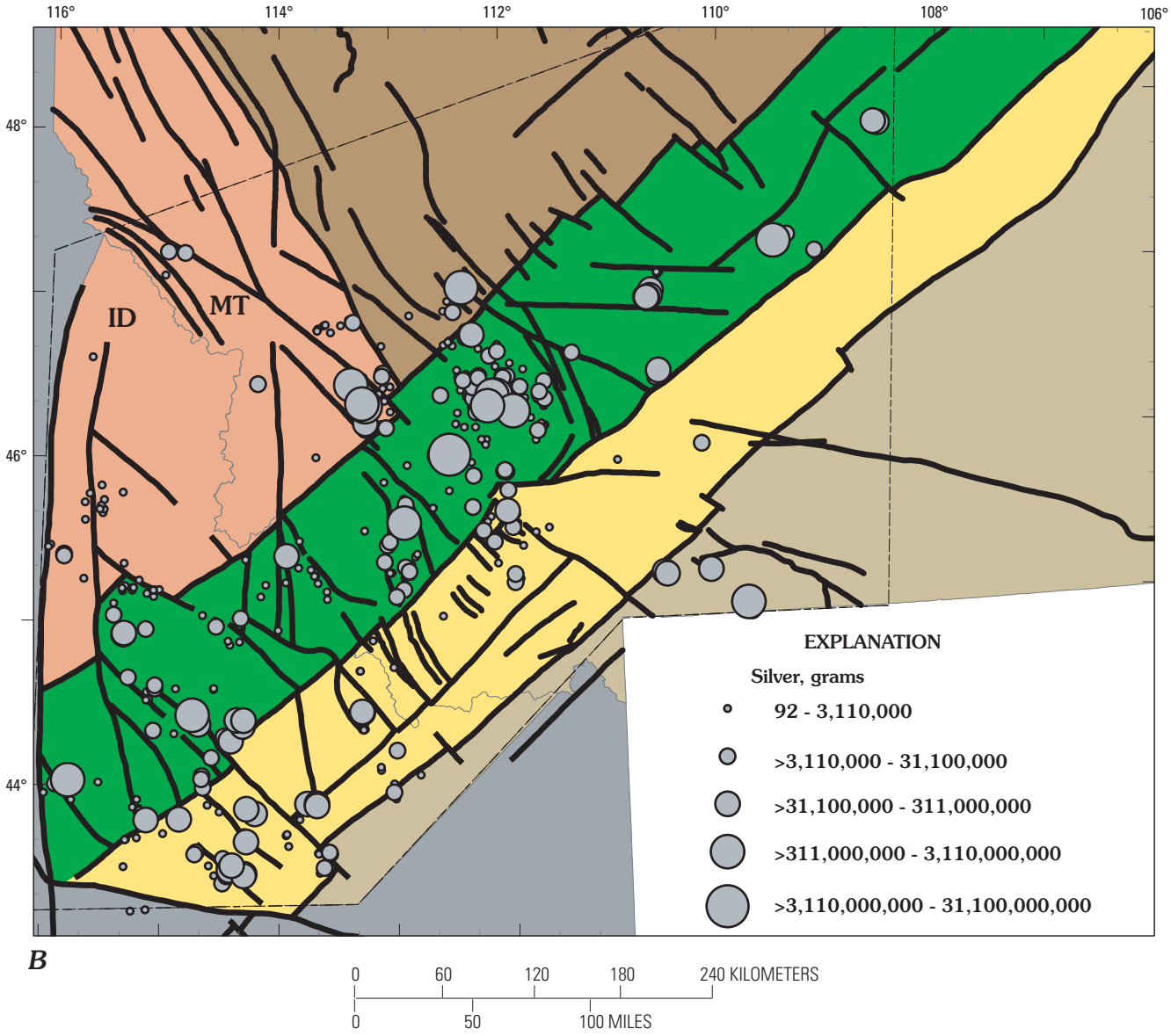
116°
114°
112°
110°
108°
106°
48°
46°
44°
ID
MT
EXPLANATION
Silver, grams
92 - 3,110,000
>3,110,000 - 31,100,000
>31,100,000 - 311,000,000
>311,000,000 - 3,110,000,000
>3,110,000,000 - 31,100,000,000
0 60 120 180 240 KILOMETERS
0 50 100 MILES

B

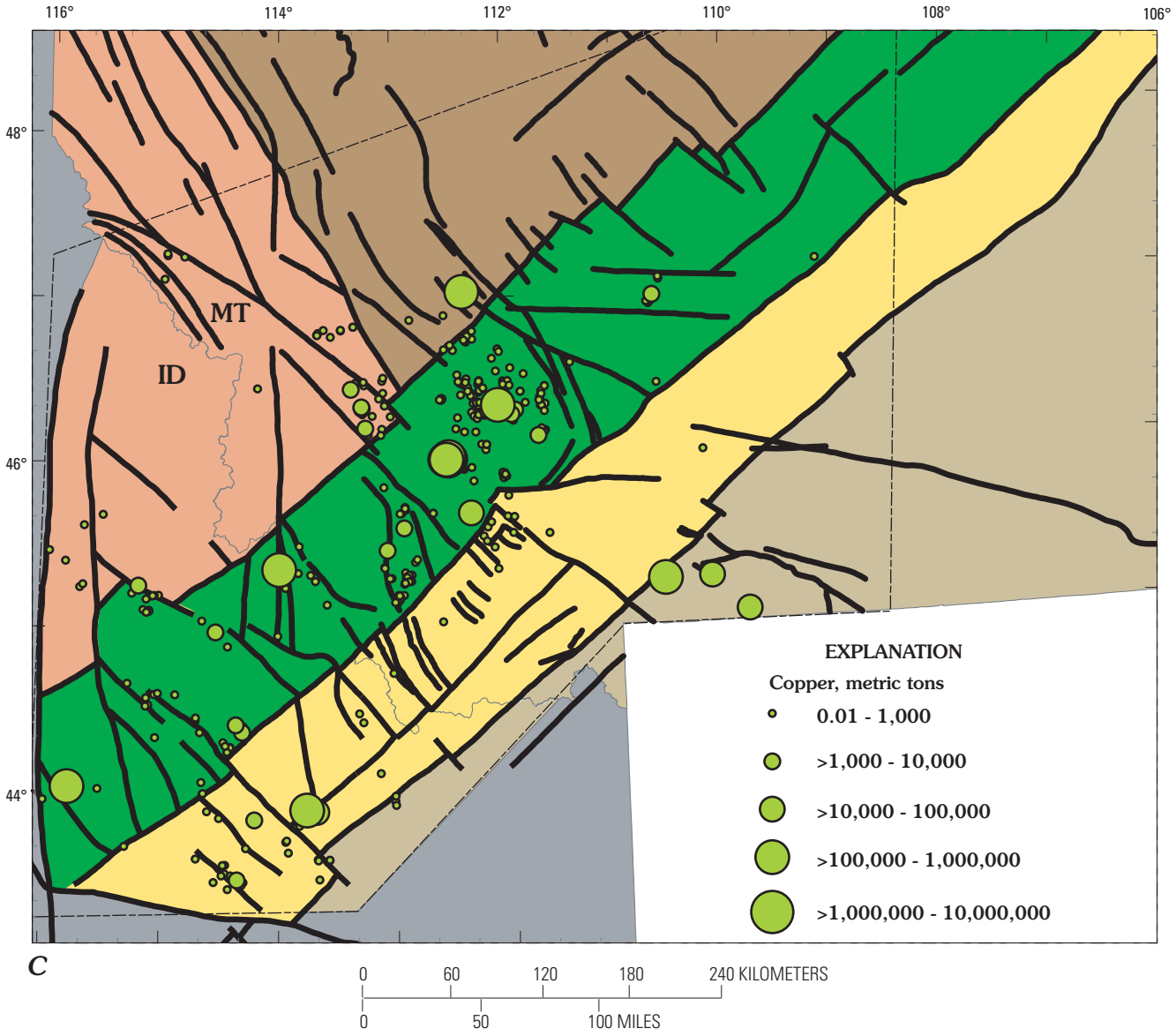

Figure 9—Continued. Location and quantity of metals produced from deposits with greater than 100 tons ore production and prospects with identified resources. *C*, copper; *D*, lead.

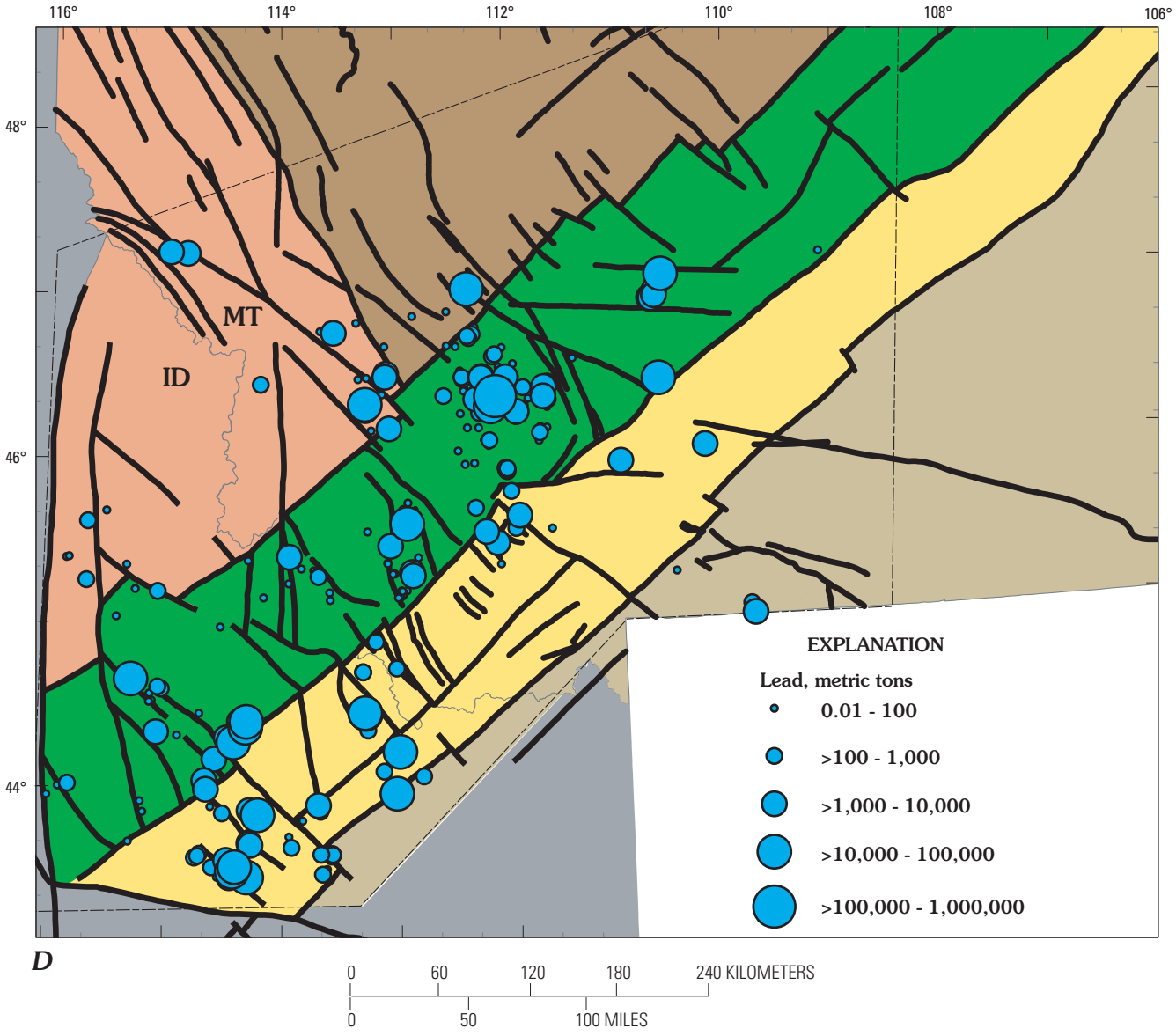
116°
114°
112°
110°
108°
106°
48°
46°
44°
MT
ID
EXPLANATION
Lead, metric tons
0.01 - 100
>100 - 1,000
>1,000 - 10,000
>10,000 - 100,000
>100,000 - 1,000,000
0 60 120 180 240 KILOMETERS
0 50 100 MILES

D

Tertiary epigenetic mineral deposits that are contained within Mesoproterozoic host rocks and which were inferred by Tweto and Sims (1963) to be localized by Proterozoic-age basement structures. Data for metal production from lode deposits in the Idaho-Montana porphyry belt and the Colorado mineral belt (compiled from Vanderwilt, 1947; Del Rio, 1960; and U.S. Bureau of Mines Mineral Yearbooks from 1959–1990) show that each area has produced similar amounts of gold, silver, and zinc. Molybdenum production is two times greater and lead production three times greater in the Colorado mineral belt than in the Idaho-Montana porphyry belt, whereas copper production is five times greater in the Idaho-Montana porphyry belt than in the Colorado mineral belt.

The tectonic history and composition of the Archean and Paleoproterozoic basement are interpreted to have greatly influenced the location, metal ratios, and size of epigenetic deposits in the Headwaters Province study area. We propose that the coincidence of the epigenetic deposits to juvenile magmatic rocks in the underlying basement resulted in melting of those fertile rocks during subsequent orogenic pulses and remobilization of metals. This permits first-order definition of permissive mineral resource assessment tracts for many deposit types. Refinement of the location and history of basement structures through more detailed studies will aid in further defining areas with higher economic potential. The close relationship between epigenetic metal deposits and basement rock compositions and preexisting structures in Archean and Paleoproterozoic terranes is not unique to the Idaho-Montana porphyry belt (see Sims and others, 2002), and it offers additional options in defining permissive tracts for national- and global-scale mineral resource assessments.

Geochronology and Geochemistry of the Idaho-Montana Porphyry Belt

By Cliff D. Taylor, Jeffrey A. Winick, Daniel M. Unruh, and Michael J. Kunk

The vast majority of the known molybdenum and copper resources in the Headwaters Province are contained in the northeast-trending Idaho-Montana porphyry belt (Rostad, 1978), a zone of porphyry-related deposits that extends from the Boise Basin in central Idaho, through southwestern Montana, to the Little Belt Mountains, and possibly as far east as the Hawkeye prospect (fig. 10) in the Zortman Landusky district of north-central Montana. The porphyry belt is truncated on the west by the Salmon River suture (fig. 10).

Two periods of silicic magmatism resulted in (1) voluminous Late Cretaceous tonalite to granite of the Idaho, Pioneer, and Boulder batholiths (related to convergent tectonism, subduction, and construction of an Andean-style cordillera along the Pacific margin) and (2) smaller Eocene plutons and associated dikes of more evolved monzogranite to granite-rhyolite composition (thought to have been emplaced during a period of crustal relaxation and rifting that followed subduction-related magmatism; Rehn and Lund, 1981). Regionally, these plutonic rocks were emplaced into the Archean Wyoming province, the Medicine Hat block, and the Paleoproterozoic Wallace terrane. Significantly, the northeast-trending porphyry belt is coincident with the Great Falls tectonic zone, the structurally complex underlying Paleoproterozoic orogenic zone originally produced by collision of the Wyoming province with Trans-Montana orogen rocks to the northwest during assembly of the Paleoproterozoic continent (fig. 5). This crystalline basement is obscured by younger sedimentary, volcanic, and plutonic rocks, including the Mesoproterozoic metasedimentary rocks of the Belt Basin, Paleozoic sedimentary rocks, Eocene volcanic rocks, and both major periods of magmatism.

Although most of the porphyry copper-molybdenum occurrences within this 750-km-long belt are economically insignificant, potentially important deposits exist at CUMO, Cannivan Gulch, and Heddleston; and major deposits at Thompson Creek and Butte have been mined. These deposits highlight the economic importance and undiscovered resource potential of the Idaho-Montana porphyry belt. Despite recognition between the 1930s and 1970s (Ross, 1934; Rostad, 1978) that deposits were aligned, very little information concerning age or geologic and geochemical characteristics is available in the literature. Thus, any attempt to discuss deposits in this belt has created controversy regarding whether deposits share similar origins, whether discrete episodes of porphyry deposit formation exist, or whether mineralization was associated with the two major periods of silicic magmatism.

Previous age data, mostly K-Ar analyses on minerals from both the host intrusions and mineral deposit-related alteration, span a range of ≈87 to 29 Ma (Armstrong and others, 1978; Rostad, 1978). Clearly, when compared with the normal lifespan of most mineral deposits, measured in hundreds of thousands to several million years (Stein and Cathles, 1997), the nearly 60 million years of igneous intrusive activity and mineralization cannot be related to a single magmatic episode or tectonic event. (1) How many periods of porphyry mineralization are present? (2) Is there a periodicity, or is deposit formation within the belt distributed evenly through time? (3) Is there a relationship between the age of formation and the geographic position of deposits within the belt? (4) What is the fundamental control resulting in the linearity of the belt in the first place? (5) What effect does the source region of the porphyries have on the size and characteristics of the deposits? (6) Do all these deposits share similar genetic origins regardless of age and nature of their source rocks?

In light of these questions, some of the important goals of the Headwaters Province project include (1) to more fully describe the characteristics of porphyry mineral deposits and occurrences, (2) to conduct a geochronological study of the

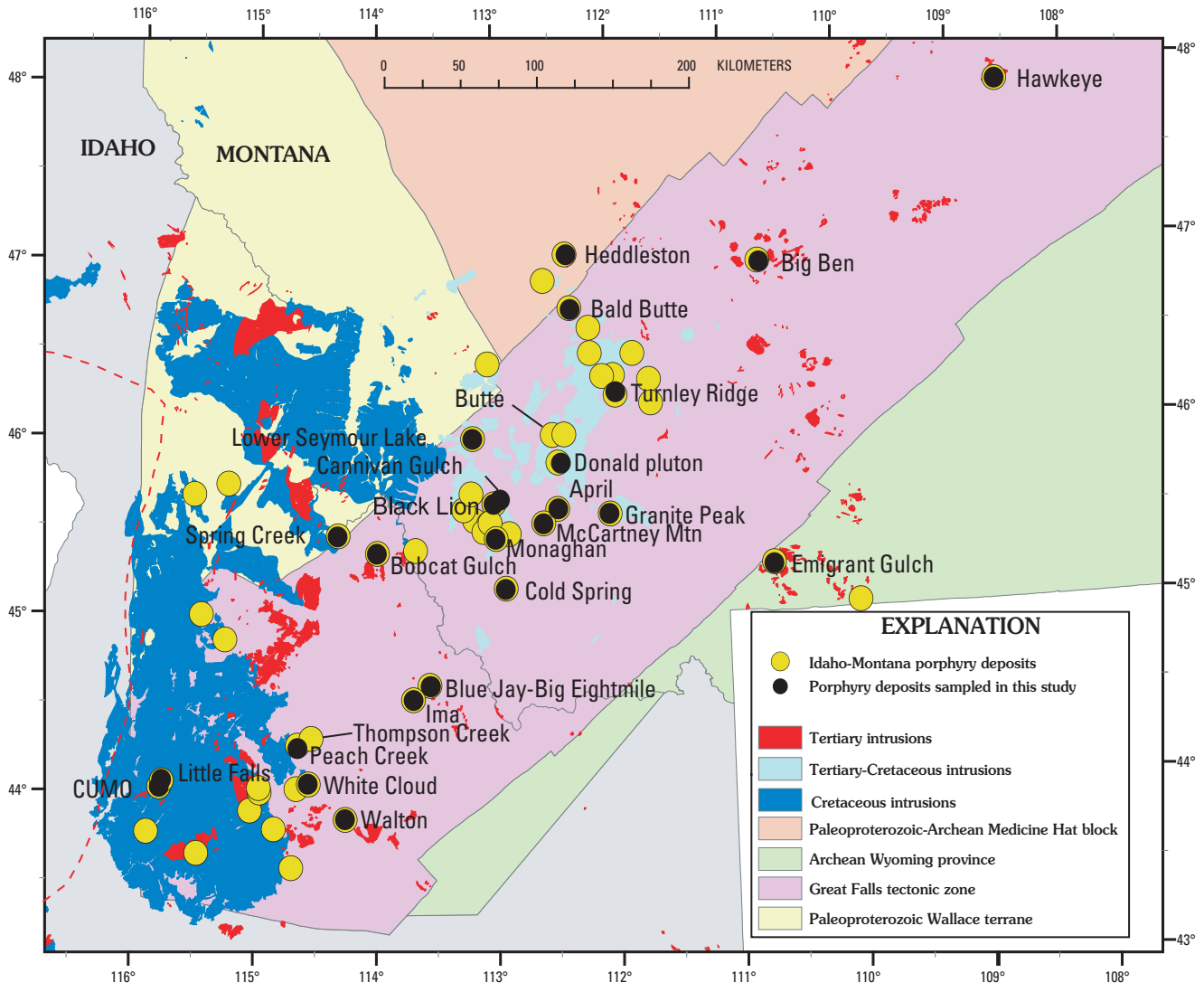

Figure 10. Location of porphyry molybdenum and copper-molybdenum deposits of Idaho-Montana porphyry belt. Pale gray shade, area not studied or not in Great Falls tectonic zone or Trans-Montana orogen. Dashed red line, Salmon River suture.

deposits within the belt using the high-precision $^{40}Ar/^{39}Ar$ method, and (3) to characterize and evaluate the genetic origins of the host plutons using modern geochemical and radiogenic isotopic analytical methods.

Field Work and Classification of Occurrences by Deposit Type

Sixty-three molybdenum and molybdenum-copper deposits and occurrences (fig. 10) are listed in the MRDS and MAS/MILS USGS mineral databases (McFaul and others, 2000); thirty of these were visited. We collected rock samples primarily to obtain new $^{40}Ar/^{39}Ar$ data (1) to determine cooling ages of the igneous host rocks (using hornblende, biotite, muscovite, or potassium feldspar mineral separates) that host deposits, and (2) to establish deposit ages for alteration minerals (using sericite mineral separates). The least altered igneous rocks were collected for whole-rock geochemical and radiogenic isotopic characterization. A subset of these samples includes Cretaceous batholith rocks and Proterozoic gneiss, collected and analyzed in order to better constrain the age and geochemistry of local country rocks.

At each site, we analyzed the mineralogical composition and texture of the host igneous rock and the form of intrusion (pluton, sill, or dike), as well as associated mineral deposit mineralogy, type and extent of alteration, and deposit style and morphology. These data were used to assign deposits to a stockwork, vein, or disseminated porphyry deposit class. Because intrusions related to porphyry molybdenum-copper deposits are generally associated with subduction-related continental arcs, molybdenum-only deposits were divided into low-fluorine, granodiorite-hosted deposits (generally associated with subduction-related Andean style continental arcs) or high-fluorine monzogranite-hosted to high-silica-rhyolite-hosted Climax-type deposits (generally related to intracontinental rift environments).

One set of deposits was difficult to characterize due to their small size and poor exposure relative to standard porphyry deposit models. Further characterization of age relationships and geochemistry (following) helped in characterization. A second group of deposits within the linear trend exhibited commonly accepted characteristics of porphyry deposits. The best known and well-studied deposits in the Idaho-Montana porphyry belt, the molybdenum-only Thompson Creek mine and the copper-molybdenum mine at Butte, are somewhat atypical examples of molybdenum and copper-molybdenum porphyry deposits. All three groups are shown in table 3.

$^{40}Ar/^{39}Ar$ Geochronology

In order to constrain the age relationships between Cretaceous and Tertiary igneous rocks and their associated mineral deposits within the Idaho-Montana porphyry belt, we obtained 54 high-precision $^{40}Ar/^{39}Ar$ analyses at 17 sites (table 4). Minerals analyzed include hornblende, biotite, potassium feldspar, and muscovite separated from the host igneous rocks, and sericite from ore-related alteration assemblages. Due to the wide and variable range (400°–250°C) of argon closure temperatures for the minerals analyzed, the $^{40}Ar/^{39}Ar$ technique provides a minimum age of the last thermal event to affect the rock. Yellow highlighted samples on table 4 represent cooling of sericite in alteration assemblages to below 250°C and, thus, represent minimum mineralization ages. Gray highlighted samples represent minimum cooling ages for igneous country rocks spatially associated with the porphyry deposits but only indirectly related to mineralizing events. For example, the analyses of potassium feldspar and biotite from the Mesoproterozoic augen gneiss at Spring Creek (Doughty and Chamberlain, 1996) probably reflect metamorphism of that unit during emplacement of the Idaho batholith. Similarly, Eocene ages for three mineral separates from the quartz monzonite of the Idaho batholith collected at Rattlesnake Gulch, about 20 km east of the Little Falls deposit, probably reflect resetting and cooling of batholith rocks near Eocene dikes related to the deposits at Little Falls and CUMO. The remainder of the samples in table 4 represent cooling ages of rock-forming minerals in intrusive rocks that are directly related to hydrothermal mineralization events.

The age of intrusion and mineralization as a function of distance from the continental margin is summarized in figure 11. Two major features are apparent. First, samples of Cretaceous age exhibit a poorly defined but consistent younging trend with increasing distance northeast of the Salmon River suture. The oldest deposits related to the Idaho batholith have a maximum age of 85.2 Ma (biotite) for the Little Boulder Creek stock (White Cloud deposit, figs. 10, 11). The youngest of the Cretaceous batholith-related deposits is located in the easternmost Tobacco Root batholith at Granite Peak, where mineralized dikes cutting the batholith have a minimum age of 69.6 Ma (potassium feldspar). Cooling ages for additional samples of batholithic country rocks, not directly related to mineralization, such as at Peach Creek and the Donald pluton, support the general eastward younging trend. Second, samples of Tertiary age show a more tightly constrained age distribution that appears to be largely independent of position relative to the continental margin. The range in age for Eocene intrusive host rocks spans an interval from 38.8 Ma (CUMO) to 51.3 Ma (Bluejay-Big Eightmile). In comparison, if ages of batholithic plutonic country rocks that host the deposits are included, the Cretaceous samples indicate a ≈34 m.y. range.

Examination of the cooling histories at six Cretaceous and six Tertiary locations for which age data for multiple mineral separates are available suggests fundamental differences between Cretaceous and Tertiary deposits. Normal age progressions of hornblende>biotite>sericite>potassium feldspar are observed at five of the six Tertiary deposits and generally indicate cooling histories of less than ≈4 m.y. The longest age span is 6.6 m.y. at the Walton deposit. Normal age progressions are also observed at four of the six Cretaceous deposits, although the age span is greater than for the Tertiary deposits. Three of six span a range of about 8 to 11 m.y., and share the characteristic of being hosted by the Idaho and Tobacco Root batholiths. The two deposits that exhibit relatively short

Table 3. Characteristics of selected molybdenum deposits and mineralized areas in the Idaho-Montana porphyry belt.[1]

Deposit name(s)	Host rock	Form	Diagnostic minerals	Alteration
		Deposits difficult to characterize relative to standard porphyry deposit models		
Peach Creek, McCartney Mountain, April Claim, Thrift Stamp.	Genetically unrelated country rock.	Sparse fracture coatings and disseminations associated with large veins or pods of quartz.	Molybdenum or molybdenum-copper minerals.	Unknown.
Walton--------	Felsic dikes peripheral to the Little Fall Creek pluton.	Large, discontinuous quartz-sericite veins.	Unknown	Unknown.
Pear Lake-Anchor Lake-Monaghan.	Granodiorite country rock.	Widely dispersed coated fractures.	Pyrite and molybdenite	Unknown.
Spring Creek--	Proterozoic gneiss that may be genetically associated with the minor occurrence of felsic dikes noted in drill core.	Highly mineralized massive quartz-sericite vein.	Molybdenite	Unknown.
Granite Peak, Emigrant Gulch.	Large felsic dikes	Unknown	Disseminated pyrite and molybdenite.	Unknown.
Bald Butte---	Unexposed quartz diorite intrusion at depth from drill core (Rostad, 1978).	Molybdenum geochemical anomaly in soils.	Molybdenum	Unknown.
Turnley Ridge	Large and continuous aplite dike cutting quartz-potassium feldspar porphyry.	Sparse mineralized rock.	Unknown	Potassium feldspar-sericite flooded.
Bluejay-Big Eightmile.	Big Eightmile stock	Disseminated mineralization in greisen developed at the top of the stock.	Pyrite, chalcopyrite, and rare molybdenite with malachite and azurite.	Unknown.
		Porphyry-related deposits		
Little Falls--	Extensive set of Eocene porphyritic calc-alkaline dikes that intrude the Idaho batholith.	Quartz vein stockworks associated with rhyolite porphyry dikes and alteration halo extending a short distance into the surrounding Idaho batholith.	Molybdenite-pyrite coated fractures and molybdenite-rich quartz vein stockworks.	Weak pyritic alteration halo.
CUMO	Extensive set of Eocene porphyritic calc-alkaline dikes that intrude the Idaho batholith.	Idaho batholith country rocks.	Significant disseminated molybdenum-copper mineralization.	Central zone of intensely silicified host rock surrounded by extensive argillic halo. Extensive pyrite-sericite alteration in country rocks.
White Cloud, Cannivan Gulch, Black Lion	Granodiorite to monzogranite porphyry intrusions. (White Cloud, Idaho batholith; Cannivan Gulch and Black Lion, Pioneer batholith).	Well-developed quartz-potassium feldspar-sericite-pyrite-molybdenite vein stockworks.	Abundant molybdenite	Concentrically zoned phyllic and argillic alteration haloes surrounding silicic and potassically altered cores.

Table 3. Characteristics of selected molybdenum deposits and mineralized areas in the Idaho-Montana porphyry belt—Continued.

Deposit name(s)	Host rock	Form	Diagnostic minerals	Alteration
		Porphyry-related deposits—Continued		
Big Ben-----	Intrusive high-silica porphyritic rhyolite.	Unknown	"Climax-type" molybdenum deposit.	Unknown.
Pipestone Pass occurrences.	Granitic Homestake and granodioritic Donald plutons of the Boulder batholith.	Disseminated mineralization.	Minor concentrations of disseminated molybdenite.	Unknown.
Heddleston, Bobcat Gulch.	Granodioritic intrusions.	Disseminated and stockwork veins in standard porphyry copper-molybdenum deposit.	Pyrite, chalcopyrite, and molybdenum. Protore and supergene enriched bodies of chalcocite.	Pervasive and concentrically zoned alteration.
Cold Spring-Grasshopper.	Sanidine-rich dacite plug.	Unknown	Unknown	Heavily altered.
		Somewhat atypical examples of molybdenum and copper-molybdenum porphyry deposits		
Thompson Creek	Outer equigranular, medium-grained, biotite granodiorite, with an inner weakly porphyritic biotite granite.	Little to no disseminated molybdenite in deposit. Tenor of orebody defined by size and density of stockwork quartz-molybdenite veining, Deposit scale: veins constitute a stockwork. Outcrop scale: widely spaced discrete veins are centimeters to a meter wide. Grade controlled by high concentrations of coarsely crystalline molybdenite in selvages of large veins.	Molybdenite associated with minor pyrite. Metals aggregate within the intrusive bodies primarily as selvages to coarse-grained, quartz-potassium feldspar-muscovite-biotite veins.	Pervasive weak argillic alteration. Potassic and phyllic alteration of the host intrusions confined to within a few centimeters of the veins.
Butte	Butte granite pluton	Concentrically arranged massive to disseminated shells of ore. Bulk of the metal (Main Stage) contained by swarm of large, subparallel polymetallic veins and coeval quartz porphyry dikes. Earlier, pre-Main Stage porphyry mineralization present at depth.	Stockwork of randomly oriented and discontinuous chalcopyrite-molybdenite veinlets with superimposed rich copper veins.	Chalcopyrite-molybdenite veinlets enclosed within sericite-biotite potassium feldspar alteration envelopes.

[1]See figure 10 for locations of studied sites.

Table 4. New $^{40}Ar/^{39}Ar$ data for mineralized rocks (gold color), genetically related plutons, and country rocks (gray) of the Idaho-Montana porphyry belt.

Field No.	Prospect	Rock type	Mineral	Age (Ma)	±1s	Type
K-01-7-19A	Walton	altered quartz monzonite adjacent to vein	Sericite	44.49	4.86	Isochron
K-01-7-19B	Walton	biotite quartz monzonite-Little Fall Creek pluton	Biotite	47.80	0.25	Total fusion
K-01-7-19B	Walton	biotite quartz monzonite-Little Fall Creek pluton	Biotite	47.23	0.55	Isochron
K-01-7-19B	Walton	biotite quartz monzonite-Little Fall Creek pluton	K-spar	41.20	4.94	Isochron
K-01-7-21C	CUMO	silicified, MoS_2-bearing quartz monzonite	K-spar	38.80	0.30	Isochron
K-01-7-21D	CUMO	altered, brecciated lamprophyre	Biotite	45.62	0.23	Total fusion
K-01-7-21D	CUMO	altered, brecciated lamprophyre	Biotite	45.71	0.25	Plateau
K-01-7-21F	CUMO	hornblende gabbro	Hornblende	39.01	0.21	Plateau
01HW-69		quartz monzonite-Rattlesnake Gulch	K-spar	44.32	0.24	Plateau
01HW-69		quartz monzonite-Rattlesnake Gulch	Biotite	47.61	0.24	Total fusion
01HW-69		quartz monzonite-Rattlesnake Gulch	Biotite	45.02	1.28	Isochron
K-01-7-23A	White Cloud	quartz-MoS_2 vein cutting Little Boulder Creek stock	Sericite	84.98	0.35	Plateau
K-01-7-23A	White Cloud	quartz-MoS_2 vein cutting Little Boulder Creek stock	Sericite	84.53	0.35	Plateau
K-01-7-23A	White Cloud	quartz-MoS_2 vein cutting Little Boulder Creek stock	Sericite	84.40	0.30	Isochron
K-01-7-23B	White Cloud	biotite quartz monzonite-Little Boulder Creek stock	K-spar	78.09	1.53	Isochron
K-01-7-23B	White Cloud	biotite quartz monzonite-Little Boulder Creek stock	Biotite	85.19	0.30	Total fusion
K-01-7-23B	White Cloud	biotite quartz monzonite-Little Boulder Creek stock	Biotite	84.67	0.22	Total fusion
K-01-7-23C	White Cloud	hornfelsed Wood River Fm.-quartz-MoS_2 vein selvage	Sericite	85.10	0.30	Plateau
01HW-73	White Cloud	quartz monzonite-White Cloud stock	Biotite	86.33	0.27	Total fusion
JW-6-17-02D	Big Ben	altered Snow Creek quartz porphyry	Sericite	49.40	1.30	Isochron
JW-6-17-02E	Big Ben	Snow Creek quartz porphyry-drill core	K-spar	47.90	0.20	Plateau
JW-6-17-02F	Big Ben	Snow Creek quartz porphyry-drill core	Biotite	47.38	0.07	Total fusion
02DU-08	Big Ben	Carpenter Creek biotite granite porphyry-drill core	Biotite	47.53	0.09	Total fusion
02DU-08	Big Ben	Carpenter Creek biotite granite porphyry-drill core	K-spar	45.95	0.26	Isochron
JW-6-18-02A	Bald Butte	diorite-Belmont dike	Biotite	42.96	0.12	Total fusion
JW-6-18-02A	Bald Butte	diorite-Belmont dike	Biotite	43.05	0.24	Total fusion
JW-6-18-02A	Bald Butte	diorite-Belmont dike	K-spar	57.45	0.17	Total gas
JW-6-19-02A	Heddleston	altered quartz monzonite porphyry	Sericite	43.83	0.18	Plateau
JW-6-19-02D	Heddleston	altered quartz monzonite porphyry	Sericite	46.50	0.60	Isochron
JW-6-21-02A		granodiorite-Boulder batholith	Biotite	72.81	0.25	Total fusion
JW-6-21-02A		granodiorite-Boulder batholith	K-spar	81.00	0.20	Plateau
JW-6-21-02A		granodiorite-Boulder batholith	Hornblende	102.31	3.34	Isochron
JW-6-22-02B	Pipestone Pass	leucocratic granite-Donald pluton	K-spar	69.10	0.30	Isochron
JW-6-22-02B	Pipestone Pass	leucocratic granite-Donald pluton	K-spar	70.07	0.62	Isochron
JW-6-23-02B	April Claim-Crystal Butte	altered quartz monzonite	Sericite	73.71	0.20	Plateau
JW-6-23-02D	April Claim-Crystal Butte	diorite	Biotite	74.78	0.26	Total fusion
JW-7-17-02A	Emigrant Gulch	rhyolite porphyry	Sericite	48.10	0.27	Plateau
JW-7-17-02C	Emigrant Gulch	rhyolite porphyry	Biotite	49.57	0.21	Total fusion
JW-7-17-02C	Emigrant Gulch	rhyolite porphyry	K-spar	47.90	0.50	Isochron
JW-7-18-02C	Granite Peak	quartz monzonite dike	K-spar	69.60	0.40	Isochron
JW-7-18-02D	Granite Peak	biotite granite	K-spar	68.60	0.40	Isochron
JW-7-18-02D	Granite Peak	biotite granite	Hornblende	79.41	0.47	Isochron
JW-7-19-02C	McCartney Mtn	biotite granodiorite stock	Biotite	75.13	0.26	Total fusion
JW-7-19-02C	McCartney Mtn	biotite granodiorite stock	K-spar	72.80	0.30	Isochron
JW-7-20-02A	Cold Spring-Grasshopper	dacite plug	Sanidine	72.50	0.20	Weighted mean
JW-7-21-02A	Black Lion	Clifford Creek granodiorite	Sericite	63.36	0.34	Plateau
JW-7-23-02A	Lower Seymore Lake	altered white mica-bearing leucomonzogranite	White mica(?)	75.40	0.26	Plateau
JW-7-23-02B	Lower Seymore Lake	leucomonzogranite	Sericite	44.75	0.13	Plateau
JW-7-25-02B	Spring Creek	quartz-pyrite-sericite-molybdenite vein	Sericite	46.53	0.55	Isochron
JW-7-25-02D	Spring Creek	biotite-hornblende augen gneiss	K-spar	89.88	0.49	Plateau
JW-7-25-02D	Spring Creek	biotite-hornblende augen gneiss	Biotite	79.91	0.49	Total fusion
JW-7-25-02E	Ima	quartz vein cutting Precambrian quartzite	Sericite	44.50	0.13	Plateau
JW-7-26-02A	Bluejay-Big Eightmile	biotite monzogranite-Big Eightmile stock	Biotite	49.52	0.14	Total fusion
JW-7-26-02A	Bluejay-Big Eightmile	biotite monzogranite-Big Eightmile stock	Biotite	47.40	2.77	Total fusion
JW-7-26-02A	Bluejay-Big Eightmile	biotite monzogranite-Big Eightmile stock	K-spar	48.00	0.30	Isochron
JW-7-26-02B	Bluejay-Big Eightmile	basaltic andesite dike cutting Big Eightmile stock	Biotite	50.60	0.22	Total fusion
JW-7-26-02C	Bluejay-Big Eightmile	quartz-sericite vein cutting altered monzogranite	Sericite	51.10	0.40	Plateau
JW-7-26-02C	Bluejay-Big Eightmile	quartz-sericite vein cutting altered monzogranite	Sericite	50.48	1.06	Isochron
JW-7-26-02D	Bluejay-Big Eightmile	heavily altered malachite-rich greisen at Bluejay	Sericite	51.30	0.40	Isochron
JW-7-27-02B	Peach Creek	quartz monzonite-Idaho batholith	K-spar	79.50	0.40	Isochron
02DU-11	Hawkeye	k-spar flooded rhyolite porphyry	K-spar	62.80	0.34	Plateau
02HW-06B	Hawkeye	rhyolite porphyry-drill core	K-spar	64.71	0.35	Plateau

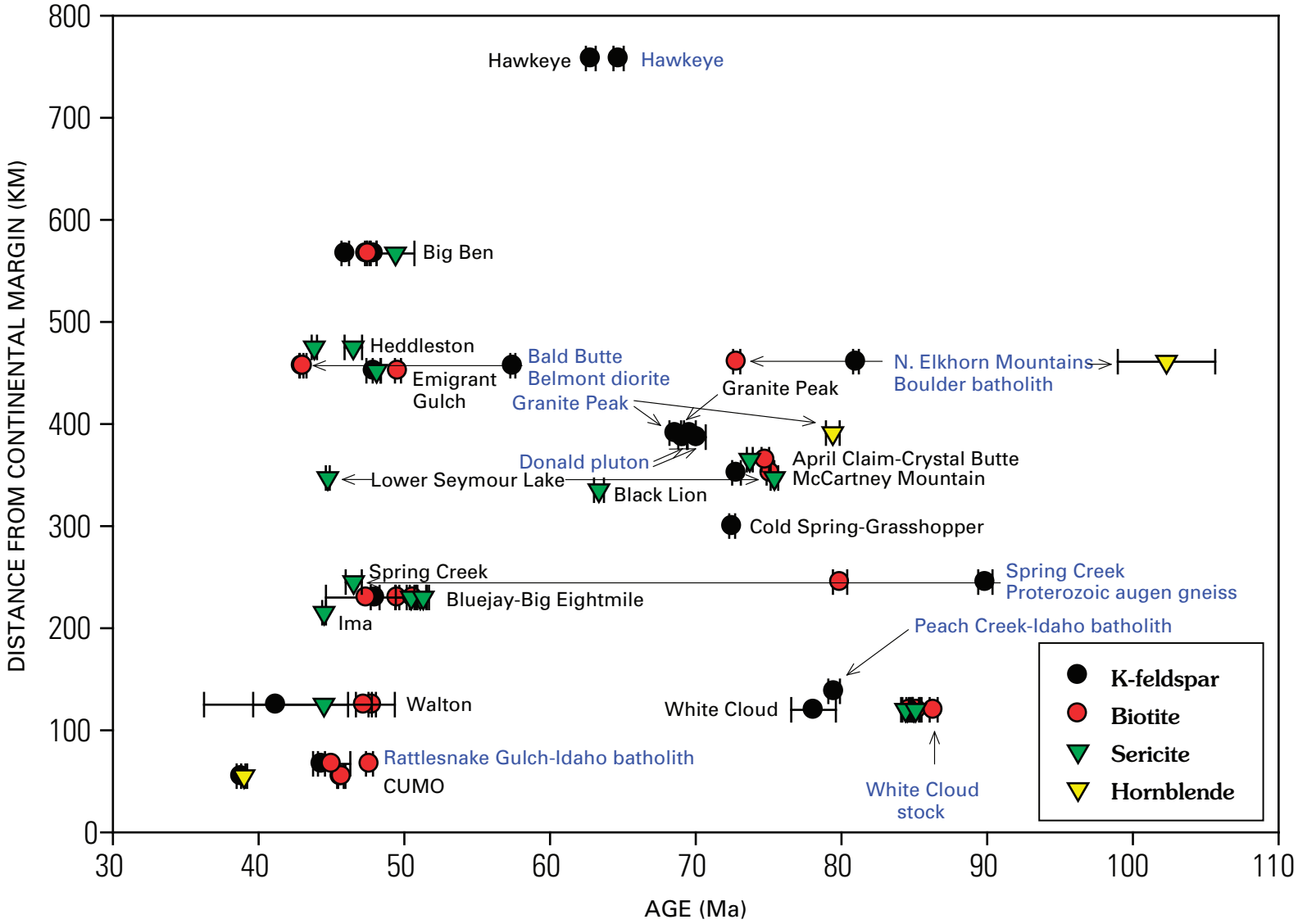

Figure 11. New ages for porphyry deposits as determined by $^{40}Ar/^{39}Ar$ geochronology versus approximate distance from pre-Cretaceous continental margin. Blue type indicates the age of igneous rock that hosts a porphyry deposit. Black type indicates the age of the porphyry intrusions or alteration related to one of the porphyry deposits.

cooling histories of 1.1 and 2.3 m.y. are in close proximity to each other and are outside known boundaries of the major batholiths. Mineral separates from rocks that host the Boulder batholith in the northern Elkhorn Mountains indicate an anomalously long cooling history of 29.5 m.y.

Whole-Rock Geochemistry and Radiogenic Isotopic Studies

Describing the host plutons helps to explain the origin of the metals as it reflects the character of the crystalline basement underlying the Idaho-Montana porphyry belt. To this end, detailed geochemical analyses were obtained on 62 samples at 29 sites of least altered Cretaceous and Tertiary igneous rocks and country rocks at and near many of the deposits. Although major-element and some minor-element data are published for the major batholiths and to a lesser extent for the Tertiary plutons, very little trace-element and REE (rare earth element) geochemistry has been reported. Similarly, radiogenic isotope abundances of strontium, neodymium, and lead were determined for a suite of selected samples. Together, these new geochemical data provide a refined perspective on the character of the Cretaceous and Tertiary plutons related to the porphyry deposits and will enhance understanding concerning the nature and origin of the porphyry belt (Taylor and others, 2004; C.D. Taylor and D.M. Unruh, unpub. data, 2003).

Whole-rock major-element variation (Harker) diagrams based on data recalculated to anhydrous compositions are displayed in figure 12. In general, most of the plots display coherent trends, suggesting that both the Cretaceous and Tertiary rocks have evolved by similar fractionation and (or) assimilation processes. The range in SiO_2, from ≈53 to 76 percent SiO_2, indicates that rock samples range from gabbro to granite-rhyolite composition. Above 68 percent SiO_2, Cretaceous rock compositions cluster from about 68 to 73 percent SiO_2, reflecting their predominantly tonalitic to granodioritic compositions. Samples with higher SiO_2 values are mostly Tertiary and reflect their more evolved compositions. Differences in the relative enrichments and depletions of major elements between the Cretaceous and Tertiary rocks are distinctive. Cretaceous rocks are enriched in Al_2O_3, CaO, and MnO, and depleted in K_2O and TiO_2 compared to Tertiary rocks. $FeTO_3$, MgO, and P_2O_5 abundances in the Cretaceous and Tertiary rocks are indistinguishable. Na_2O and Zr abundances show no consistent variation relative to SiO_2 variation. Loss on ignition (LOI) provides a useful proxy for the alteration intensity of a rock; data points >2 percent LOI indicate samples that are from within the alteration haloes of the porphyry deposits. The higher LOI values of Tertiary rocks suggest that those rocks are more likely to be altered, or alternatively that they intrinsically have a higher magmatic volatile content. The smooth decrease in abundance of Al_2O_3, $FeTO_3$, MgO, CaO, TiO_2, P_2O_5, and MnO, as well as the increase in K_2O with increasing SiO_2 for both Cretaceous and Tertiary rocks, is characteristic of normal calc-alkaline fractionation processes.

Plots of chondrite-normalized REE data for Cretaceous batholiths and plutons related to the porphyry deposits are in figure 13. REE data for Tertiary plutons and dikes in the southwestern and central parts of the porphyry belt are shown in figure 14*A*, and those in the northeastern part in figure 14*B*. REE patterns of basic and intermediate rocks are not considered here. The shape of REE patterns of the Cretaceous plutons is significantly different from that of most of the Tertiary intrusions. In general, the Cretaceous rocks exhibit moderately negative sloping light REE (LREE) profiles (starting at abundances 60–250 times chondrites), they include minor to no negative Eu anomalies, and they have gently negatively sloping heavy REE (HREE) abundances (2–20 times chondrites). In contrast, REE profiles of Tertiary igneous rocks in the southwestern and central portions of the porphyry belt (fig. 14*A*) display weak to moderately well developed negative Eu anomalies. Light REE abundances are 50–200 times chondrite, whereas HREE abundances are 2–20 times chondrite. With the exception of the negative Eu anomalies characteristic of the Tertiary samples, the overall shapes of the REE patterns are very similar, as are their REE abundances. A possible interpretation is that both the Cretaceous and the Tertiary samples are derived from the same source material but are melting under slightly different conditions. Negative Eu anomalies may indicate plagioclase retention in the source prior to extraction of the Tertiary melts or plagioclase fractionation during solidification. The comparatively flat and somewhat elevated HREE profiles (with respect to chondrites) suggest that both Cretaceous and Tertiary melts experienced no HREE fractionation resulting from either retention of HREE-bearing phases in the source region or removal by crystal settling during solidification.

Tertiary plutons and dikes in the northeastern part of the porphyry belt (fig. 14*B*) have REE patterns slightly different from those for plutons in the southwestern part of the belt. Most noticeably, the northeastern plutons have moderately negative slopes, with slight or no Eu anomalies, like the Cretaceous rocks. Reasons for the differences exhibited by these Tertiary rocks, specifically those from the Heddleston, Emigrant Gulch, and Big Ben deposits, are unclear. However, these patterns may reflect melting of fundamentally different Archean and Paleoproterozoic basement rocks that underlie these deposits outside the boundaries of the Great Falls tectonic zone (fig. 10). Possible differences in the basement blocks include basic geochemical differences in the disparate crustal blocks, melting of source rocks at shallower levels in the crust where garnet remains in the residuum, and (or) melting of rocks that did not undergo metasomatic changes resulting from the Paleoproterozoic compression and orogenesis.

Sr-Nd-Pb radiogenic isotopic data from a subset of the samples from the Headwaters Province project area (fig. 15) provide a powerful tool to evaluate plutonic evolution. Radiogenic isotopes serve as tracers of the original material

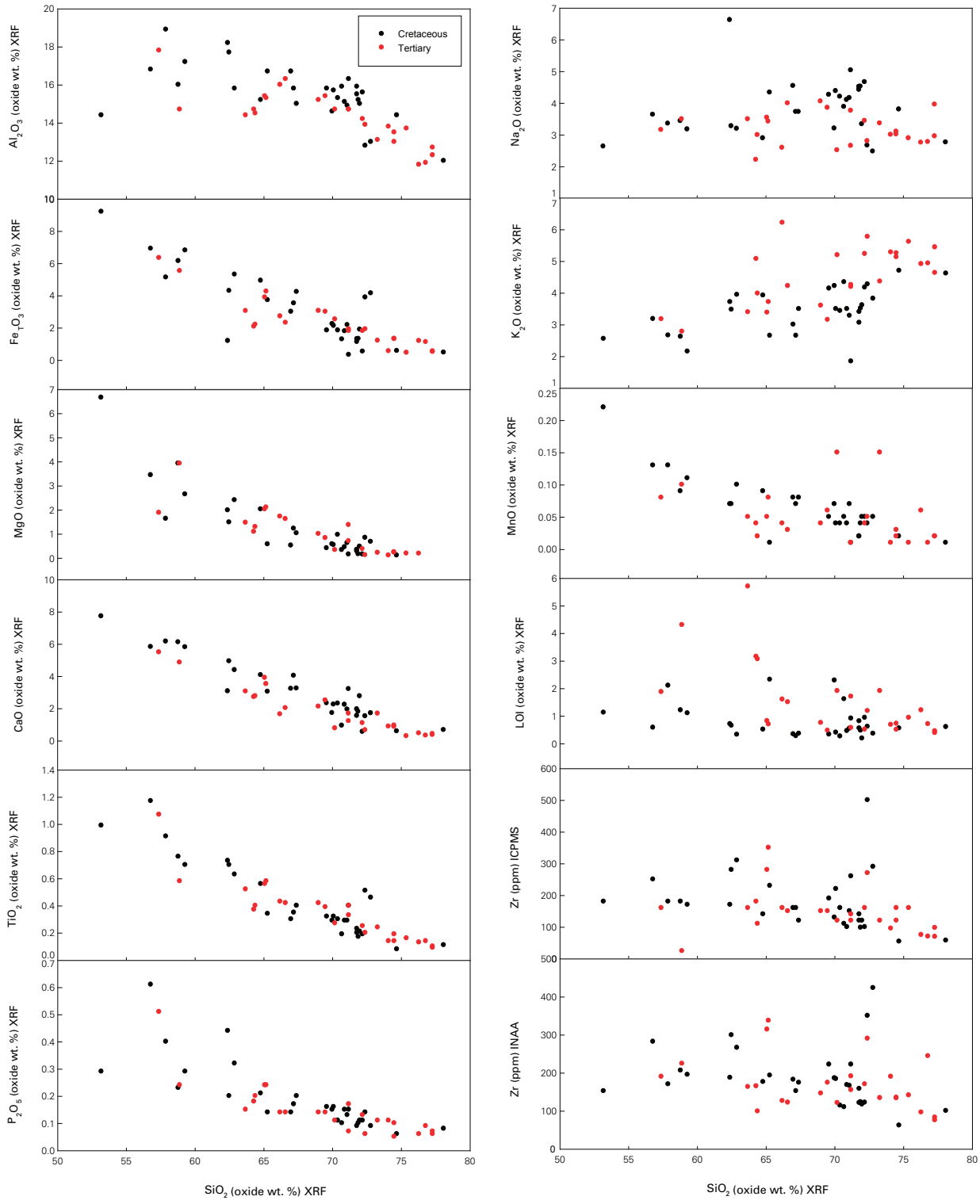

Figure 12. New whole-rock geochemical data for intrusive porphyry bodies at mineral deposits of Idaho-Montana porphyry belt. INAA, instrumental neutron activation analysis; ICPMS, inductively coupled plasma–mass spectrometry; XRF, X-ray fluorescence.

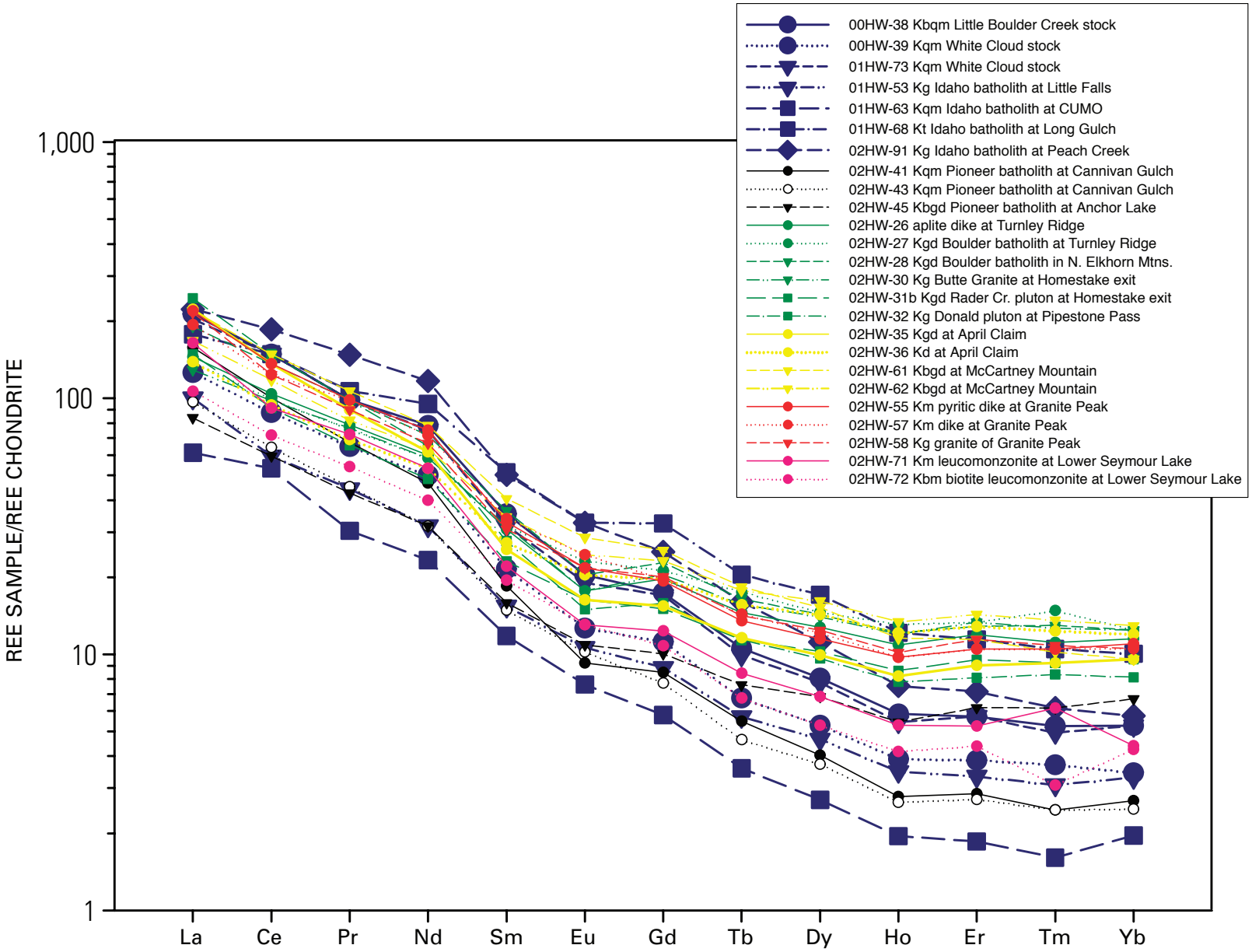

Figure 13. Chondrite-normalized rare earth element plots for Cretaceous porphyry intrusions and Cretaceous batholithic rocks of Idaho-Montana porphyry belt. Numbers are field numbers. K, Cretaceous; bqm, biotite quartz monzonite; qm, quartz monzonite; g, granite; t, tonalite; bgd, biotite granodiorite; gd, granodiorite; d, diorite; m, leucomonzonite; bm, biotite leucomonzonite.

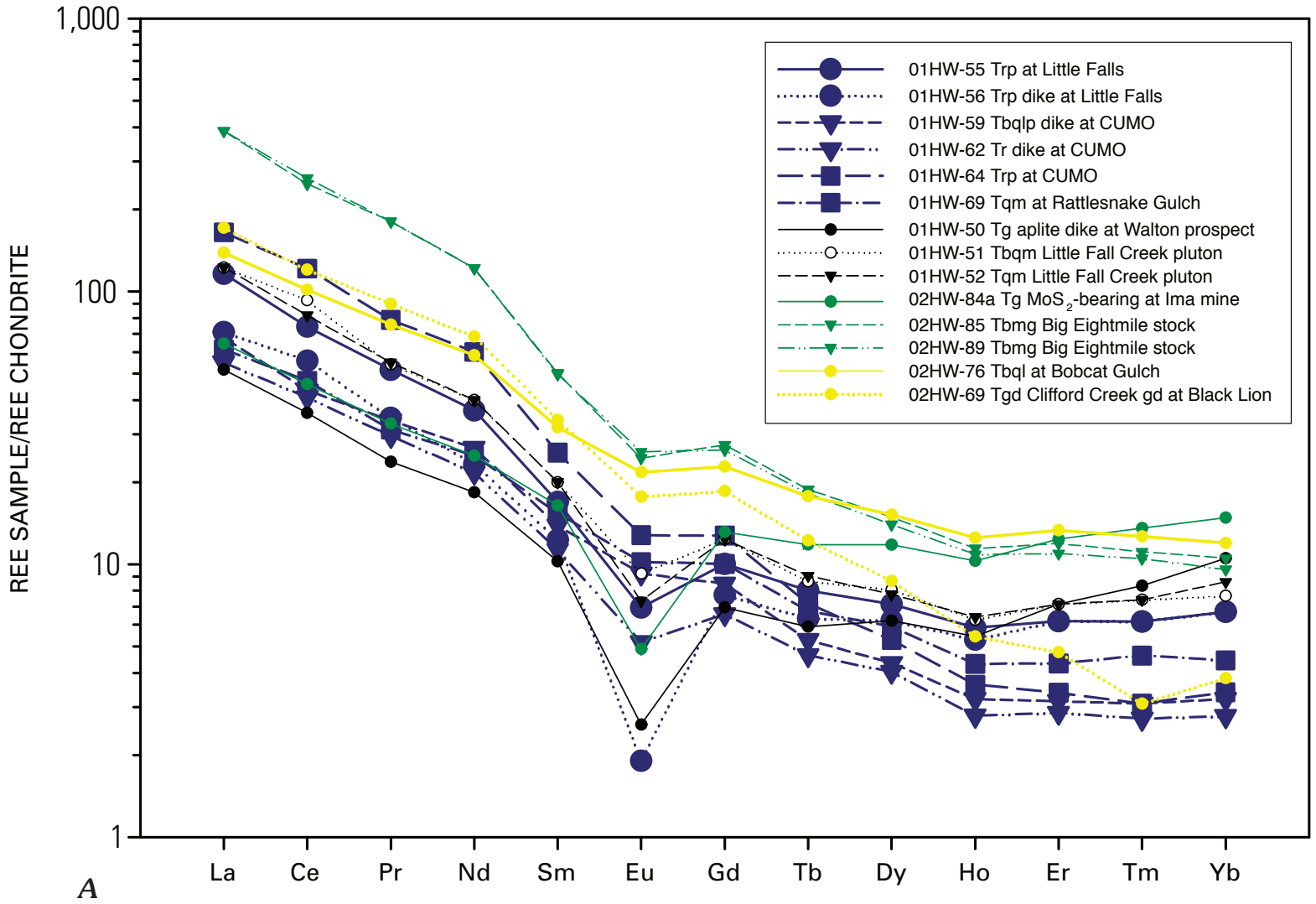

Figure 14. Chondrite-normalized rare earth element plots of Eocene porphyry intrusions and Cretaceous batholithic rocks. *A*, Intrusions in southwestern and central part of Idaho-Montana porphyry belt. Numbers are field numbers. T, Tertiary; rp, rhyolite porphyry; bqlp, biotite quartz latite porphyry; r, rhyolite; qm, quartz monzonite; g, granite; bqm, biotite quartz monzonite; qm, quartz monzonite; bmg, biotite monzogranite; bql, biotite quartz latite; gd, granodiorite.

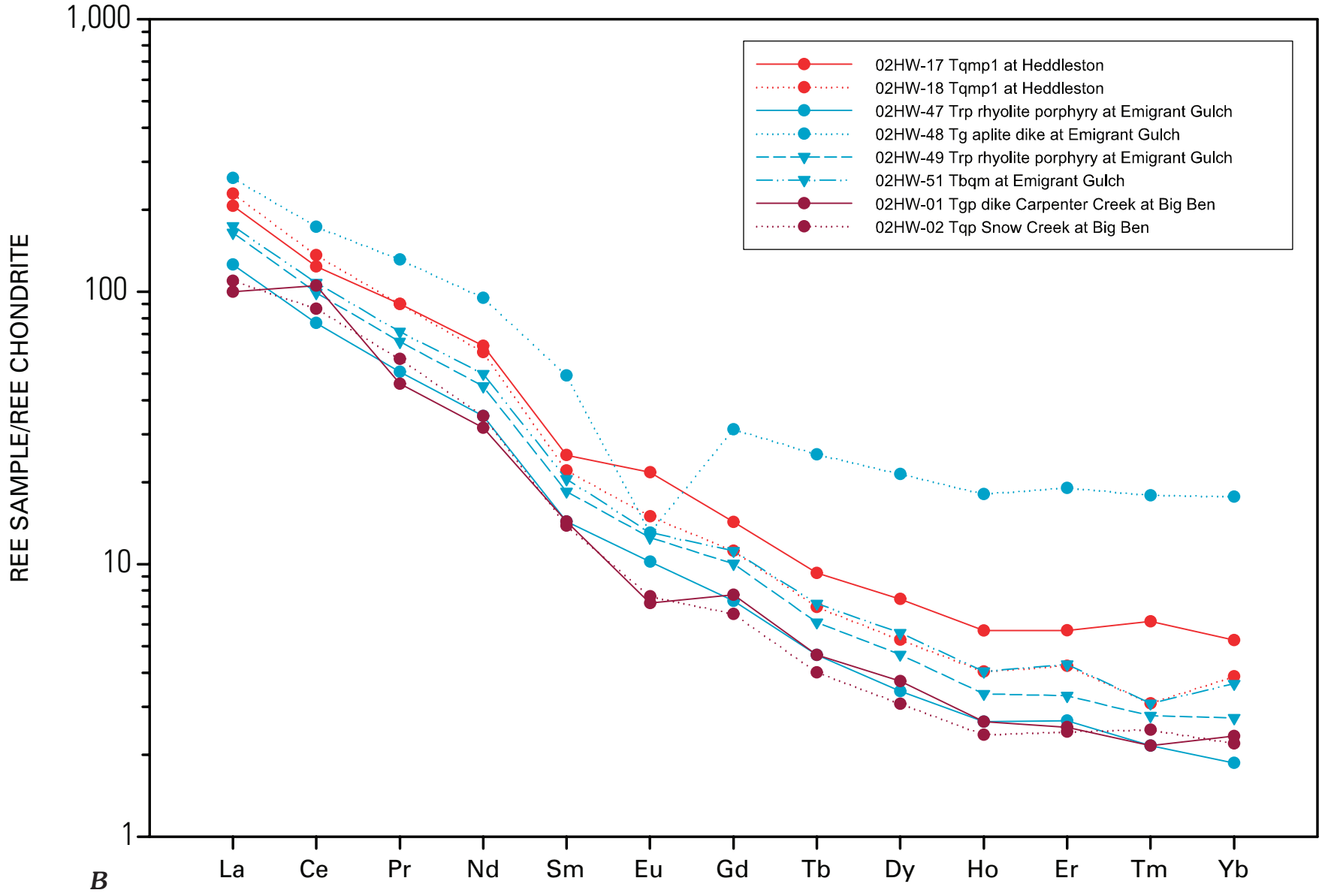

Figure 14—Continued. Chondrite-normalized rare earth element plots of Eocene porphyry intrusions and Cretaceous batholithic rocks. *B*, Intrusions in northeastern part of Idaho-Montana porphyry belt. Numbers are field numbers. T, Tertiary; qmp1, quartz monzonite porphyry #1; rp, rhyolite porphyry; g, granite; bqm, biotite quartz monzonite; gp, granite porphyry; qp, quartz porphyry.

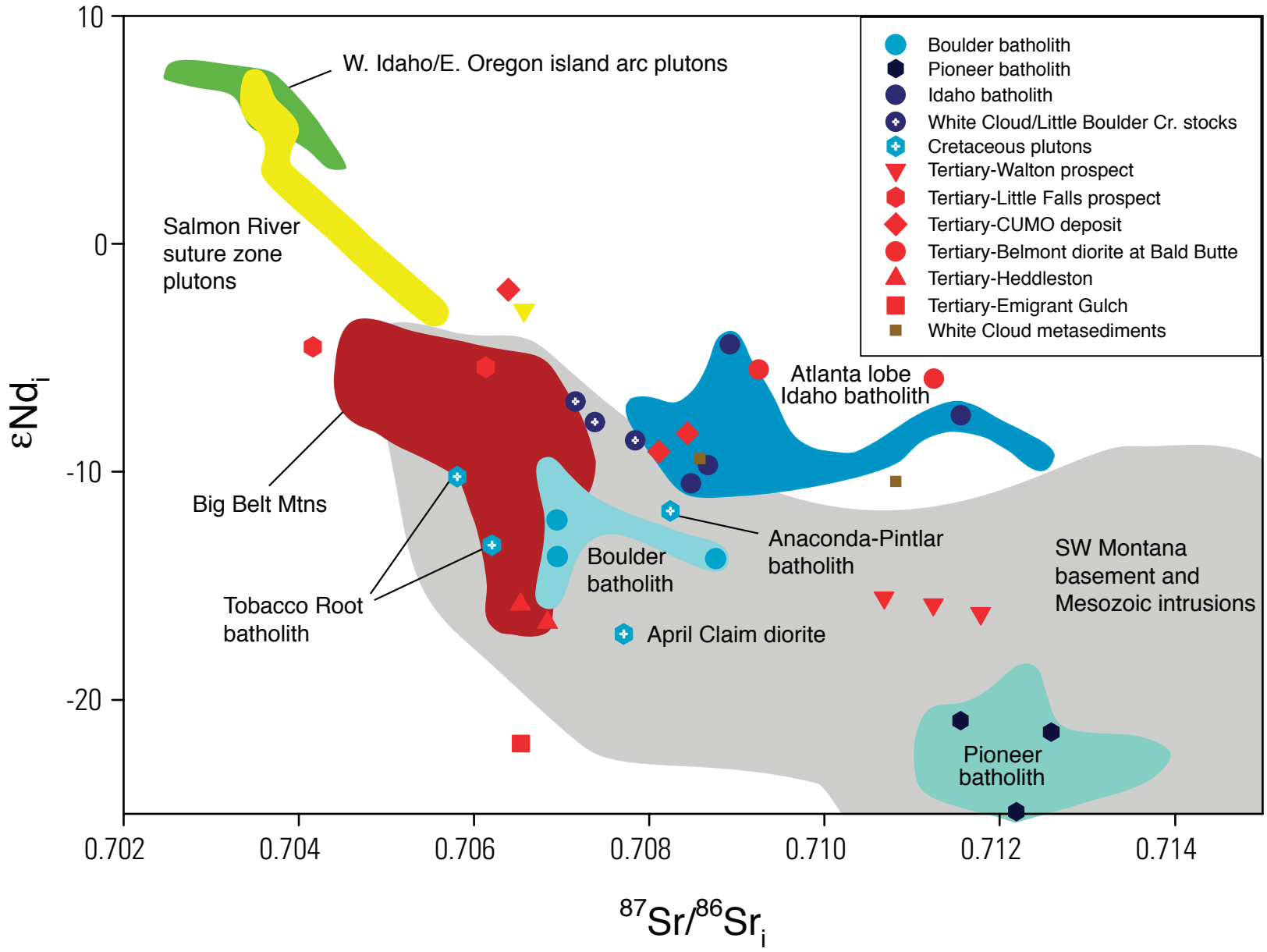

Figure 15. Plot of strontium-neodymium (initial) isotopic values for porphyry intrusions and Cretaceous batholithic rocks from Idaho-Montana porphyry belt. New Sr-Nd analyses are shown as discrete points relative to a larger database (colored fields) of published and unpublished analyses (Big Belt Mountains: E.A. du Bray and D.M. Unruh, unpub. data, 2004; Idaho batholith, island arc plutons, and suture zone plutons: M.A. Kuntz, D.M. Unruh, and Karen Lund, unpub. data, 2001, and Karen Lund and D.M. Unruh, unpub. data, 2002; Boulder batholith: Karen Lund, J.M. O'Neill, and D.M. Unruh, unpub. data, 1999; southwest Montana: Gunn (1991); Pioneer batholith: Zen and others (1975); Arth and others (1986); Hammarstrom and others (1993, and unpub. data, 1992).

from which crustal rocks are derived. They provide insights into magma genesis and the nature and degree of subsequent magma contamination by assimilation of preexisting crustal rocks. Our data are limited, but they include isotopic abundances for the Idaho batholith in the vicinity of the Little Falls and CUMO deposits; Tertiary intrusions from Little Falls, CUMO, and Walton; and the White Cloud stock and the Paleozoic metasedimentary rocks it intruded (fig. 15). These data, compared with a larger database of published and unpublished analyses, provide the opportunity to evaluate basement compositions within the Idaho-Montana porphyry belt and to compare those trends to the isotopic character of the basement elsewhere in the project area.

A general and expected evolutionary trend of both neodymium and strontium towards more radiogenic or evolved from west to east reflects compositions that form a transition from oceanic to continental interior. Thus, the most unradiogenic (primitive) rocks (fig. 15) are from allochthonous island arc terranes west of the Salmon River suture where melting of oceanic crust produced magmas with relatively unradiogenic isotopic composition. Compared to rocks derived from the allochthonous terranes, all of the remaining analyses exhibit more radiogenic compositions typical of continental granitic rocks (Faure, 1986). Therefore, rocks of the Idaho and Boulder batholiths and those of the Big Belt Mountains, which are thought to be derived primarily by relatively deep melting of old, radiogenic cratonic crust (Armstrong and others, 1977), have more evolved compositions (fig. 15).

Another, lesser trend (fig. 15) may enhance our understanding of the genesis of the Cretaceous and Tertiary rocks. Isotopic data for rocks from the Idaho and Boulder batholiths and the Big Belt Mountains define discrete clusters that suggest distinct source region differences. These data depict a weakly defined trend of progressively less radiogenic strontium and to a lesser extent progressively more radiogenic neodymium with distance from the continental margin. Previous strontium isotope studies (Armstrong and others, 1977) noted that the Idaho batholith is more radiogenic than the Boulder batholith and credited a possibly higher proportion of melting and mixing of Mesoproterozoic sediments into the Idaho batholith parent magmas. Alternatively, the Boulder batholith and Big Belt Mountains plutons may reflect less radiogenic Archean sources in the Medicine Hat and Wyoming Archean crustal blocks compared to the source chemistry of the Paleoproterozoic Wallace terrane, which probably was a source for the Idaho batholith magmas.

Conclusions

New mineralization ages, whole-rock geochemical data, and radiogenic isotopic data represent the most extensive collection of constraints available with which to evaluate the timing of emplacement, cooling history, and mineralization associated with the Idaho-Montana porphyry belt. These new data suggest that the location and type of mineral deposits in the Headwaters Province are less controlled by the composition, age, or emplacement depth (cooling conditions) of magmatic systems than by the composition and (or) structural character of the underlying basement.

SHRIMP U-Pb and $^{40}Ar/^{39}Ar$ Age Constraints for Relating Plutonism and Mineralization in the Boulder Batholith Region, Montana

By Karen Lund, John N. Aleinikoff, Michael J. Kunk, and Daniel M. Unruh

The composite Boulder batholith, Montana, hosts a variety of mineral deposit types including important silver-rich polymetallic quartz vein districts in the northern part of the batholith and the giant Butte deposit (porphyry copper-molybdenum pre-Main Stage system and crosscutting copper-rich Main Stage vein system) in the southern part of the batholith (Smedes and others, 1973; fig. 16; table 5). Limited dating studies previously identified ambiguous relationships among igneous and mineralizing events (see discussion in Lund and others, 2002). Mineralizing hydrothermal fluids for these types of deposits and magma for quartz porphyry dikes at Butte have all been considered to be late-stage differentiates of the Boulder batholith.

Geochronologic Results

To resolve ages of magmatism and mineralization, single age domains within zircon crystals from plutonic rock samples were dated using the Sensitive High Resolution Ion Microprobe (SHRIMP), and $^{40}Ar/^{39}Ar$ geochronology was used to date white mica, biotite, and potassium feldspar from mineralized samples (table 6; figs. 17, 18).

Outlying 74.4 Ma silver-rich polymetallic quartz veins (samples 98BL010, 98BL011, 98BL016, fig. 18) of the Basin and Boulder mining districts probably are directly related to the 74.5 Ma Butte Granite (sample 98BL004, fig. 17), having formed less than a million years after crystallization age of the hosting pluton. At Butte, east-west-trending quartz porphyry dikes (named Steward-type) cut the Butte Granite and crystallized from 66 to 65 Ma (samples 98BL006 and 98BL013, fig. 17); and the copper-molybdenum porphyry system formed at about 63.6 Ma (sample 98BL014B, fig. 18). Thus, quartz porphyry dikes and Butte pre-Main Stage deposits are parts of a 66–64 Ma magmatic/mineralization system unrelated to emplacement of the Boulder batholith (table 6). The age of the crosscutting Main Stage veins may be about 61 Ma as originally

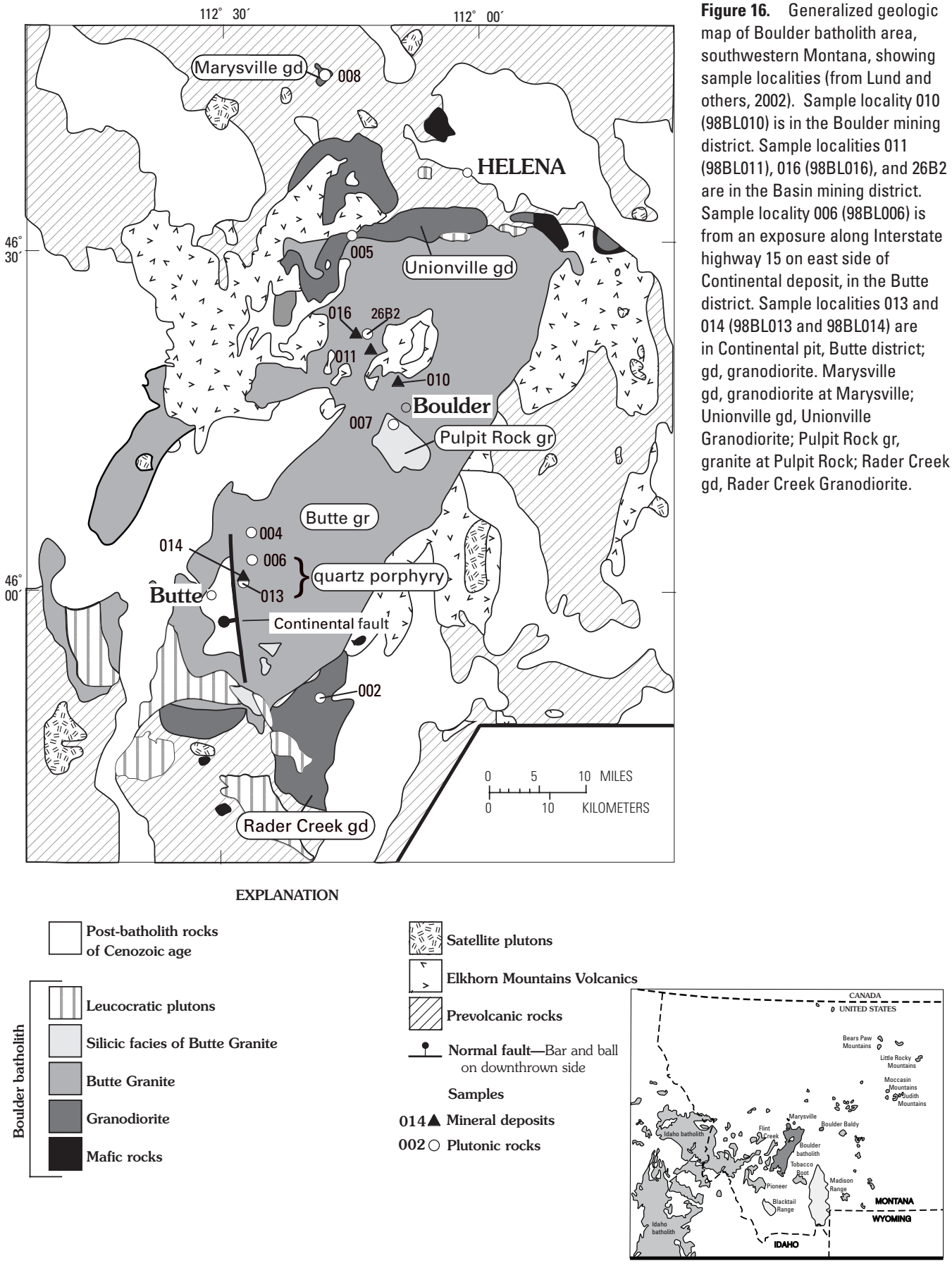

Figure 16. Generalized geologic map of Boulder batholith area, southwestern Montana, showing sample localities (from Lund and others, 2002). Sample locality 010 (98BL010) is in the Boulder mining district. Sample localities 011 (98BL011), 016 (98BL016), and 26B2 are in the Basin mining district. Sample locality 006 (98BL006) is from an exposure along Interstate highway 15 on east side of Continental deposit, in the Butte district. Sample localities 013 and 014 (98BL013 and 98BL014) are in Continental pit, Butte district; gd, granodiorite. Marysville gd, granodiorite at Marysville; Unionville gd, Unionville Granodiorite; Pulpit Rock gr, granite at Pulpit Rock; Rader Creek gd, Rader Creek Granodiorite.

Table 5. Summary of mineral deposit characteristics for Boulder and Butte mining districts.

Deposit type	Commodities	Vein type	Sulfide mineralogy	Alteration zones
Basin and Boulder mining districts				
Silver-rich quartz veins	Ag, Pb, Zn, Cu	1 cm anastomosing quartz veinlets to 15 m quartz veins. Overall tabular geometry with E.-W. trend. Rare open-space textures. Several episodes of brecciation and sealing with vein material. Pink carbonate veinlets are late stage and cross-cutting.	Ubiquitous pyrite ± chalcopyrite, galena, arsenopyrite, sphalerite, and tetrahedrite. Reported stibnite, bornite, cosalite, enargite, chalcocite, ruby silver, boulangerite, bournonite, and albandite.[1]	Sericite zone nearest vein several centimeters wide. Argillic zones as much as several meters wide. Propylitic zones as much as several decimeters wide.
Butte				
Pre-Main Stage: Porphyry copper and molybdenum porphyry systems	Cu, Mo	Biotite breccia dikes: biotite and potassium feldspar matrix with breccia fragments.[2] "Early dark mica" veinlets:1- to 5-mm- wide veinlets of quartz, potassium feldspar, muscovite, and biotite.[3] Quartz-molybdenite veinlets: form main part of deposit.[4]	"Early dark mica" veinlets: chalcopyrite, pyrite, and magnetite. Quartz-molybdenite veinlets: molybdenite.	Porphyry copper: complex overlapping potassium-silicate alteration systems.[5] Porphyry molybdenum: biotitic alteration dome above molybdenum mineralization.[2,3]
Main Stage: Copper-rich veins in center of district gradational to silver-rich veins in periphery	Cu, Zn, Pb, Ag, Mn, Au	2- to 10-m-wide veins; some are as wide as 30 m.[4]	Central deposits: Pyrite± chalcocite, digenite, covellite, and enargite. Chalcocite and enargite with bornite at higher levels. Chalcopyrite more common in outer and deeper parts.[4] Peripheral deposits: silver-rich zinc mineralization, sphalerite, galena, tennantite, tetrahedrite.	Central deposits: overlapping acid-sulfate alteration zones.[5] Peripheral deposits: sericitic zones close to veins and outer intense argillic assemblages with manganese carbonate gangue.[4]

[1]Becraft and others (1963) and Ruppel (1963).
[2]Miller (1973).
[3]Brimhall (1973); Brimhall and others (1984).
[4]Meyer and others (1968).
[5]Sales and Meyer (1948); Brimhall (1973); Roberts (1973); and Brimhall and others (1984).

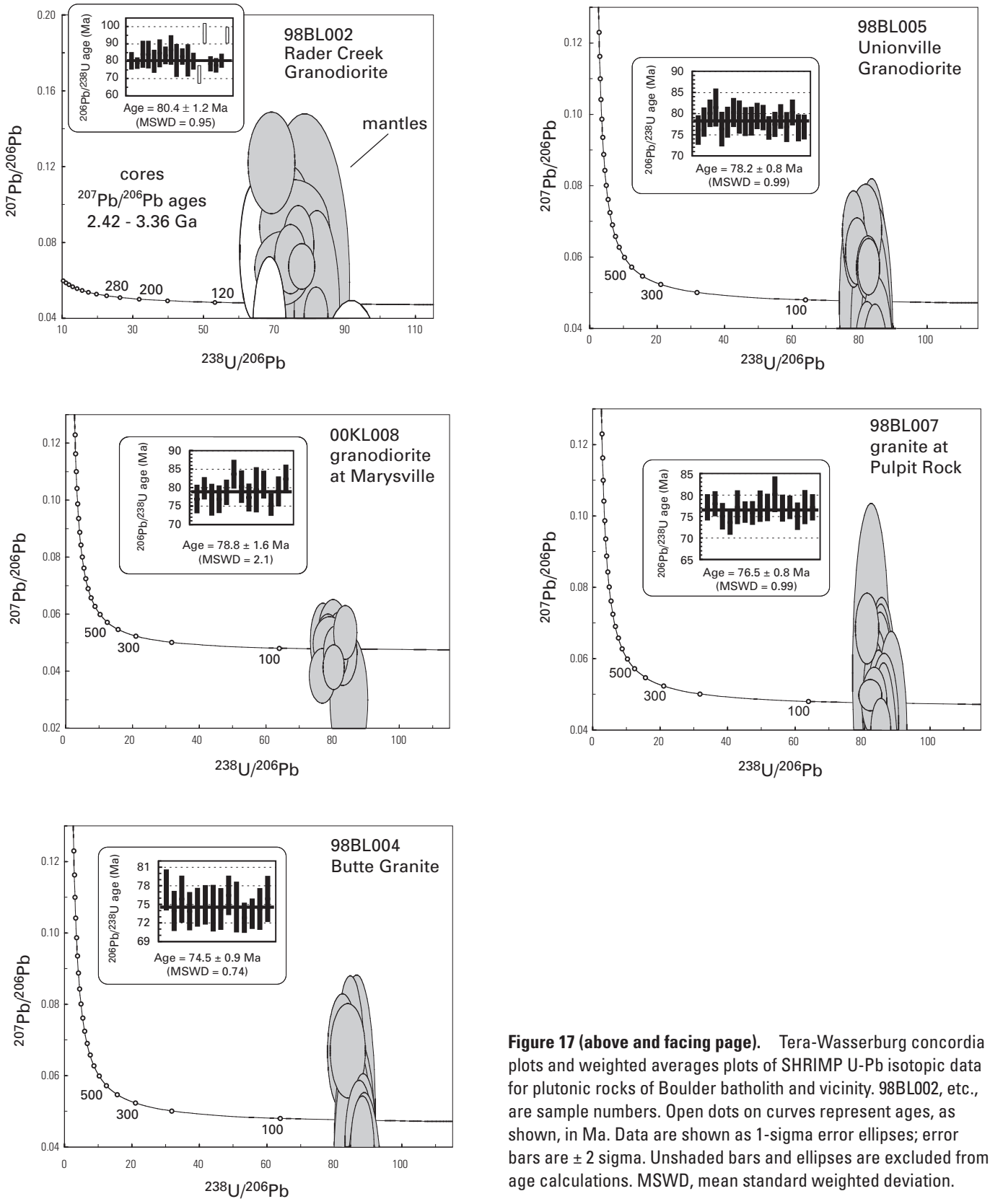

Figure 17 (above and facing page). Tera-Wasserburg concordia plots and weighted averages plots of SHRIMP U-Pb isotopic data for plutonic rocks of Boulder batholith and vicinity. 98BL002, etc., are sample numbers. Open dots on curves represent ages, as shown, in Ma. Data are shown as 1-sigma error ellipses; error bars are ± 2 sigma. Unshaded bars and ellipses are excluded from age calculations. MSWD, mean standard weighted deviation.

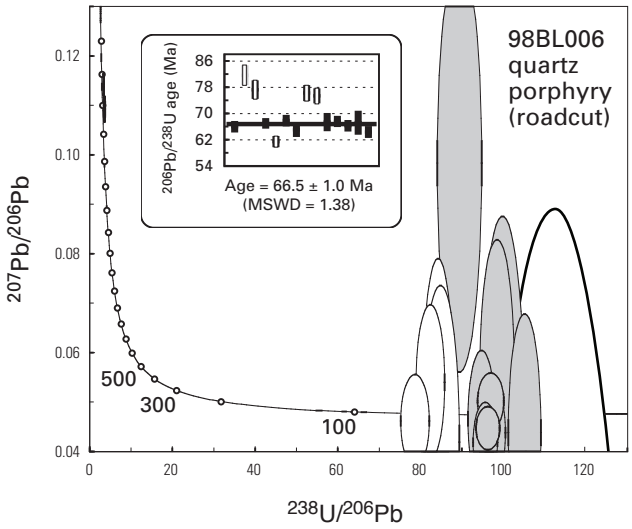
98BL006
quartz
porphyry
(roadcut)
Age = 66.5 ± 1.0 Ma
(MSWD = 1.38)
206Pb/238U age (Ma)
207Pb/206Pb
238U/206Pb
500
300
100

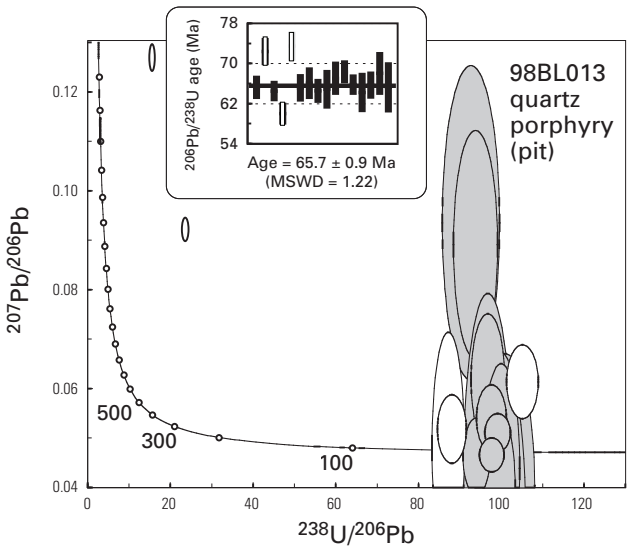
98BL013
quartz
porphyry
(pit)
Age = 65.7 ± 0.9 Ma
(MSWD = 1.22)
206Pb/238U age (Ma)
207Pb/206Pb
238U/206Pb
500
300
100

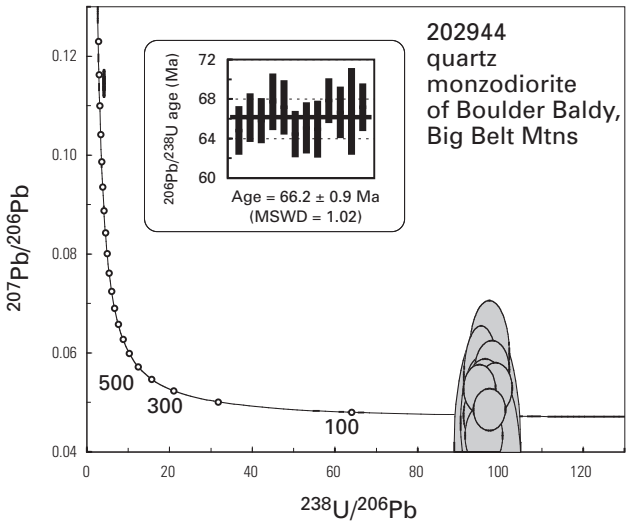
202944
quartz
monzodiorite
of Boulder Baldy,
Big Belt Mtns
Age = 66.2 ± 0.9 Ma
(MSWD = 1.02)
206Pb/238U age (Ma)
207Pb/206Pb
238U/206Pb
500
300
100

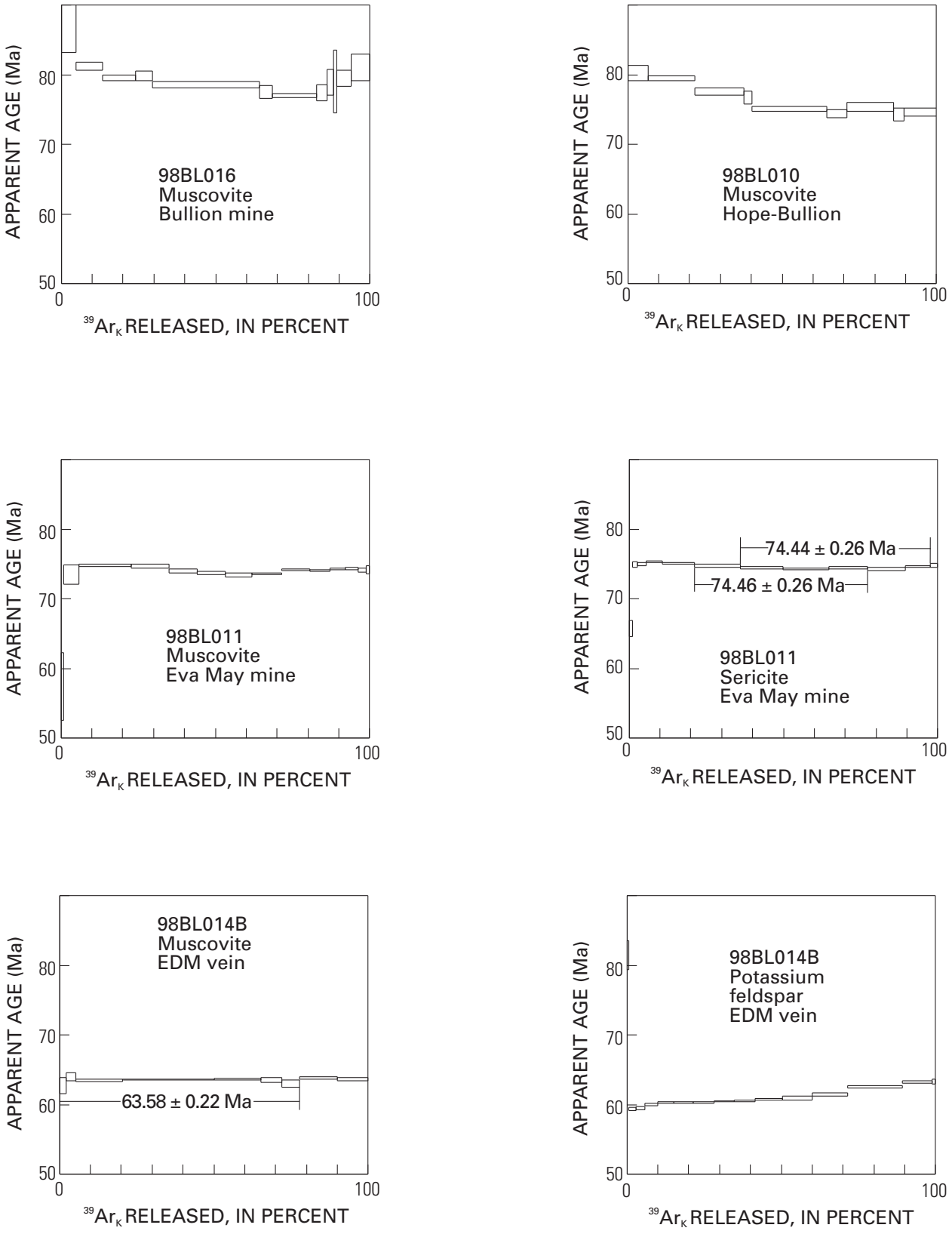

Figure 18. $^{40}Ar/^{39}Ar$ age spectra for mineralized and altered samples. Rectangles in age spectra depict ± 2 sigma uncertainties.

Table 6. Summary of isotopic data for Boulder and Butte mining districts.
[Error estimates for U-Pb data are ±2 sigma, those for $^{40}Ar/^{39}Ar$ data are ±1 sigma]

Sample No.	Unit or mine	Mineral[1]	Dating method[2]	Age (Ma)
		U-Pb data		
Boulder batholith:				
98BL002	Rader Creek Granodiorite	zrn	SHRIMP	80.4 ± 1.2
98BL005	Unionville Granodiorite	zrn	SHRIMP	78.2 ± 0.8
00KL008	Granodiorite at Marysville	zrn	SHRIMP	78.8 ± 1.6
98BL007	Granite at Pulpit Rock	zrn	SHRIMP	76.5 ± 0.8
			TIMS	74.7 ± 1.2
26B2	Granophyric phase of Butte Granite.	zrn	TIMS	74.5 ± 0.7
98BL004	Butte Granite	zrn	SHRIMP	74.5 ± 0.9
Quartz porphyry dikes at Butte:				
98BL006	Steward-type quartz porphyry dike (I-15 roadcut).	zrn	SHRIMP	66.5 ± 1.0
			TIMS (1 grain)	71.2 ± 0.3
98BL013	Steward-type quartz porphyry dike (Continental pit).	zrn	SHRIMP	65.7 ± 0.9
			TIMS (1 grain)	65.9 ± 0.8
Regional magmatic event related to quartz porphyry dikes:				
202994	Quartz monzodiorite of Boulder Baldy.	zrn	SHRIMP	66.2 ± 0.9
		$^{40}Ar/^{39}Ar$ data		
Mineralization in Boulder and Basin mining districts:				
98BL016	Bullion mine	mu	Minimum	77.0 ± 0.4
98BL010	Hope-Bullion mine	mu	Isochron	74.4 ± 1.2
98BL011	Eva May mine	mu	Isochron	73.9 ± 0.7
98BL011	Eva May mine	ser	Plateau	74.4 ± 0.3
			Isochron	74.6 ± 0.3
Copper-molybdenum porphyry mineralization in Butte mining district:				
98BL014A	Biotite breccia dike	bt	Total fusion	63.6 ± 0.2
98BL014B	"Early dark mica" vein	mu	Plateau	63.6 ± 0.2
		bt	Total fusion	63.6 ± 0.2
98BL014B	"Early dark mica" vein	ks	Maximum	63.3 ± 0.2
			Minimum	59.4 ±0.2

[1]Mineral abbreviations: zrn, zircon; mu, muscovite; ser, sericite; bt, biotite; ks, potassium feldspar.
[2]SHRIMP, Super high resolution ion microprobe. TIMS, Thermal ionization mass spectrometry.

reported (Woakes, 1960), but the veins are only known to be older than the ≈50 Ma intrusions of the Eocene Lowland Creek Volcanics.

Interpretations

Resolution of the age and probable magmatic source of the Butte pre-Main Stage porphyry copper-molybdenum system and of the silver-rich polymetallic quartz vein systems in the northern part of the Boulder batholith indicates that these deposits formed from two discrete periods of hydrothermal mineralization related to two discrete magmatic events. The approximately 64 Ma porphyry copper-molybdenum systems at Butte and porphyry gold mineralization at Miller Mountain (Lang and others, 2000) are indicative of regionally important, ≈66 million year old, small plutonic and associated hydrothermal mineralizing systems that may be common in the Boulder batholith region, especially to the northeast (du Bray, 1995; Lund and others, 2002). Deposits at Butte and in the Boulder batholith overlie an important basement juncture between the Paleoproterozoic suture zone of the Great Falls tectonic zone and a multiple-times-reactivated Mesoproterozoic northwest-trending fracture system along the Lewis and Clark line, probably indicating metal-enriched basement and reactivated basement structural flaws.

Use Of Multiple Techniques

U-Pb zircon dating of plutonic rocks results in magma crystallization ages. This technique avoids problems resulting from slow cooling of plutonic systems that are inherent in the original K-Ar dates for both the Boulder batholith plutons and the quartz porphyry dikes. Our study documents the degree of inheritance of older zircon cores (fig. 19); inheritance probably caused conventional thermal ionization mass spectrometry U-Pb geochronologic methods to produce the inconclusive results identified by Martin and others (1999). Those results illustrate the importance of using single-grain SHRIMP U-Pb techniques, by which the complex genetic history of each grain can be carefully documented.

Alteration minerals were dated by $^{40}Ar/^{39}Ar$ geochronology for corroborating evidence of the age of mineralization relative to intrusion of the Boulder batholith and the Steward-type quartz porphyry dikes. Samples of silver-rich polymetallic quartz vein deposits in mining districts northwest of Boulder (fig. 16) were also analyzed by $^{40}Ar/^{39}Ar$ methods, for the first time, to determine their age relative to the age of emplacement of the Boulder batholith and of mineralization at Butte.

Impacts

Determination of ages for mineralization and magmatic systems demonstrated that porphyry copper-molybdenum and copper-vein deposits at Butte resulted from a different magmatic source than silver-vein deposits in the northern part of the batholith. The silver-rich polymetallic vein systems are related to fluid accumulations in cooling fractures at the roof of Late Cretaceous Butte Granite. The huge mineralizing systems at Butte are related to latest Cretaceous-Paleocene, shallowly emplaced, quartz-porphyry systems that can now be related on a regional basis to other magmatic systems of this age. This clarification of models for the two deposit systems allows exploration and topical studies of these deposits to be considerably more meaningful. The new temporal framework also more clearly defines the scale of the two deposit types. Specifically, the silver-rich polymetallic vein systems are relatively older and not genetically related to the magmatic source associated with younger porphyry copper-molybdenum systems at Butte. These conceptual breakthroughs yield better predictive models for (1) mineral resource exploration; (2) regional mineral resource potential, which is of interest to FLMA; (3) scale of natural environmental degradation, potentially associated with these deposits; and (4) the areal extent of metal contamination potentially resulting from metallic resource development as a function of mining techniques and deposit types.

Stratigraphy and Structure of Proterozoic Strata of Central Idaho

Much of the Headwaters Province is underlain by Proterozoic strata. In northern Idaho and western Montana, these units are the thick succession of the Mesoproterozoic Belt Supergroup. The south-central part of the Headwaters Province, east-central Idaho, is underlain by Mesoproterozoic strata whose internal stratigraphy is poorly understood. Their age and their stratigraphic relationships to the better known, nearby Belt Supergroup are likewise unknown. Additionally, vast areas of western and central Idaho (west-central Headwaters Province) are underlain by metamorphosed rocks about which little information on age, composition, or origin is available. Geologic mapping of west-central Idaho is complicated by difficulty of access and by the metamorphic grade of the area's stratified rocks. In the absence of age data, correlations are unreliable, and workers have universally accepted ages of Archean or Mesoproterozoic for rocks that underlie the area; Neoproterozoic strata, present along the rest of the Cordillera, were assumed to be absent (Stewart, 1991). Because so many regional questions exist about these rocks whose ages could range from about 2.5 to 0.5 Ga, the possible geologic settings in which the rocks formed and the possible predictions for associated mineral deposit types, scale of probable alteration systems, and regional buffering characteristics are very poorly defined. Many questions remain about much of this terrain.

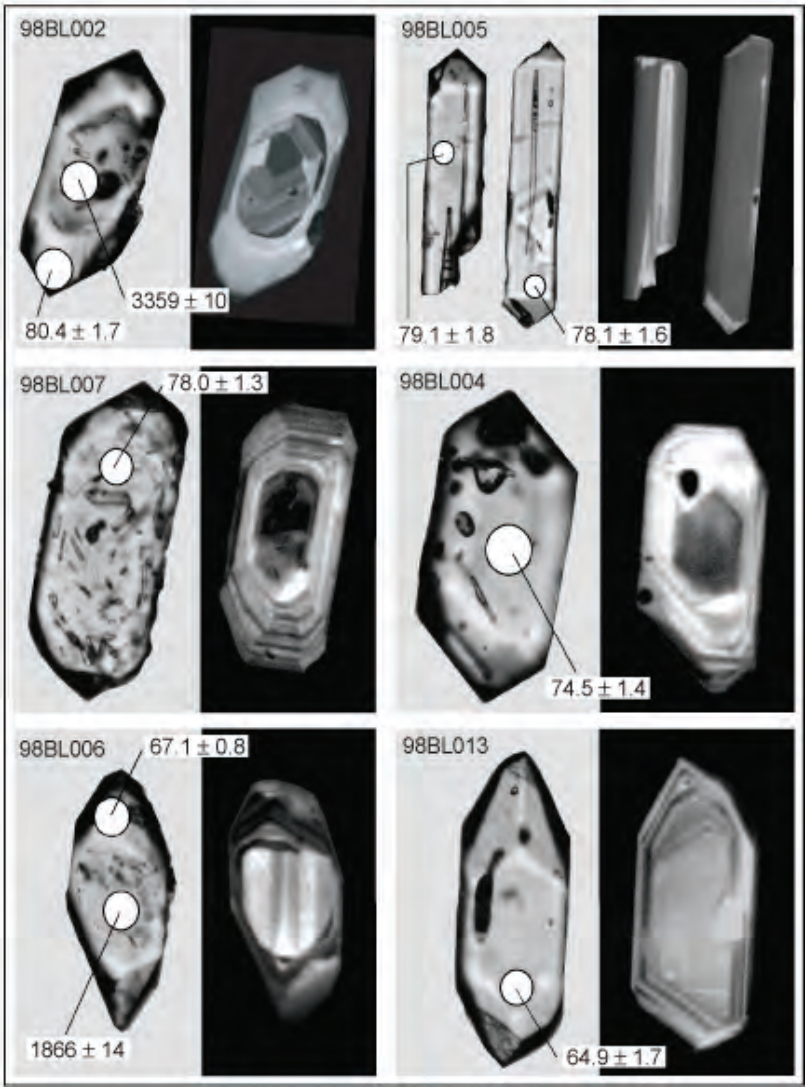

A

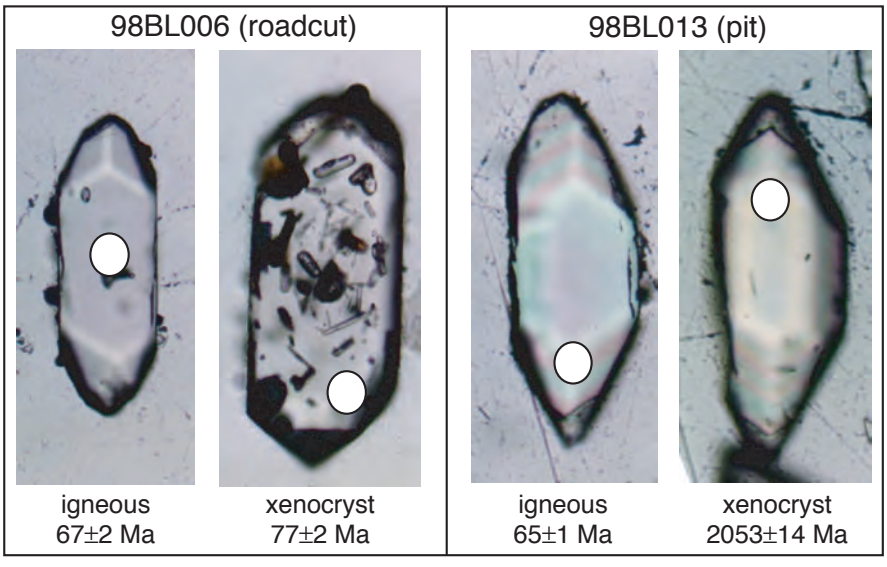

B

Figure 19. Transmitted light (left) and cathodoluminescence (right) image pairs for representative zircons from samples of granitic rocks dated as part of the Headwaters Province project. *A*, 98BL002 (Rader Creek Granodiorite), 98BL005 (Unionville Granodiorite), 98BL007 (granite at Pulpit Rock), 98BL004 (Butte Granite), 98BL006 and 98BL013 (Steward-type quartz porphyry). White circles show locations of ion microprobe analyses, in all cases about 25 micrometers in diameter. Ages are shown as ± 1 sigma uncertainties. Note rounded cores with incomplete oscillatory zoning that yield very old ages in samples 98BL002 and 98BL006. *B*, Xenocrystic zircon grains, which were incorporated into Steward-type quartz porphyry dikes (samples 98BL006 and 98BL013), illustrate the problem of zircon inheritance for conventional U-Pb dating. Zircon from sample 98BL006 is a Late Cretaceous xenocryst related to the Boulder batholith and is remarkably similar to the zircon shown in *A* from the granite at Pulpit Rock. Zircon from sample 98BL013 is an inherited grain of Proterozoic age.

Topical studies of Proterozoic rocks in the Headwaters Province study area focused on specific areas and topics regarding Proterozoic rocks of western and central Idaho. Geologic mapping combined with detailed stratigraphic and structural studies in east-central Idaho resulted in unraveling the stratigraphy and structural geometry of Mesoproterozoic strata there. (See Evans, Tysdal, and Lund, this page.) Advances in the understanding of regional stratigraphic and structural setting set the framework for a detailed topical study of the structural setting of the Blackbird gold-cobalt-copper deposit, east-central Idaho. This study resulted in limiting the strata that host Blackbird-type deposits and in documenting origin of metamorphic and transpositional features of the deposits. (See Lund, Tysdal, Evans, and Kunk, p. 50.) Stratigraphic, structural, and dating studies resulted in recognition of an important belt of Neoproterozoic rocks crossing the area (Lund, Aleinikoff, and Evans, p. 55). With respect to Neoproterozoic rocks worldwide, recent studies led some to suggest that, at least twice, the entire surface of the Earth was frozen (Snowball Earth), thus producing simultaneous worldwide glacial deposits (Hoffman and others, 1998). Lund, Aleinikoff, and others (2003) firmly dated one of those two events using rocks from central Idaho, but also questioned whether the glaciation was truly synchronous on a global scale.

Mesoproterozoic Strata of East-Central Idaho

By Karl V. Evans, Russell G. Tysdal, and Karen Lund

During the past decade, our understanding and ability to correlate Proterozoic rocks across central Idaho have increased considerably (fig. 2, the reduced version of USGS Map I–2765). Deciphering unknown structure and unknown stratigraphy is always an iterative process, as these two aspects are interdependent. Detailed studies, especially by Tysdal (2000a, 2002; compare Ruppel and Lopez, 1988) in the well-exposed Lemhi Range have both built on and revised previous mapping of Mesoproterozoic strata and provided a speculative template for evaluation of the less accessible areas of central Idaho. In addition, Lund, Tysdal, and others (2003) have firmly established the presence of Neoproterozoic glacial and volcanic rocks across a large part of the Frank Church–River of No Return Wilderness (Evans and Green, 2003; Lund, 2004).

Unlike the results of most previous studies which assumed little or no tectonic transport of rocks in the area (Armstrong, 1975; Ruppel, 1978), the Headwaters Province study indicates that the structural geology of central Idaho is characterized by several major northwest-striking Mesozoic thrust faults. These faults juxtapose blocks of differing stratigraphy and (in places) metamorphic grade. Further work remains to establish the full continuity of these thrust faults, especially in the least accessible areas, but the thrust faults are now adequately documented and form an integral connecting link between the well-known parts of the Cordilleran thrust belt in northern Idaho and those in southeastern Idaho, as was conceptually hypothesized by Skipp (1987) based on much less information. Complicating the interpretation of structure, there is evidence that, prior to the dominant Mesozoic folding and thrusting, Mesoproterozoic deformation, metamorphism, and probably migmatization took place at least locally. Furthermore, Cenozoic faulting has superimposed large-magnitude extension on the previously contractional orogen (Janecke and others, 1998).

The metasedimentary Proterozoic rocks of central Idaho have long been considered to be temporal correlates of the Mesoproterozoic Belt Supergroup of Montana and northern Idaho. Determination of the time span necessary for deposition of the Belt strata was for many years a persistent problem; early isotopic dating, for instance, suggested a span of about 600 m.y. (Obradovich and Peterman, 1968). Fortunately, improved isotopic techniques combined with recognition of volcanic units within the Belt have greatly improved our understanding of Mesoproterozoic geochronology in Idaho and Montana. Evans and others (2000) used SHRIMP U-Pb techniques to analyze zircons from several stratigraphic levels throughout the Belt sequence. Their results, combined with recent studies in Canada (for example, Anderson and Davis, 1995), have established that nearly all of the Belt Supergroup was deposited in about 70 m.y. (1,470 to 1,400 Ma).

Within the Headwaters Province project area, considerable new mapping indicates that some previous stratigraphic assignments and correlations of Mesoproterozoic strata required revision. Table 7 summarizes the historical development of Mesoproterozoic stratigraphic terminology in central Idaho, and presents the results compiled and used in the present study. Perhaps most significantly, the formerly widespread "Yellowjacket Formation" is restricted to its original definition (Ross, 1934). Other units to which the name Yellowjacket had been extended (Ruppel, 1975; Ruppel and Lopez, 1988; Evans, 1998) are now considered to be parts of the Lemhi Group (Tysdal, 2000b). In this light, the Yellowjacket strata are now everywhere separated from the Lemhi Group by faults, thereby leaving correlations between the two stratigraphic packages unresolved. Furthermore, the stratigraphically controlled gold-bearing cobalt-copper deposits of the Blackbird mine and Idaho cobalt belt (Nash and Hahn, 1989) are now known to occur mostly within the banded siltite member of the Apple Creek Formation. This member pinches out in the Lemhi Range to the southeast of Blackbird, making it unlikely that undiscovered cobalt deposits are present in that area. Additional work is ongoing in an attempt to establish regional correlations with the classic Belt basin deposits (for example, Link and others, 2003; R.G. Tysdal, unpub. data); new findings could greatly enhance understanding of Mesoproterozoic basin development and distribution of associated stratigraphically controlled mineral deposits.

Table 7. Correlation diagram for Mesoproterozoic rocks of east-central Idaho.

[From Tysdal, 2000b]

Ross (1947), upper column. Ross (1934), lower column.	**Ruppel (1975)**	**Lopez (1981)**	**Ruppel and Lopez (1988)**	**Bennett (1977)**	**Connor and Evans (1986); Connor (1990A); Evans and Connor (1993); Evans (1999)**	**Ekren (1988)**	**Winston and Link 1993)**	**Tysdal and Moye (1996), Tysdal (1996a, b, 2000) and THIS REPORT**	**Tietbohl (1981, 1986)**	**Anderson (1961)**
			Lawson Creek Fm				Lawson Creek Fm	Lawson Creek Fm		
Swauger Fm	Swauger Fm	Swauger Fm	Swauger Fm				Swauger Fm	Swauger Fm		Swauger Fm
	Gunsight Fm		Gunsight Fm				Yellow- Mem E	Gunsight Fm		Lemhi Quartzite
	Apple		Apple				Mem B, C, D	Apple *c. siltite*	Apple Creek Fm	Apple
Lemhi	Creek		Creek				jacket	Creek *diamictite*	diamictite	Creek Fm
	Fm		Fm				Fm	Fm *f. siltite*	Big	
Quartzite	Big		Big				Big		Creek	
	Creek Fm		Creek Fm	Hoodoo Quartzite			Creek Fm	Big Creek Fm	Fm	
	West Fork Fm		West Fork Fm				West Fork Fm	West Fork Fm		
	Inyo Creek Fm		Inyo Creek Fm				Inyo Creek Fm	Inyo Creek Fm		
								FAULT		
Unnamed unit						Unnamed unit		Unnamed unit		
Hoodoo Quartzite	**THRUST FAULT**	**FAULT**	**THRUST FAULT**			Hoodoo Quartzite		Hoodoo Quartzite		
Yellowjacket Fm	Yellow-	Yellow- Mem E	Yellow- Mem E	Yellowjacket	Yellow- U	Yellowjacket Fm		Yellowjacket Fm		
		Mem D	Mem D	Fm Phylite L	M					
	jacket	jacket Mem C	jacket Mem C		jacket L					
		Mem B	Mem B		Hoodoo Quartzite L					
	Fm	Fm Mem A	Fm Mem A		Fm L					

Blackbird Gold-Bearing Cobalt-Copper Deposits, East-Central Idaho—Reevaluation of Stratigraphic and Structural Setting

By Karen Lund, Russell G. Tysdal, Karl V. Evans, and Michael J. Kunk

The Blackbird gold-bearing cobalt-copper deposit is the most important of a unique type of sediment-hosted cobaltiferous massive sulfide deposits and is located within a 50-km-long northwest-trending zone in east-central Idaho (Hughes, 1983; Hahn and Hughes, 1984; Nold, 1990; fig. 20). The Blackbird deposit is hosted in a thick Mesoproterozoic siltite-metasandstone sequence, first placed in the Mesoproterozoic Yellowjacket Formation (Vhay, 1948; Nash and Hahn, 1989). Early work suggested that the gold-cobalt-copper deposits in the Blackbird district may have been epigenetic hydrothermal deposits (Anderson, 1947) or hydrothermal replacement along shear zones (Vhay, 1948). More recently they were interpreted as synsedimentary exhalative and diagenetic brine-remobilization deposits that formed in a Mesoproterozoic rift basin (Hahn and Hughes, 1984; Nash and Hahn, 1989); post-diagenetic processes were deemphasized.

Reconciling new broader scale understanding with previous local information caused the stratigraphic and structural setting of the Blackbird deposits to be refined such that the original setting of individual prospects can be geometrically related. Thus, the origin, diagenetic character, and amount of remobilization can be reconsidered.

Stratigraphy

Revision of the formations, definition of environment of deposition for the strata, and new delineation of their areal distribution require that the stratigraphic setting of the host rocks for Blackbird deposits be significantly revised. Although long thought to be hosted in the Mesoproterozoic Yellowjacket Formation, which was mapped as the dominant formation throughout central Idaho, deposits of the Blackbird mineral deposit type throughout this region are now known to be hosted by strata in the upper Apple Creek Formation and strata transitional to the basal Gunsight Formation (fig. 20). The Yellowjacket Formation is now limited to fault-bounded exposures west of the district and does not contain sediment-hosted deposits. These reevaluations resolve the conflict between the interpretation that Blackbird type deposits formed in a deep-water rift environment and the interpretation that the Yellowjacket Formation, as originally described, formed in relatively shallow water. Placement of the Blackbird deposit in the Apple Creek Formation and strata transitional to the basal Gunsight Formation limits the distribution of the formation that hosts the cobalt-copper-gold deposits in a way that is critical to future exploration for such deposits. The conclusion also limits the distribution of exposures of strata that formed in this deep basinal (rift) setting to a northwest-trending belt.

Metamorphism and Deformation

Regional understanding of the metamorphism and the location and style of Cretaceous compressional deformation in the Headwaters Province is changed by recent regional subdivision of the Mesoproterozoic stratigraphic units and discrimination of structures (Tysdal, 2000a, 2000b; Lund, Tysdal, and others, 2003; Tysdal and others, 2003; K. Lund, unpub. mapping, 2001–2002). Metamorphic grade, which increases northwest and northward across the district (Vhay, 1948; Cater and others, 1975; Lund and others, 1983), and the garnet isograd, which loops across part of the Blackbird mine area (Vhay, 1948), were attributed to contact metamorphism during emplacement of granitic rocks (which were first interpreted as Cretaceous but later as Mesoproterozoic; Cater and others, 1975; Nash and Hahn, 1989). The Blackbird district lies in the complexly deformed upper footwall to the northwest-trending Iron Lake fault (figs. 20, 21). Deposits in the district are located at the northeast-trending hinge zone of a down-to-the-north lateral ramp in the Iron Lake thrust fault (fig. 21). This structural setting resulted in folds of all scales from megascopic to microscopic, in axial-planar and shear zone schistosity in lower grade rocks, and in widespread transposition of features in the most deformed rocks. The most deformed zone is at the top of the footwall to the Iron Lake, herein called the Indian Creek subplate (figs. 20, 21); these rocks are essentially part of the thrust fault zone and contain the rocks above the garnet isograd. $^{40}Ar/^{39}Ar$ dating of white mica below the Iron Lake fault indicates that the white mica formed during thrust faulting, at about 84 Ma. Most of the previously explored deposits lie in the Blackbird subplate, at intermediate structural levels (figs. 20, 21). A few deposits lie in the structurally lowest Haynes-Stellite subplate that is in the gradational zone between Apple Creek and Gunsight Formations (figs. 20, 21).

The area of the Blackbird deposit was modified by post-mineralization normal faults (figs. 20, 21). The north-trending White Ledge shear zone marks the west edge of mineralized rock, and the Slippery Creek fault marks the east edge (Vhay, 1948; Bennett, 1977). Most of the thrust faults were reactivated by normal faults (figs. 20, 21).

Deposits

Recent stratigraphic studies (Sobel, 1982; Tysdal, 2000a, b) corroborate conclusions of Nash and Connor (1993) that the Blackbird deposits formed in a deep-water environment. However, observations of metamorphic or structural disruption and remobilization of the deposits, described by early studies (Anderson, 1947; Vhay, 1948), were not reconciled with more

recent sediment-hosted deposit models (for example, Nash and Hahn, 1989). Studies conducted during the Headwaters Province project demonstrated that mineral deposits in the Blackbird district formed in three related sedimentary environments that underwent different degrees of dynamothermal overprinting and that were structurally stacked in an inverted sequence (Lund and Tysdal, 2007).

1. Tourmalinite diatreme deposits, now at the structurally lowest levels in the Haynes-Stellite subplate, formed during diagenesis and by remobilization during later tectonism in the upper banded siltite member of the Apple Creek Formation and where it is transitional to fine-grained sandstone strata of the basal Gunsight Formation. These deposits formed relatively higher in the stratigraphic succession as the deep host basin began to fill with sediment and water level shallowed. Thus, they are not feeder pipes for the stratigraphically layered synsedimentary deposits in the main deposits of the Blackbird district to the west as suggested by earlier work (Hahn and Hughes, 1984; Nash and Hahn, 1989).

2. Silica-facies iron-formation tourmalinite and biotitite ("mafic") layers and their diagenetically disrupted equivalents (which host cobaltite deposits in the central structural levels of the Blackbird subplate; fig. 21) underwent deformation and mild localized metamorphism; metals as well as the tourmaline biotite-silica synsedimentary exhalative layered system were remobilized to some degree. Tectonic remobilization resulted in veins and veinlets of quartz-biotite-tourmaline and in a more sulfide-rich metal suite.

3. Tourmalinite-biotitite zones, which host gold-cobalt-copper deposits in the Indian Creek (higher structural level) subplate (fig. 21), are strongly metamorphosed, transposed, and deformed. Chloritoid-garnet-feldspar-quartz-biotite schist that hosts the deposits formed by regional dynamothermal metamorphism during thrust faulting; deposits in these rocks are chemically and mineralogically different from those of the Blackbird subplate. The schists are in structural, not stratigraphic, contact with underlying strata. Deposits of the Indian Creek subplate contain lower sulfide but higher silica, arsenic, and gold abundances than deposits in other subplates. Whether these were original characteristics or whether they developed as a result of dynamothermal and related hydrothermal processes during deformation is indeterminate at present. Subsequent normal faulting juxtaposed different structural levels and reduced the amount of apparent thrust fault separation. Deformation may have been localized near the deposits because of physical properties of metal-rich zones and, as a corollary, deposits may have been enriched by remobilization processes related to the local nature of deformation.

Conclusions

Deposits in the Blackbird district are related to ancient basement structures (northwest-trending fracture system) that may have controlled the orientation of depositional basins that crossed central Idaho parallel to the present structural fabric. Blackbird-type deposits have many synsedimentary and diagenetic characteristics similar to those observed in the less structurally disturbed Mesoproterozoic Sullivan-type deposits in British Columbia, but these two deposit types probably formed in separate or subsidiary depositional basins. Thus, although the Blackbird- and Sullivan-type deposits are remarkably similar with respect to chemistry and associated iron-formations, differences in age, tectonic setting, basement, and chemistry of underlying rocks probably contributed to metallogenic features that are unique to the Blackbird cobalt-copper deposits.

Poorly understood stratigraphic relations, metamorphism, and deformation all contributed to the uncertainty about the geometry of Blackbird deposits. Heterogeneous deformation in the Blackbird district is now known to be confined to distinct structural domains that controlled metal paragenetic variation in the district.

Implications

A wide array of information previously gathered from this mining district fits well in the newly developed, more comprehensive framework concerning the depositional setting and subsequent dynamothermal processes that contributed to the genesis of these deposits. Ultimately, establishing a better understanding of the origin and tectonic history of the unique Blackbird sediment-hosted massive sulfide deposits will improve genetic models for massive sulfide deposits in the Mesoproterozoic of North America and elsewhere. Information concerning the Blackbird district provides a useful point of comparison with other more dismembered massive sulfide deposits, such as the Broken Hill type, because the array of Blackbird-type deposits ranges from being largely undisturbed by dynamothermal processes to nearly completely transposed during upper greenschist facies metamorphism and deformation. Characterization and consideration of the basinal setting for distal deposits hosted in the Apple Creek Formation may result in better understanding of the similarities and differences among sediment-hosted massive sulfide deposit types, such as Sullivan, Broken Hill, and possibly Olympic Dam types that are presently considered to be distinct deposit types.

The Headwaters Province study has contributed to a more complete understanding of the stratigraphic and structural setting that prevails near the Blackbird mining district, and with this knowledge, the genesis of known Blackbird gold-cobalt-copper deposits can be reconstructed. These insights contribute to (1) development of better exploration models and more effective geoenvironmental assessment of Blackbird-type deposits; (2) more precise reconstruction of the sedimentary basin(s) in which these deposits formed; and (3) better understanding of how Blackbird-type deposits are related in time, space, and tectonic setting to deposits, such as Sullivan, which formed in part of the same or a related basin.

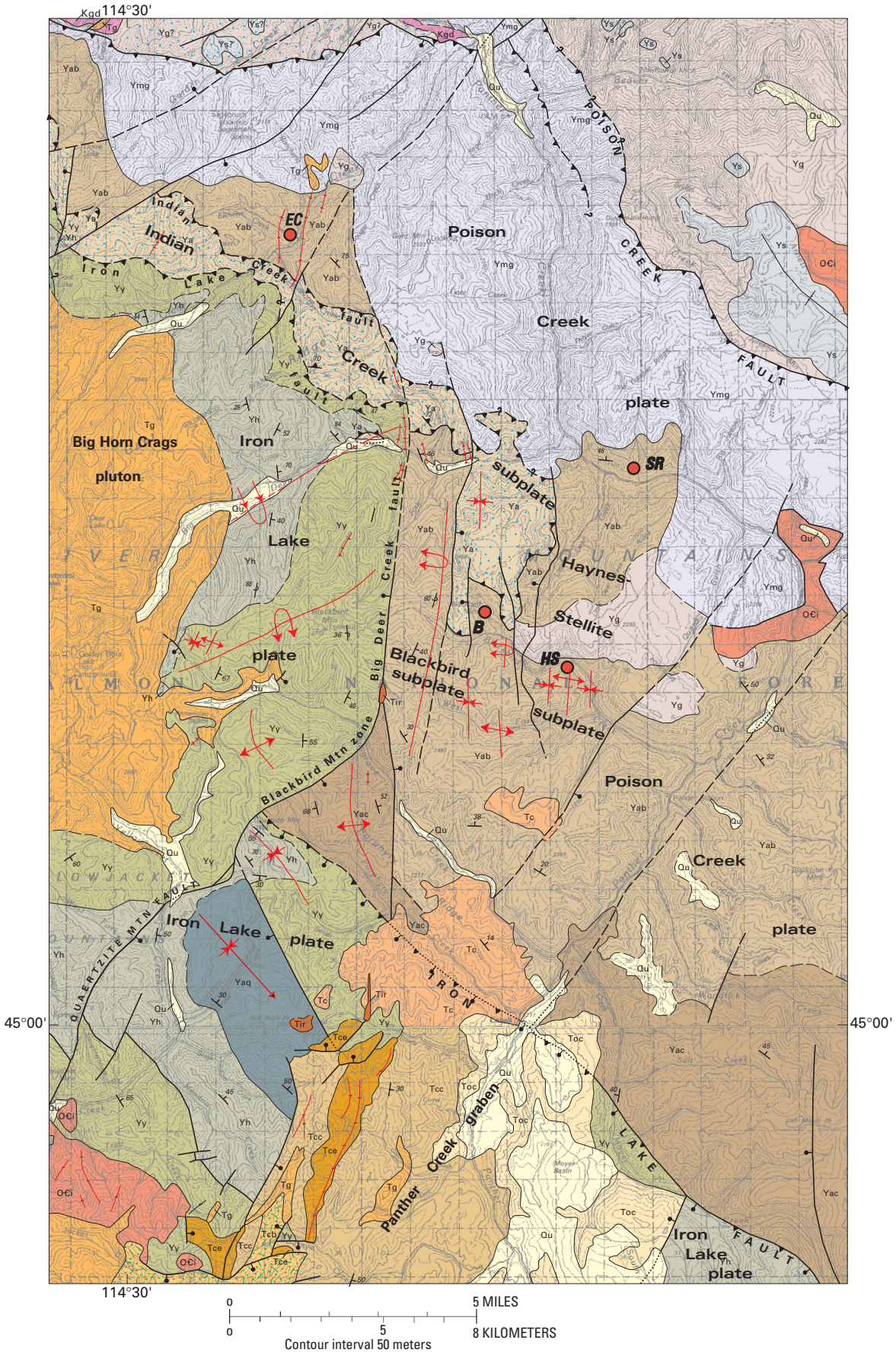
114°30'
45°00'
Big Horn Crags pluton
Iron Lake plate
Indian Creek fault
Indian Iron Lake Creek
Poison Creek plate
POISON CREEK FAULT
Big Deer Creek fault
Blackbird subplate
Blackbird Mtn zone
Haynes Stellite subplate
Iron Lake plate
QUARTZITE MTN FAULT
IRON CREEK graben
Panther Creek
LAKE FAULT
EC
SR
B
HS
0 5 MILES
0 5 8 KILOMETERS
Contour interval 50 meters

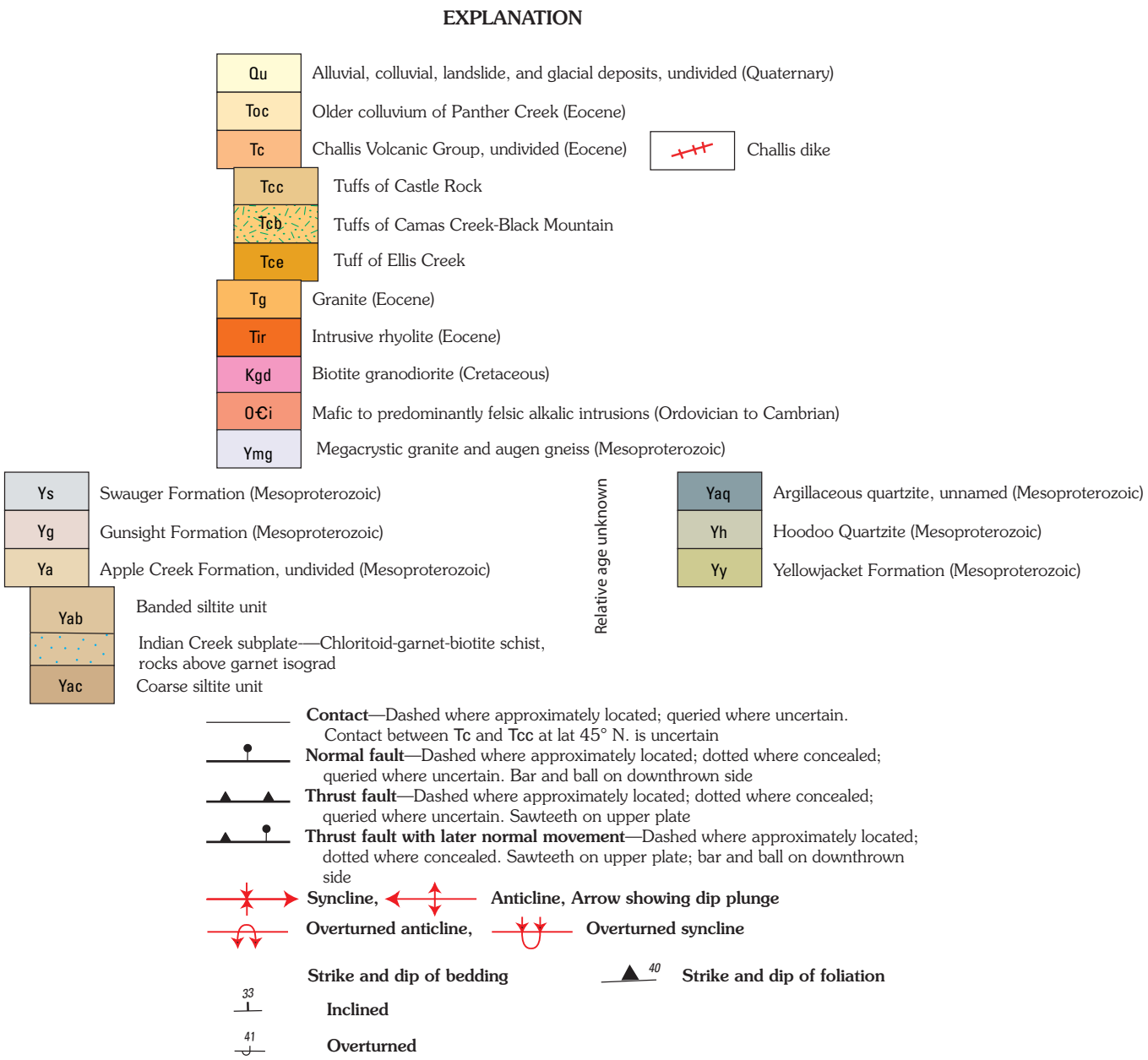

Figure 20. Regional geologic and location map, showing cobalt-copper deposits in exposed belt of banded siltite of the Apple Creek Formation. Compiled from Tysdal and others (2003), Vhay (1948); Karen Lund, unpub. mapping, 2001–2002. Rocks above garnet isograd are patterned. B, Blackbird mine; EC, Elkhorn Creek prospect; HS, Haynes-Stellite deposit; SR, Sweet Repose mine.

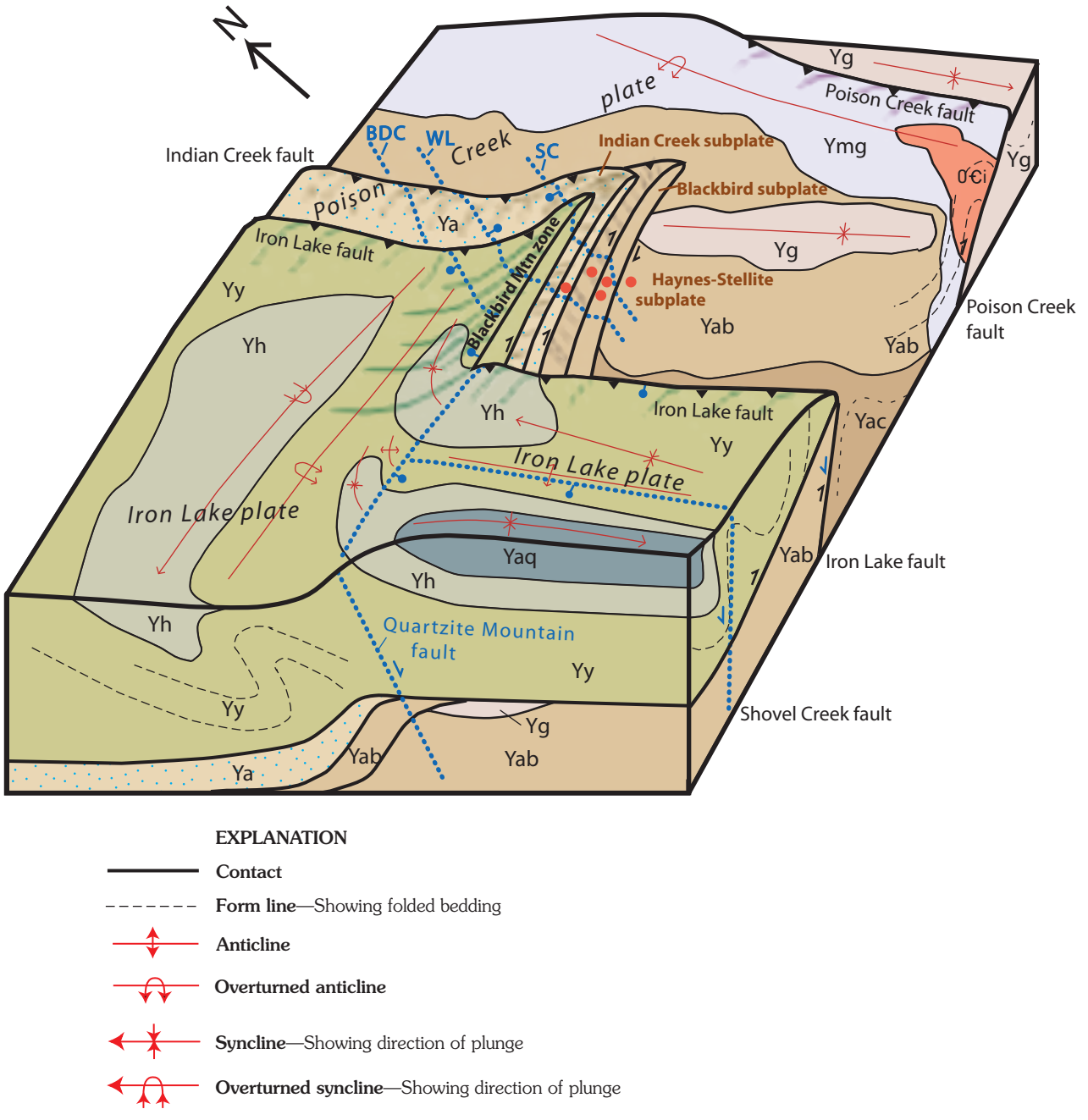

Figure 21. Block diagram showing structures of Blackbird district. 0€i, Ordovician to Cambrian intrusion; Ymg, Mesoproterozoic porphyritic granite; Yg, Gunsight Formation; Yab, banded siltite unit, Apple Creek Formation; Yac, coarse siltite unit, Apple Creek Formation; Ya, Apple Creek Formation, undivided, rocks above garnet isograd; Yaq, argillaceous quartzite; Yh, Hoodoo Quartzite; Yy, Yellowjacket Formation; barbs, relative fault movement; blue dotted lines, position of normal faults, block shows restored position before normal faulting; BDC, Big Deer Creek fault; WL, White Ledge shear zone; SC, Slippery Creek fault; red dots, location of major deposits in Blackbird district.

Identification of Neoproterozoic Windermere Supergroup, Central Idaho, using Geologic Mapping and SHRIMP U-Pb Geochronology—Implications for Neoproterozoic Rifting and Glaciation

By Karen Lund, John N. Aleinikoff, and Karl V. Evans

Vast areas of central Idaho are underlain by poorly known metamorphic rocks isolated within voluminous Mesoproterozoic to Eocene magmatic rocks. New mapping identified metamorphosed sedimentary and volcanic rocks that form a discontinuous northwest-southeast belt across central Idaho. New Sensitive High Resolution Ion Microprobe (SHRIMP) U-Pb age determinations on zircon in the volcanic rocks show that these rocks are part of the Neoproterozoic glacial and continental margin sediments of the western margin of Laurentia (pre-Cretaceous North America). The ages and location of these previously unrecognized strata require revision of mineral resource potential estimates across the Headwaters Province and reevaluation for models of Proterozoic supercontinent development and disintegration as well as models of global climate change.

Stratigraphy

As part of the Headwaters Province project, geologic mapping in central Idaho (fig. 22) and subsequent geochronologic studies determined that roof pendants in the northern Atlanta lobe of the Idaho batholith include strata correlative with (1) Mesoproterozoic strata of east-central Idaho, (2) the Neoproterozoic Windermere Supergroup, and possibly (3) the lower Paleozoic miogeocline (Lund, Aleinikoff, and others, 2003; Lund, 2004). The presence of Neoproterozoic Windermere Supergroup and related rocks in central Idaho provides a link between strata extending from the Alaska-Yukon region to California (fig. 22; Crittenden and others, 1972; Gabrielse, 1972; Stewart, 1972, 1991; Ross and others, 1989; Link and others, 1993; Dehler and others, 2001). Consequently, much of the Neoproterozoic western margin of Laurentia is preserved in central Idaho and was not removed by Mesozoic rifting or transcurrent faulting. As a result, the geometries of the Neoproterozoic rift belt and subsequent Mesozoic accretionary tectonics require redefinition.

In the northwestern part of the Headwaters Province, a succession of nine newly named Neoproterozoic formations of the Gospel Peaks succession A–D (fig. 23) record middle Neoproterozoic preglacial, rift-glacial, and postglacial events as well as late Neoproterozoic glacial and rift events (Lund, Aleinikoff, and others, 2003; Lund, 2004). Gospel Peaks succession A includes three newly named formations composed of schist, quartzite, and calc-silicate gneiss or marble—Plummer Point, Square Mountain, and Anchor Meadow Formations—that may correlate with Neoproterozoic strata found below glaciogenic rocks elsewhere in the Cordillera. Gospel Peaks succession B includes three new formations (bottom to top): (1) the Edwardsburg Formation (which is divided into four members composed of interfingered bimodal rift-related volcanic and glaciogenic diamictite strata), (2) the Moores Station Formation, and (3) the Goldman Cut Formation. The latter two are postglacial deeper water successions. Gospel Peaks succession C includes two newly established formations, the coarse siliciclastic Moores Lake Formation and the laminated siltite-carbonate Missouri Ridge Formation, which represent younger glacial and postglacial events. Gospel Peaks succession D is dominantly quartzite of the Umbrella Butte Formation, which contains evidence of continental extension.

The strata of the Edwardsburg Formation are particularly important, as dating of the interlayered volcanic and diamictite rocks provides ages for regional to global rifting and glacial events. From bottom to top, the rift-glaciogenic succession in the Edwardsburg Formation (shown in fig. 23) is (1) the Wind River Meadows Member, metamorphosed very coarse grained glacial sediments (diamictite) interlayered with rhyodacite flows and volcanogenic rocks; (2) the Golden Cup Member, mafic volcanic flows; (3) the Placer Creek Member, volcanogenic rocks, volcanic-clast conglomerate, and heterogeneous clast-supported diamictite; and (4) the Hogback Rhyolite Member, a local rhyolite flow.

Geochronology

Zircon crystals were separated from intermediate-composition volcanic rocks in the upper and lower members of the Edwardsburg Formation. Zircon from the Wind River Meadows Member is tan, clear, and blocky to prismatic (length to width ratios of 2–6); most grains contain longitudinal cracks and (or) partially filled fluid inclusion tubes (fig. 24*A*). These imperfections rendered isotopic analysis difficult. In contrast, zircon from the Hogback Rhyolite Member is relatively pristine; crystals are tan, clear, blocky (length to width ratios of about 1–3), and contain few cracks or inclusions (fig. 24*B*). These zircons were dated using a Sensitive High Resolution Ion Microprobe (SHRIMP). The rhyodacite of the Wind River Meadows Member yielded a weighted average age of 687±10 Ma whereas the Hogback Rhyolite Member yielded a weighted average of 687±7 Ma (fig. 25).

Results

Geologic mapping was used to identify distinct stratigraphic packages in roof pendants of the Idaho batholith. Our subsequent geochronologic studies document the existence of Neoproterozoic strata in these pendants. Identification of

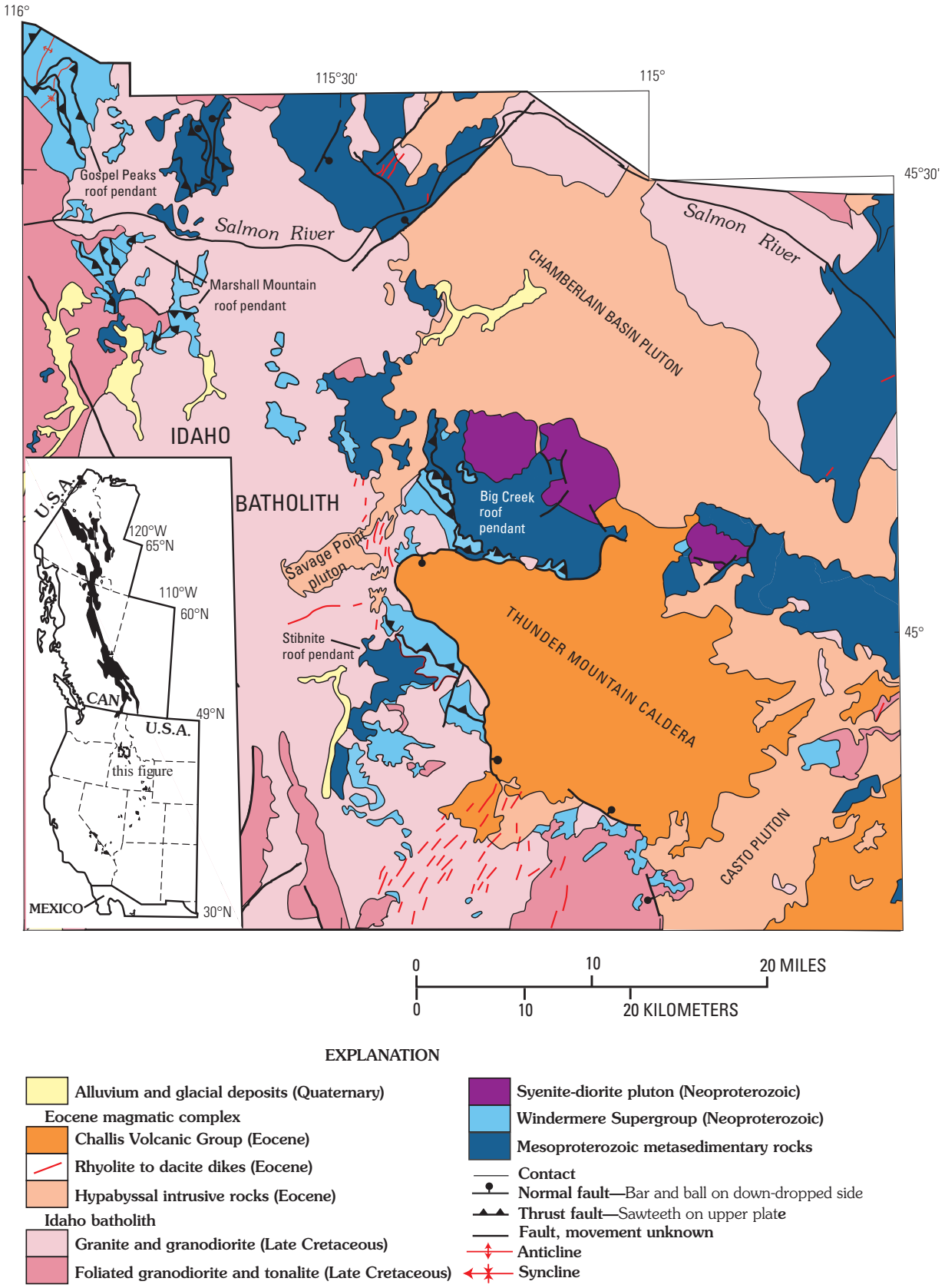

Figure 22. Windermere Supergroup rocks of central Idaho and surrounding area. Index map shows Windermere and equivalent rocks of the North American Cordillera. Canadian Cordillera from Ross and others (1989); southern U.S. Cordillera from Stewart (1991), Link and others (1993), and Dehler and others (2001); and central Idaho from Lund, Aleinikoff, and others (2003).

previously unrecognized Neoproterozoic strata in the belt across central Idaho poses many new questions. Of particular importance to local or global mineral resource assessments is that the potential for rift-related mineral deposits, which could be present in Neoproterozoic rift environments, has never been considered for this region. Possible deposits include sediment-hosted deposits of several types associated with silicate-facies iron-formation, carbonate-hosted deposit types, and conglomerate-related deposit types peculiar to the atmospheric/climatic/tectonic conditions of the developing Neoproterozoic Earth.

The presence of carbonate-bearing units in the Neoproterozoic section is important relative to the ability of country rocks to buffer acid drainage emanating from undisturbed as well as mined Cretaceous and Eocene sulfide-bearing mineral deposits across central Idaho. The presence of buffering capacity in newly defined geologic formations interspersed through several kilometers of stratigraphic section is an important new observation for FLMA relative to potential future mineral resource development and associated environmental issues.

Implications for Models of Snowball Earth and Rifting of Rodinia

Correlation of central Idaho metamorphic rocks to strata of the Neoproterozoic Windermere Supergroup (fig. 23) provided the first direct age determinations for the Windermere strata in the Cordillera. The consequence of identifying western Laurentian events at 687 Ma is that it alters models for Neoproterozoic Rodinia[1] paleogeography and resultant paleolatitude of Neoproterozoic glaciations. In that time frame, several Snowball Earth events may have enveloped the planet in glaciers due to unique climatic factors while the supercontinent Rodinia broke apart (Hoffman, 1999). However, our new dates and correlations particularly impact the number, synchroneity, and paleolatitude of possible Snowball Earth events. In particular, our study indicates that the time of rifting and glaciation was as much as 65 million years younger than previously thought.

Middle Neoproterozoic Rapitan glaciation of western Laurentia is often included as part of a worldwide glacial period, internationally called "Sturtian," hypothesized to have plunged the Earth into a global ice age that included glaciers even in equatorial regions (Hambrey and Harland, 1985; Hoffman and others, 1998). A reevaluation of this glacial record indicates that (1) two associated glacial intervals at about 687 Ma in the Edwardsburg Formation correlate with the Rapitan glaciation; (2) the Sturtian Snowball Earth event must be reevaluated based on revision of the age of Rapitan glaciation from 750–700 Ma to about 687 Ma, and (3) several different, older glaciations are known on other continents. Consequently, either there were more Snowball Earth events than previously inferred or the glaciations identified as "Sturtian" were not globally synchronous. The new, relatively young age for the Rapitan glacial event raises questions: (1) was this glaciation unique to western Laurentia rather than contemporaneous with (less well dated) Sturtian deposits worldwide and, thus, (2) was the Earth indeed a planetary snowball during the Sturtian glacial?

Our dates for interlayered volcanic and sedimentary rocks indicate that they formed about 687 Ma, as a result of rifting along the length of Laurentia during breakup of the Rodinian supercontinent (Stewart, 1972; Bond and Kominz, 1984; Young, 1995). This age clarifies a step-wise history of rifting that ultimately culminated in breakup of Rodinia about 570 million years ago (Bond and Kominz, 1984); however, this brings into question the timing of specific continental reconstructions and separations. Reevaluation of geochronology and correlations indicates that middle Neoproterozoic rifting (1) may have been protracted between 780 and 687 Ma; (2) may have been diachronous along the Cordillera; or (3) may have proceeded step-wise, including a Cordilleran-wide event at about 687 Ma that initiated onset and geometry of the Cordilleran miogeocline.

Mineral Resources in Relation to Potential Regional Environmental Effects

Federal Land Management Agencies (FLMA) are responsible for the stewardship of nearly one-third of the land in the United States. These agencies are faced with a variety of issues related to mineral resources, ranging from the permitting of new mines and the regulation of active mines to prioritizing inactive and abandoned mines for cleanup. Increasingly, FLMA incorporate principles of ecosystem management in planning and management processes.

Mineral deposits are natural concentrations of minerals formed by geologic processes. Materials from mineral deposits, whether mined or undisturbed by humans, disperse into the environment through natural and anthropogenic processes. Natural processes include physical and chemical weathering and erosion by wind and water, landslides, and wildfire. Anthropogenic (human) activities, such as mining and milling of ores, smelting, agriculture, logging, and road construction, also disperse mineral deposits and their components. (See Kesler, 1994, for an overview of mineral environmental issues.) A mineral deposit represents a potential resource, but it can also represent an existing or potential threat to ecosystems or human health. As FLMA seek the best available science for

[1]Rodinia was a Neoproterozoic-age supercontinent that formed by collisional events at about 1 Ga and broke apart into eight separate continents starting at about 750 Ma. The name is from Russian, meaning "motherland."

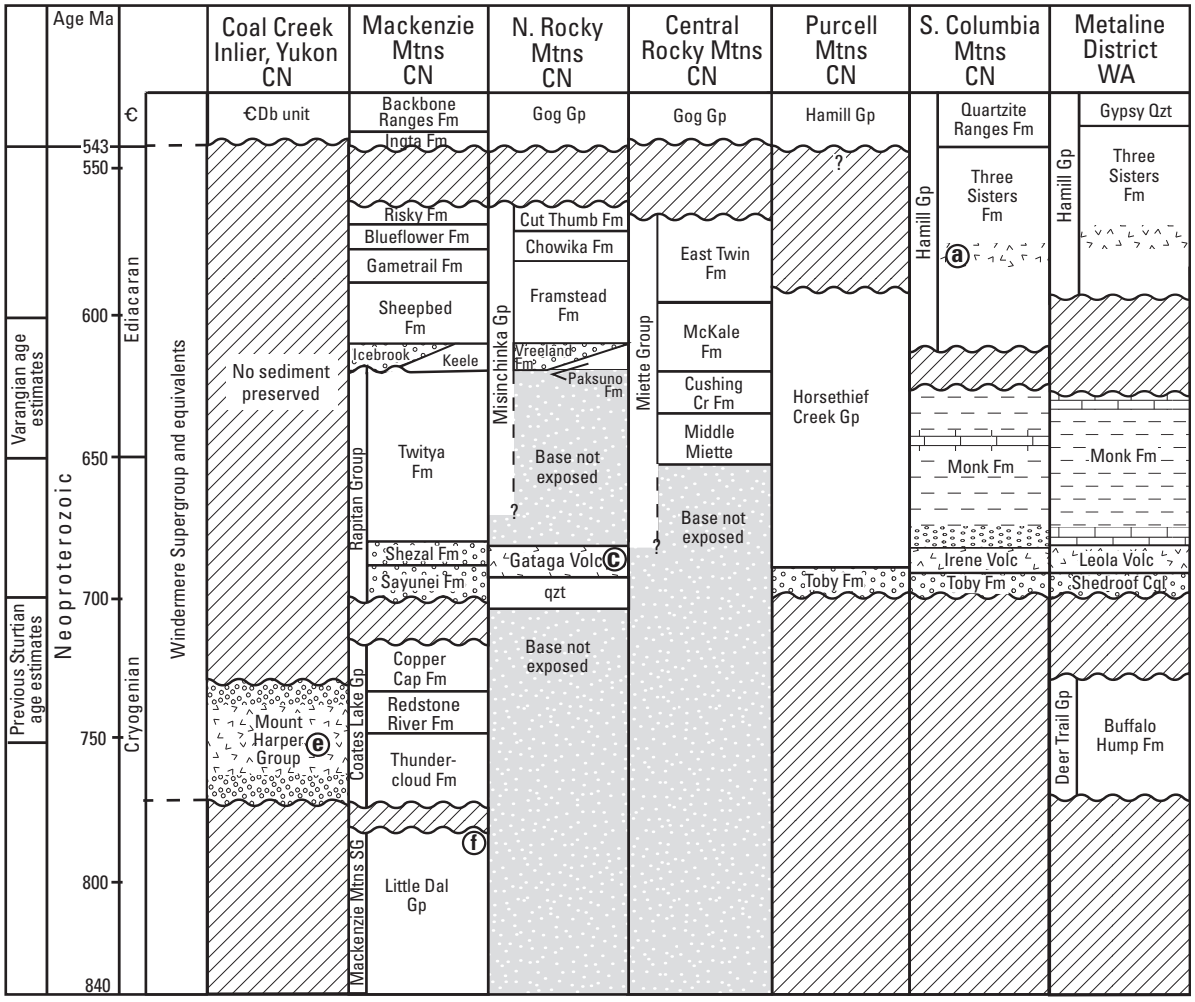

* This report

[1] Crittenden and Wallace (1973)

[2] Christie-Blick and Levy (1989)

[3] Prave (1999)

Figure 23. Composite correlation chart of Neoproterozoic and lower Paleozoic rocks, central Idaho and other sections in the Cordillera (see Lund, Aleinikoff, and others, 2003 for references), showing isotopic ages. Note that although an attempt has been made to tie rock units to geologic time in constructing this diagram, the lack of dates throughout the Cordillera results in much interpretation in intervals indicated for units as well as in individual correlations. Letters in Central Idaho column are designations for Gospel Peaks succession A–D. CN, Canada. SG, Supergroup; Gp, Group; Fm, Formation; M, Member; Cgl, Conglomerate; Dol, Dolomite; Ls, Limestone; Qzt, quartzite; Volc, Volcanic; Cn, Canyon, Cr, Creek; Lk, Lake; Mdw(s), Meadow(s); Rdg, Ridge; Rv, River.

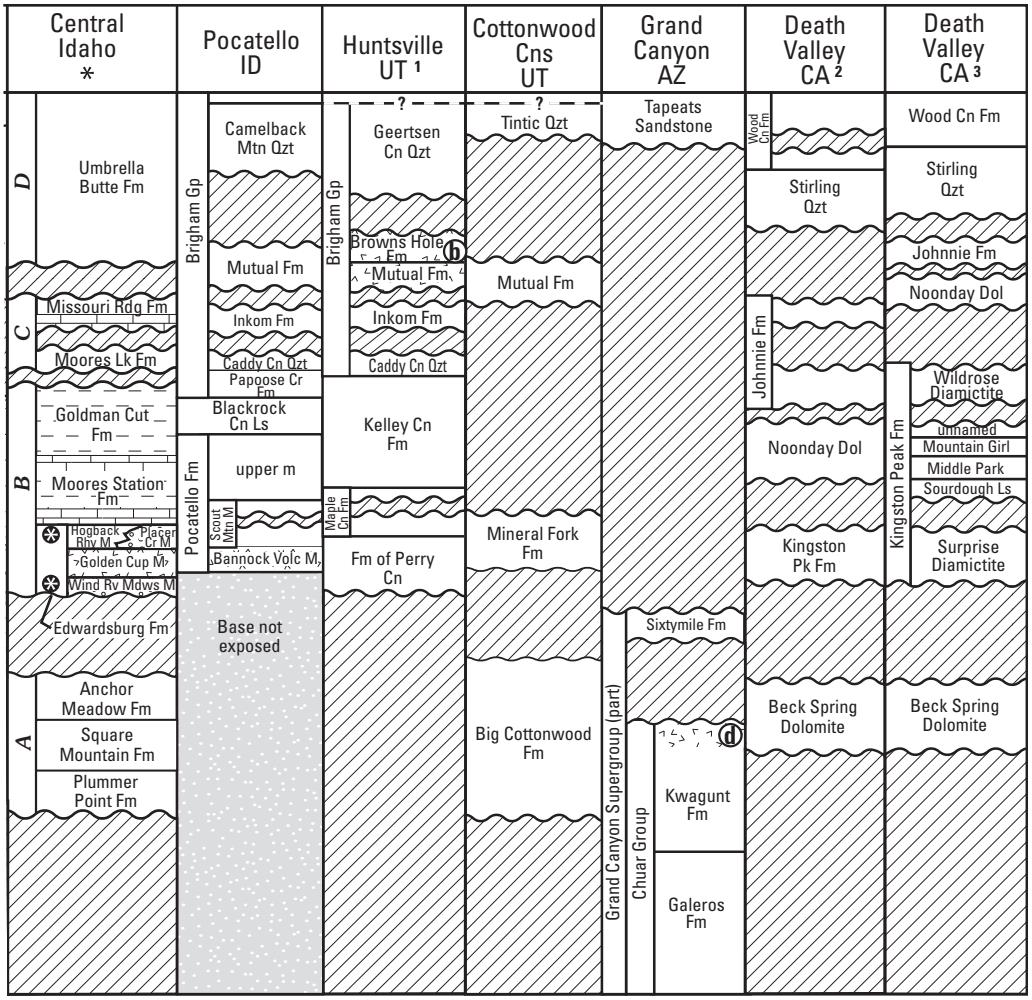

Dates:

ⓐ 569.6 ± 5.3 Ma, U-Pb, Colpron and others (2002)
ⓑ 580 ± 7 Ma, $^{40}Ar/^{39}Ar$ total fusion, Crittenden and Wallace (1973); Christie-Blick and Levy (1989)
ⓒ 689 ± 4.6 Ma, U-Pb, Ferri and others (1999)
ⓓ 742 ± 6 Ma, U-Pb, Karlstrom and others (2000)
ⓔ 751 +46/-18 Ma, U-Pb, Roots and Parrish (1988)
ⓕ 777 +3/-2 Ma, U-Pb, Jefferson and Parrish (1989)
✪ Basal: 685 ± 7 Ma; Upper: 684 ± 4 Ma, U-Pb, this paper

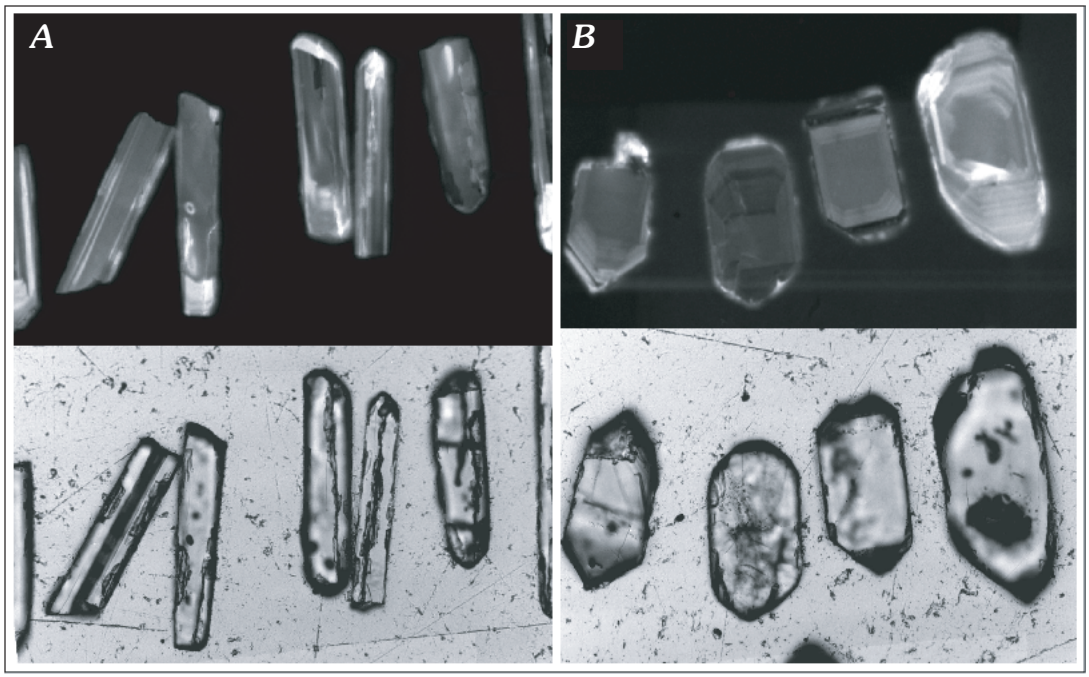

Figure 24. Photomicrographs of zircon crystals from metavolcanic rocks of the Edwardsburg Formation. Upper images in cathodoluminescence; lower images in transmitted light. *A*, Zircons from rhyodacite of Wind River Meadows Member of the Edwardsburg Formation. *B*, Zircons from Hogback Rhyolite Member of the Edwardsburg Formation.

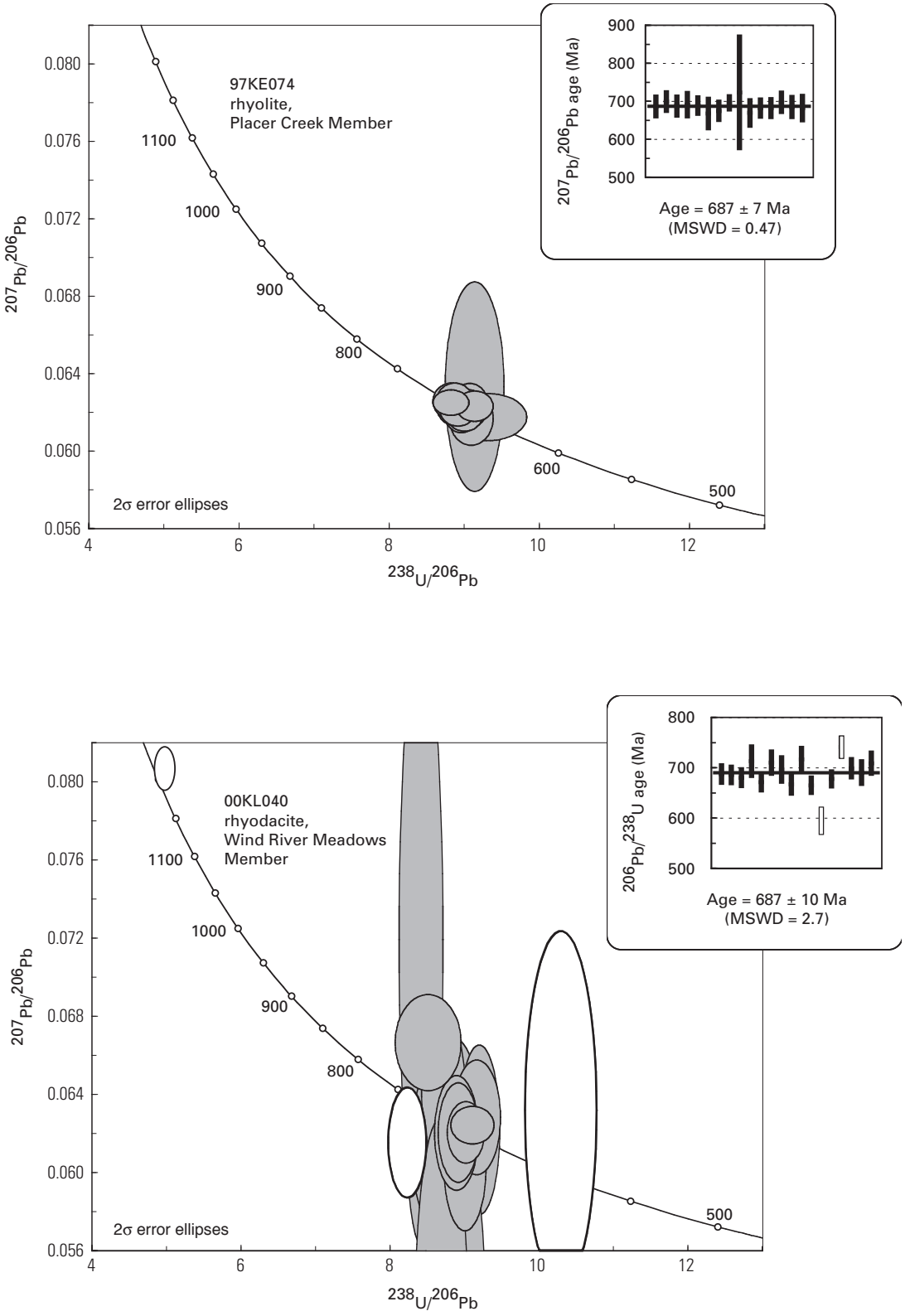

Figure 25. Tera-Wasserburg concordia plots and weighted averages plots of SHRIMP U-Pb isotopic data for metavolcanic rocks of the Edwardsburg Formation. Open dots on curves represent ages, as shown, in Ma. Data are shown as 2 sigma error ellipses; error bars are ± 2 sigma. Unshaded bars and ellipses are excluded from age calculations. MSWD, mean standard weighted deviation.

land-use planning, data on environmental signatures of mineral deposits and on unmineralized country rocks are needed in addition to data on location and economic aspect of known or potential mineral resources. Different types of mineral deposits have different environmental signatures, depending largely on the nature of the ore minerals and the host rock. In addition, climate variation can cause a single deposit type to have significantly different environmental contributions. A single watershed can contain a large variety of mineral deposit and host rock types.

Baseline Geochemistry of a Part of the Salmon River Drainage—Two Examples

By Robert G. Eppinger, Paul H. Briggs, and Betsy Rieffenberger[1]

A baseline geochemical study was undertaken in the Salmon River drainage basin to provide a geochemical "snapshot" of the area for the Salmon-Challis National Forest. A stream-sediment and stream-water baseline study covered tributaries of the Middle Fork Salmon River, Panther Creek, and the Salmon River from Dump Creek to Corn Creek (fig. 26). The drainage basins chosen for study are underlain by similar geologic units but represent a pristine, largely unmined basin, an adjacent basin heavily impacted by past mining activity, and a stretch of river connecting these two basins. Described here are two ways these baseline geochemical data can be used. The first contrasts geochemical differences between the pristine, unmined basin and the adjacent, heavily mined basin. The second describes how these data were used in assessing the effects of wildfires that swept through the region in the summer of 2000. The area is underlain predominantly by Cretaceous Idaho batholith granitoids, Proterozoic to lower Paleozoic metasedimentary rocks, and Eocene granitic plutons.

The Middle Fork Salmon River, hereafter called the Middle Fork, drains a large (2,830 mi^2, 7,330 km^2) basin largely within the Frank Church–River of No Return Wilderness. The Middle Fork basin is pristine, mostly unimpacted by resource extraction activities (such as logging, mining, roads, grazing) since the early part of the 20th century; any early extraction activities were generally minor. In the last few decades, however, the Middle Fork has become internationally recognized as a whitewater river rafting and fishing destination. Currently between 10,000 and 11,000 people visit the river yearly on self-guided or commercially guided multi-day raft trips.

In contrast, Panther Creek, adjacent to and partly within the Frank Church–River of No Return Wilderness, has had a long, rich logging and mining history and contains numerous inactive mines and some areas in which exploration activity is ongoing. The Panther Creek basin is about 532 mi^2 (1,378 km^2) in size. It is roughly parallel to, and lies east of the Middle Fork (fig. 26). Most of the mines in the Panther Creek basin were small base- and precious-metal mines that operated into the early 20th century. However, the two largest mines, Blackbird and Beartrack, were active in the latter decades of the 20th century and are presently undergoing remediation and reclamation activities.

The Blackbird mine exploited sediment-hosted cobalt-copper deposits through the 1960s. The metal-rich belt of Mesoproterozoic metamorphosed sedimentary rocks is within the Apple Creek Formation and extends well beyond the limits of the Blackbird mine. Deposits hosted by the Apple Creek Formation contain the Nation's largest cobalt resources. Exploration within this belt continues to the present day (see Formation Capital Corporation website http://www.formcap.com), although no cobalt-copper mines are currently active in the area. The Blackbird mine produced at least 5.7 million t (metric tons) of ore, grading 1.4 percent copper, 0.74 percent cobalt, and 0.015 ounces gold/t (Nash and Hahn, 1986, 1989). A descriptive model of Blackbird-type deposits is found in Earhart (1986). Mine site remediation work is well underway at the Blackbird mine and presently involves work to meet mandatory water-quality objectives, including removal of contaminated sediments and installation of ground-water wells to capture and remove contaminated ground water.

The Beartrack mine, Idaho's largest gold producer, was a recent open-pit, heap leach gold mine, along Napias Creek, a tributary to Panther Creek. The deposit is classified as a distal-disseminated gold deposit (Klein, 2004; Cox, 1992). The Beartrack mine operated from 1995 through 2000, when reserves were exhausted. Through 2001, the mine produced about 44 million t of ore, with gold grades of 0.85 g/t (Klein, 2004). Residual gold was being produced from the remaining leach pads through 2003. Mine site reclamation is ongoing as of 2004.

The Salmon River is one of the larger rivers of the Snake River system. The part of the Salmon included in this study is about 61 km long and extends from about 32 km upstream of the confluence with Panther Creek to about 11 km downstream of the confluence with the Middle Fork (fig. 26), and lies within Salmon-Challis National Forest. Tributaries of the Salmon River along this stretch contain numerous small mineral deposits that were historically mined for precious and base metals.

Methods

Bedload stream-sediment and water samples were collected from main river channels and major tributaries at 82 sites during a 3-week period in July 1996, and sampling was repeated in June 2001. For water samples, time constraints

[1]USDA Forest Service, Salmon-Challis National Forest, Rural Route 2, Box 600, Salmon, ID 83467.

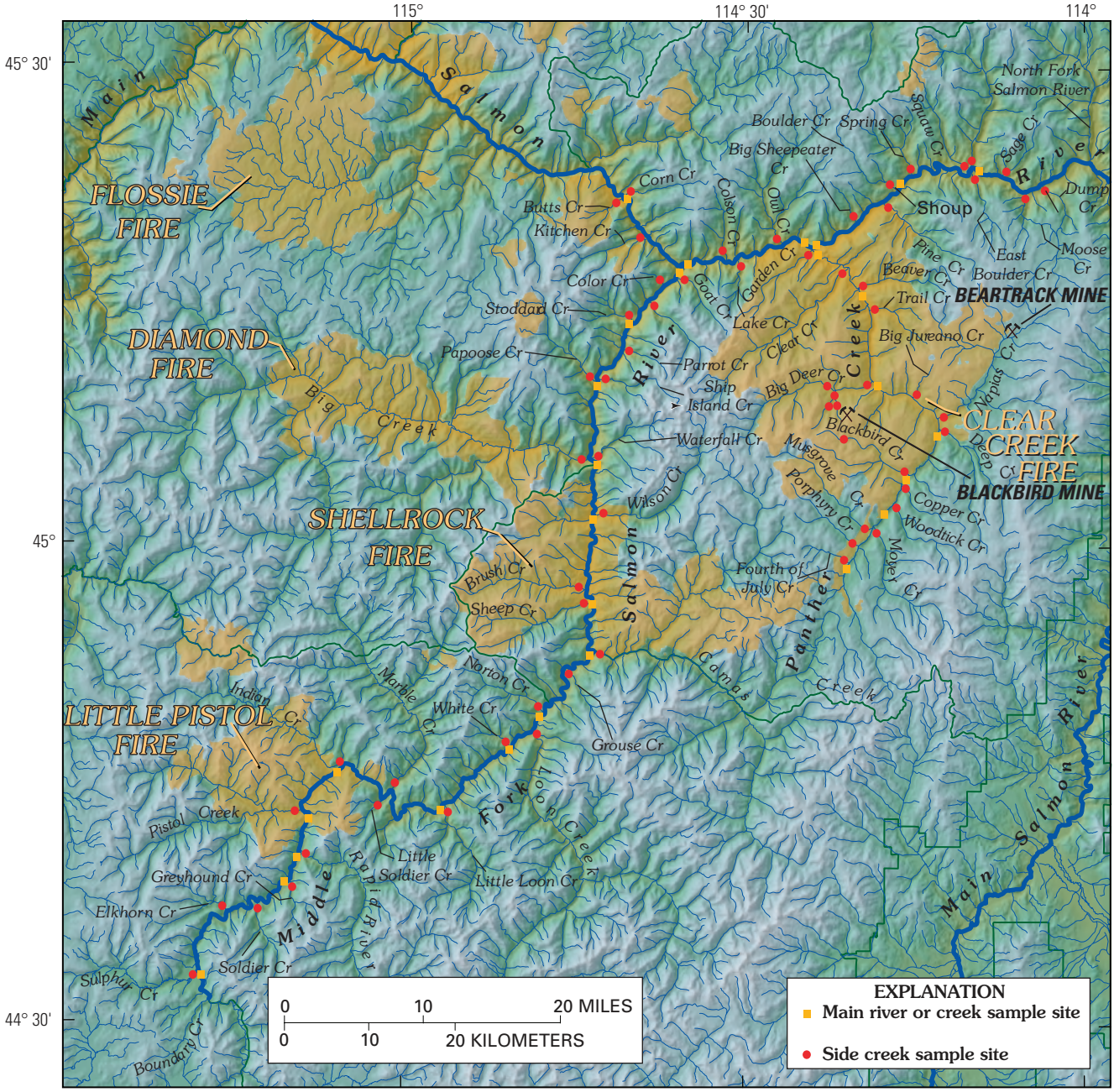

Figure 26. Location map for stream-sediment and surface-water samples collected from Panther Creek, Middle Fork Salmon River, and Salmon River. Wildfire perimeters and names for year 2000 wildfires shown in orange. Base from U.S. Geological Survey EROS Data Center digital elevation map data.

and access precluded strict adherence to USGS ppb-protocol water sampling procedures, but clean procedures were used throughout. On-site measurements included pH, conductivity, alkalinity, dissolved oxygen, water temperature, ferrous iron, turbidity, and a flow estimate.

Mixed water samples were filtered at 0.45 μm (micrometer), collected in acid-rinsed polypropylene bottles, and acidified with ultra-pure nitric acid. Water samples for mercury analysis were filtered as just noted, collected in acid-rinsed glass bottles with Teflon lids, and preserved with potassium dichromate/nitric acid. Unacidified water samples were refrigerated prior to analysis.

Bedload stream sediments were composited 1 kg (kilogram) samples from active alluvium. A minimum of 30 increments were collected at each site. Samples were air dried, sieved to minus-80 mesh (0.177 mm), and pulverized for chemical analysis. Clean quartz sand was pulverized between samples to reduce risk of contamination.

Samples were analyzed by a variety of methods including inductively coupled plasma–atomic emission spectroscopy (ICP-AES), ICP mass spectrometry, ion chromatography, and various atomic absorption methods. Quality assurance and quality control concerns were addressed through the use of site duplicates, analytical duplicates, and standards, which made up approximately 15 percent of the samples analyzed. Further details on methodology are found in Eppinger and others (2001) and Eppinger, Briggs, Rieffenberger, Van Dorn, and others (2003).

Example 1. Geochemical Contrasts Between Two Adjacent Basins

The Middle Fork and adjacent Panther Creek basins show strong geochemical contrasts in stream-sediment samples. These contrasts are largely due to differences in the geologic substrates of the basins. The Middle Fork basin is underlain largely by granodiorites and lesser granite of the Cretaceous Idaho batholith in its upper reaches and by quartz-rich Proterozoic biotite gneisses in its lower reaches. These rocks are intruded throughout much of the length of the Middle Fork basin by Eocene granitic plutons (Evans and Green, 2003; Lund, 2004; Fisher and others, 1992). In contrast, the Panther Creek basin is underlain in its upper reaches by Mesoproterozoic sedimentary rocks, including the Hoodoo Quartzite and the Yellowjacket, Gunsight, and Apple Creek Formations; and by Mesoproterozoic granite and augen gneiss in its lower reach (Evans and Green, 2003). The rich legacy of mining in the Panther Creek basin compared to the relative lack of mineral deposits exploited in the Middle Fork basin is a function of the differing geologic settings in the two basins.

The geochemical differences between the two basins are well illustrated by a plot of two variables, cobalt and the combined rare earth elements (REE), from stream-sediment samples. For simplicity, the variables are plotted in terms of average crustal abundance values. The average crustal abundance value for cobalt used here is 29 ppm (parts per million; Fortescue, 1992), which agrees closely with the new recommended average continental crust value of 26.6 ppm (Rudnick and Gao, 2004). For the combined REE (cerium, europium, holmium, lanthanum, neodymium, and ytterbium), the average crustal abundance value used here is 147 ppm (Fortescue, 1992), which is high compared with the new recommended average continental crust value of 88 ppm (Rudnick and Gao, 2004). The higher value was used here because of the generally felsic nature of the rocks in the region; felsic rocks tend to have higher REE contents than mafic rocks.

Cobalt in the Middle Fork basin is uniformly well below average crustal abundance (fig. 27). These low abundances are commensurate with the granitic to intermediate character of most rocks in the basin. Granitic rocks have low cobalt abundances, around 1 ppm on average, whereas intermediate-composition igneous rocks contain around 10 ppm Co (Rose and others, 1979; Levinson, 1980). The average cobalt content in stream sediments from 42 sites within the Middle Fork basin is 5 ppm. In contrast, considerably higher concentrations of cobalt are found in stream sediments from the Panther Creek basin (1.5 to greater than 3.5 times crustal abundance; fig. 27). In the Panther Creek basin, cobalt was mined from sediment-hosted deposits in several areas within the Apple Creek Formation, most notably at the Blackbird mine. The highest concentrations of cobalt in stream sediment (>250 ppm Co; nearly nine times crustal abundance) were from Blackbird Creek and Big Deer Creek, which both drain and are proximal to the Blackbird mine area. Cobalt concentrations in excess of 2.5 times crustal abundance are common around Blackbird and downstream along Panther Creek. Elevated cobalt abundances in stream sediments and upstream outcrops of the Apple Creek Formation are closely associated (fig. 27). This association is a predictable consequence of the sediment-hosted nature of the cobalt deposits. In fact, outcrops of the Apple Creek Formation closely define the limits of the Idaho cobalt belt (Evans and Connor, 1993; Tysdal, 2000b). Similar to cobalt, concentrations of arsenic and copper are high in stream sediments from the Panther Creek basin (hundreds and thousands of parts per million, respectively) but are negligible in the Middle Fork basin (generally <10 ppm for both elements). Arsenic and copper are closely associated with cobalt in Blackbird-type cobalt deposits (Nash and Hahn, 1989).

The sum of the REE cerium, europium, holmium, lanthanum, neodymium, and ytterbium provides another geochemical contrast between the Middle Fork and Panther Creek basins (fig. 28). Concentrations of these elements are clearly elevated in Middle Fork basin; most stream-sediment samples have REE concentrations in excess of 2.5 times crustal abundance. In fact, stream sediments from 22 of the 42 sites within the Middle Fork have REE concentrations more than 3.5 times crustal abundance (515 ppm, fig. 28). A strong spatial correlation exists between stream sediments with high REE concentrations and bodies of Eocene granite (fig. 28). Eocene granites in the region contain elevated concentrations of REE, radiogenic elements, and other lithophile elements (Kiilsgaard and Bennett, 1995; Rehn, 1983). Rare earth element-bearing

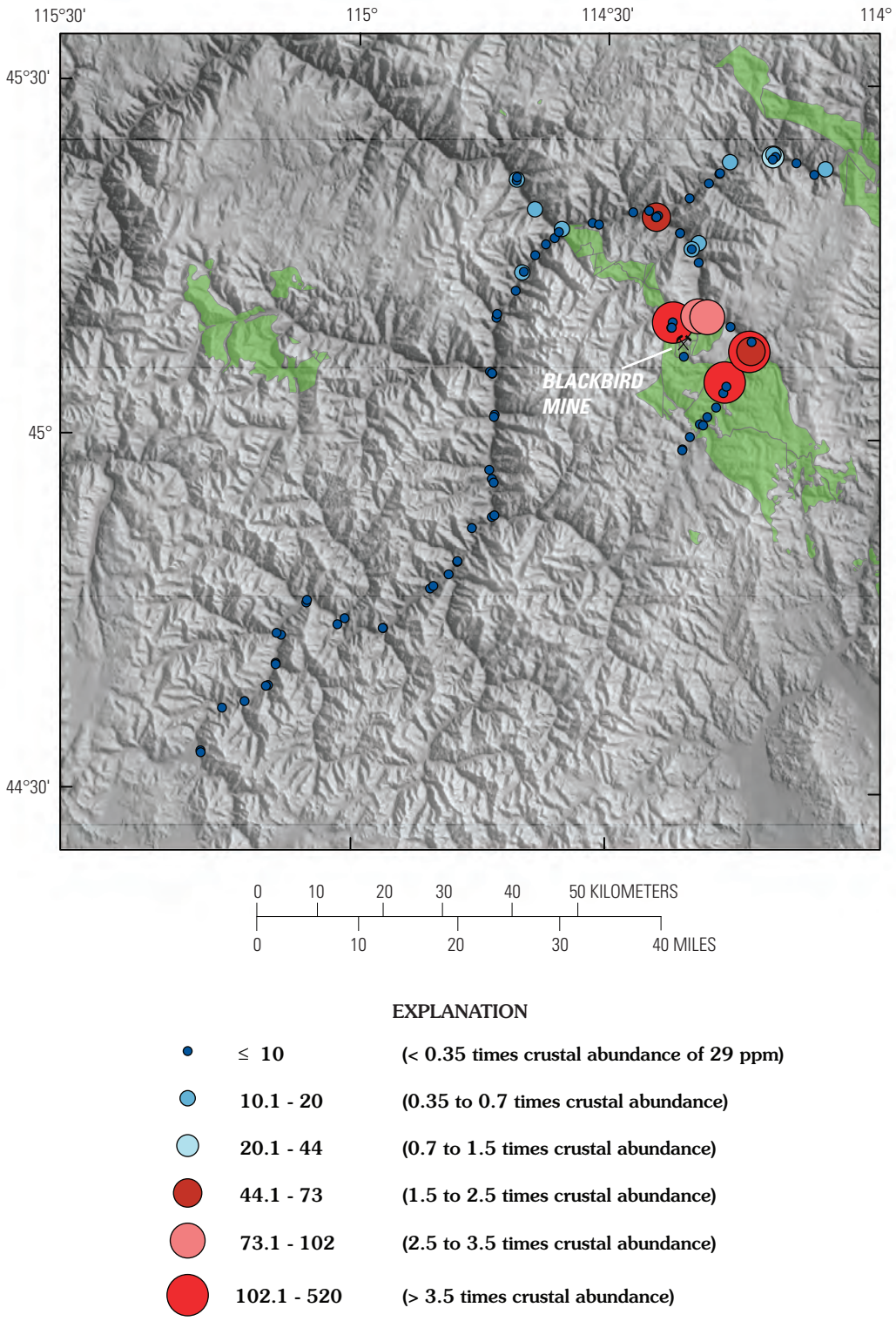

Figure 27. Cobalt in stream-sediment samples. Green polygons, outcrops of Proterozoic Apple Creek Formation; geology from Evans and Green (2003) and Lund (2004); crustal abundance value is from Fortescue (1992); see figure 26 for stream and river names.

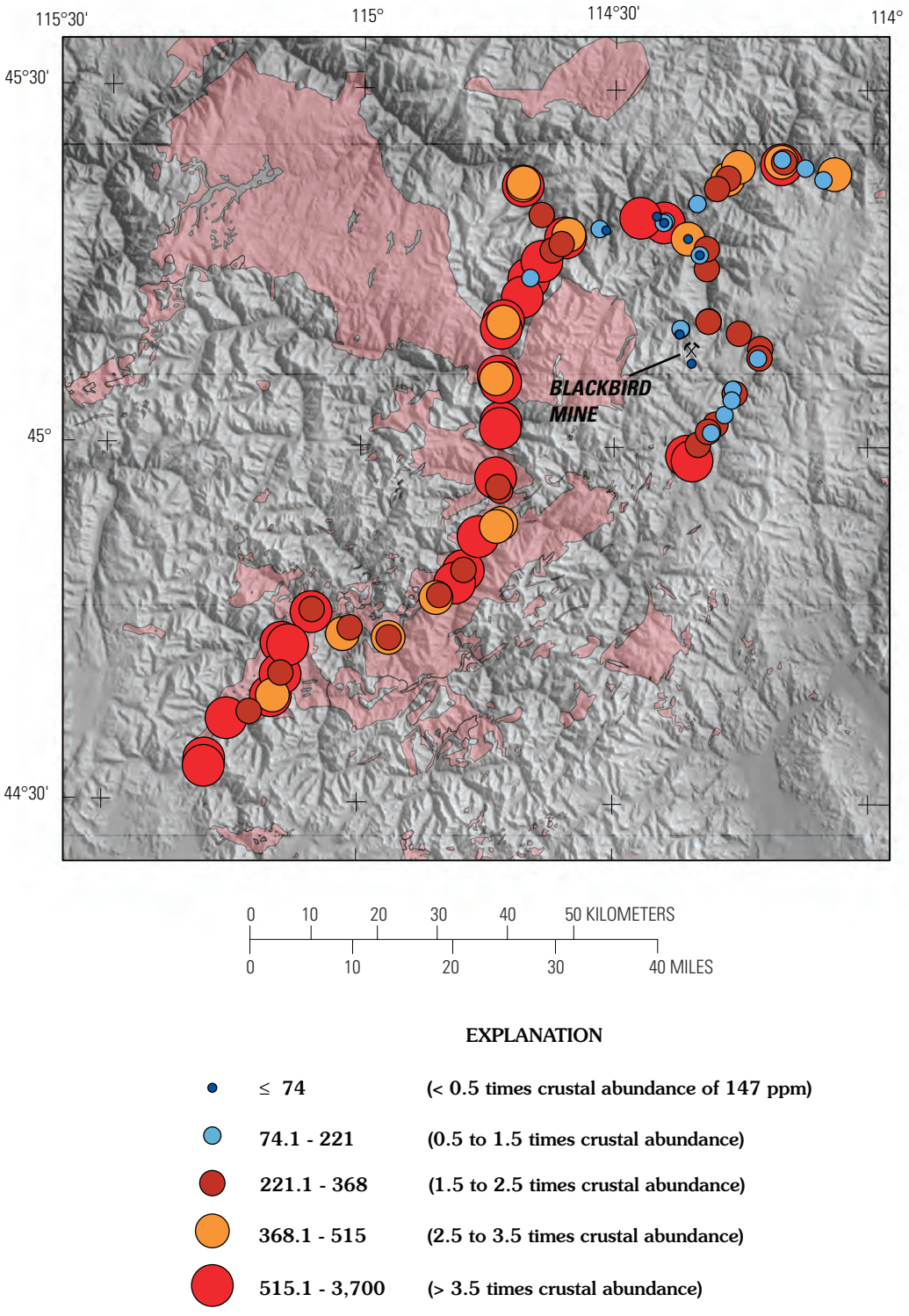

Figure 28. Sum of rare earth elements in stream-sediment samples. Pink polygons, outcrops of Eocene intrusive igneous rocks; geology from Evans and Green (2003) and Lund (2004); crustal abundance value is from Fortescue (1992); see figure 26 for stream and river names.

minerals sphene, allanite, monazite, zircon, and apatite are common accessory minerals in the Eocene granites (Kiilsgaard and Bennett, 1995). These heavy, resistate minerals are concentrated in alluvial sands. The rare-earth phosphate monazite, and the rare-earth oxide euxenite, were placer mined along Bear Valley Creek, in the headwaters of the Middle Fork, and their bedrock source is believed to be Eocene intrusive rocks (Kiilsgaard and Hall, 1995). Collectively, these features indicate that high REE concentrations in stream sediments are derived from the surrounding Eocene granite. Other elements that follow the overall pattern of enrichment in stream sediments from sites proximal to Eocene granite include barium, phosphorus, and, to a lesser degree, beryllium, lead, thorium, and yttrium. In contrast, REE concentrations are generally much lower in sediments from the Panther Creek basin, where, not coincidentally, only a minor volume of Eocene granitic rocks is present (fig. 28). Throughout the majority of the Panther Creek basin, stream sediments from 21 sites have REE concentrations that are about 1.6 times crustal abundance (240 ppm). Two exceptions to this are at the uppermost and lowermost ends of the Panther Creek basin, where high REE concentrations exceeding 3.5 times crustal abundance are present. High REE concentrations in upper Panther Creek are likely related to isolated outcrops of Eocene intrusive rhyolite. At the mouth of Panther Creek and along the Salmon River to the east, high REE concentrations are probably related to surrounding Mesoproterozoic megacrystic granites (Evans and Green, 2003), which locally contain accessory sphene, monazite, apatite, and zircon (Evans and Zartman, 1990).

Example 2. Assessing Effects of Wildfire on Stream Sediment and Water Geochemistry

The baseline geochemical study conducted in 1996 was principally undertaken to address issues of inactive or abandoned mines in the region. However, resulting data assumed a new significance when, in the summer of 2000, much of the previously sampled area was burned by the Clear Creek (>206,000 acres; >83,300 hectares) and Wilderness Complex (>182,000 acres; >73,600 hectares) wildfires. Ten months after the fires, in a jointly funded USGS–USDA Forest Service study, the area was revisited, in June 2001. The 82 sites initially sampled during the baseline study were resampled over a 3-week period, in order to determine whether the wildfires caused stream-sediment and water geochemistry to change. Samples were analyzed for the same suite of elements as in the initial study. Analytical results for this wildfire study were compiled by Eppinger and others (2001) and Eppinger, Briggs, Rieffenberger, Van Dorn, and others (2003). Interpretive results are presented by Eppinger (2002), Eppinger and others (2002), Eppinger, Briggs, Rieffenberger, and Van Dorn (2003), and Eppinger (2003).

Two statistical tests, called Wilcoxon matched pair and sign tests (Helsel and Hirsch, 2002), were used to determine whether pre- and post-wildfire data sets include statistically significant differences (fig. 29). The sign test simply computes the number of times that the value of the first chemical element (such as Mg (magnesium) in 2001 samples) is larger than that of the second element (Mg in 1996 samples). The Wilcoxon matched pair test also considers the magnitude of the difference between the two and is thus a more rigorous test. In figure 29, data for elements in the blue box are statistically significant (all have p-values <0.05) for both the sign and Wilcoxon matched pair tests relative to the pre- and post-fire sample sets. Elements plotting progressively closer to the origin at the lower left corner of the box depict differences that are progressively more statistically significant.

In stream-sediment samples, no statistically significant differences were found for Bi, Ca, CO_3^{2-}, Ce, Fe, Ho, K, La, Nb, Nd, Sb, Te, Th, or Ti (all are abundances beyond the blue box of fig. 29). However, post-wildfire sediment samples are more enriched in the major elements Al, organic C, total C, and Mg, and the trace elements Ba, Co, Cu, Li, Mn, Ni, Sc, V, and Zn. In contrast, post-wildfire stream-sediment samples are slightly depleted in As. Higher total and organic C in post-wildfire stream sediments probably results from the abundant charcoal and ash observed in sediments at most sites downstream of burned areas. In post-wildfire sediments, higher concentrations of the rock-forming elements, such as Al, Ba, Li, Mg, Mn, Ni, Sc, V, and Zn, are likely the result of addition of fine, immature, unwinnowed sediment from debris flows and landslides derived from granitoids and black slates (fig. 30). In the Panther Creek basin, Co and Cu enrichments in post-fire sediment samples may be due to new entrainment of metalliferous soils into debris flows and landslides, from areas of metal-rich rocks (Apple Creek Formation) containing sediment-hosted cobalt-copper deposits. Most of the area that contains these sediment-hosted deposits was extensively burned by the wildfire.

For stream-water samples, no statistically significant differences (p-levels >0.05) for the major ions Ca, F^-, K, Mg, Na, and Si in pre- and post-wildfire samples were identified. Water samples collected in 1996 had variably elevated temperature, conductivity, alkalinity, and concentrations of Ba, Cl^-, Co, Cu, Mn, Ni, SO_4^{2-}, U, V, and Zn (all p-levels <0.05). These effects are probably seasonal and reflect the fact that waters collected in early June of 2001 were dilute compared to those collected in mid-July of 1996. Except for pH changes (pH slightly higher in the 2001 post-wildfire samples), differences in stream-water samples collected following the wildfires were not discernible from the pre-wildfire samples.

Of particular interest in the pre-and post-fire analyses is the observation that the seven stream-sediment samples with the highest arsenic concentrations were all from the vicinity of or downstream from the Blackbird cobalt-copper mine (fig. 31). However, arsenic concentrations were lower in post-fire sediment samples than in pre-fire samples from the same sites. For these seven samples, the difference in arsenic concentrations between the two sampling periods was greater than that expected from combined analytical and sample site variation. In the most extreme cases, nearest the mine, arsenic concentrations decreased by more than

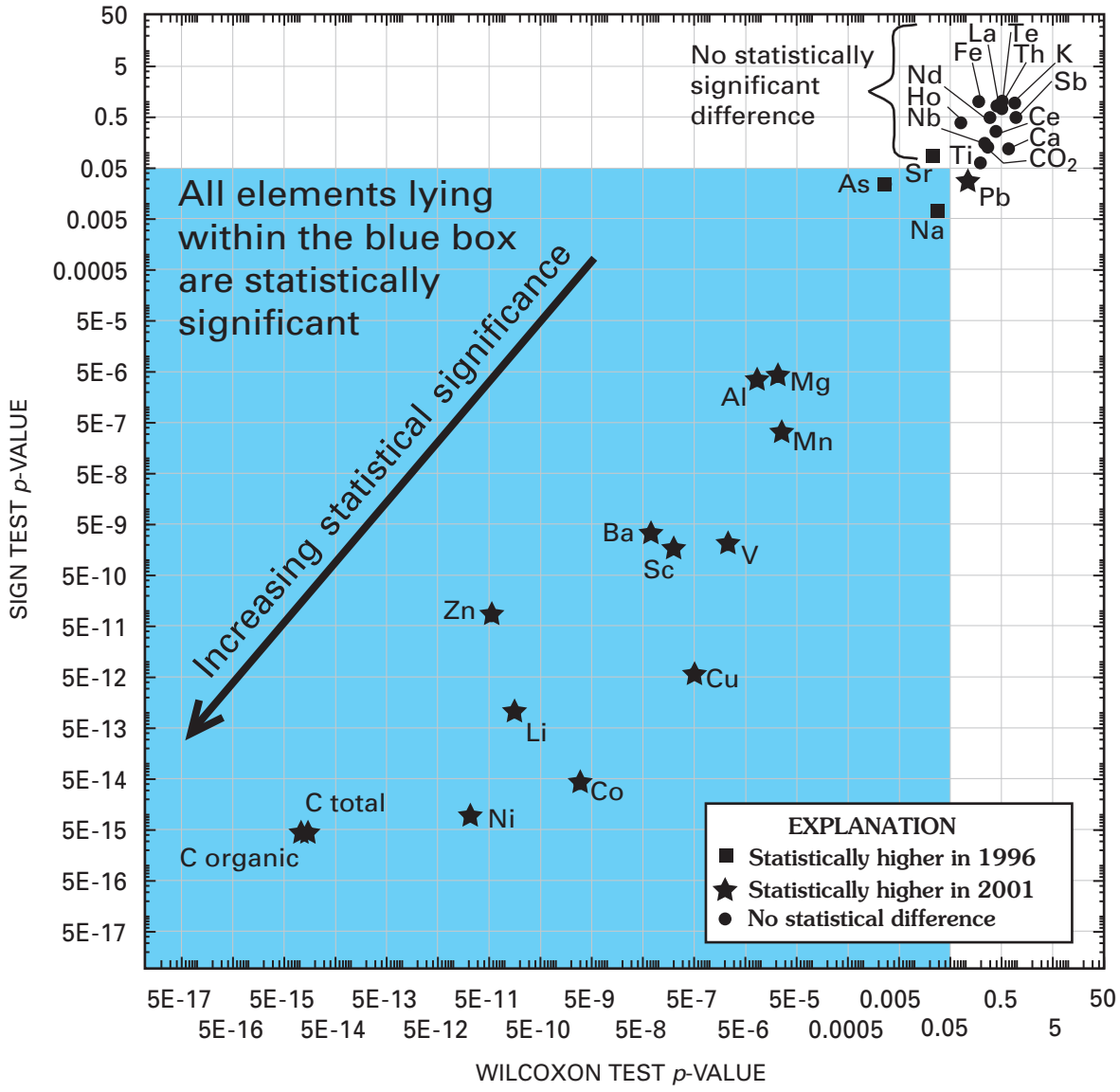

Figure 29. Elements in stream sediments showing statistically significant differences between pre-wildfire and post-wildfire sampling periods, based on 82 sample pairs.

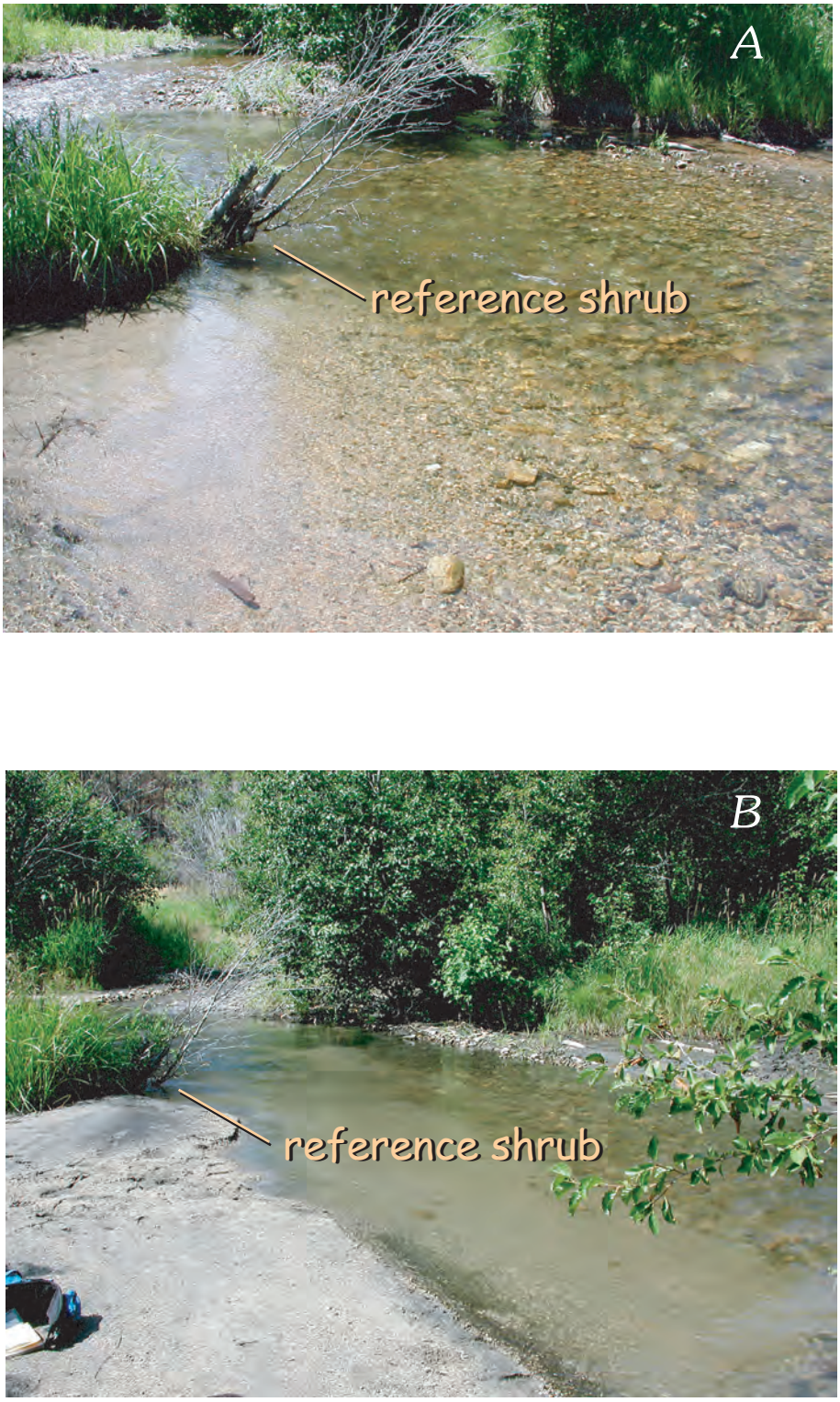

Figure 30. Photographs of Clear Creek. *A*, June 8, 2001, 10 months after the wildfire, prior to significant thunderstorm activity. *B*, July 7, 2001, same site as *A*, following thunderstorm. Note increase in fine, ash-laden, immature, unwinnowed sediment deposited by storm water.

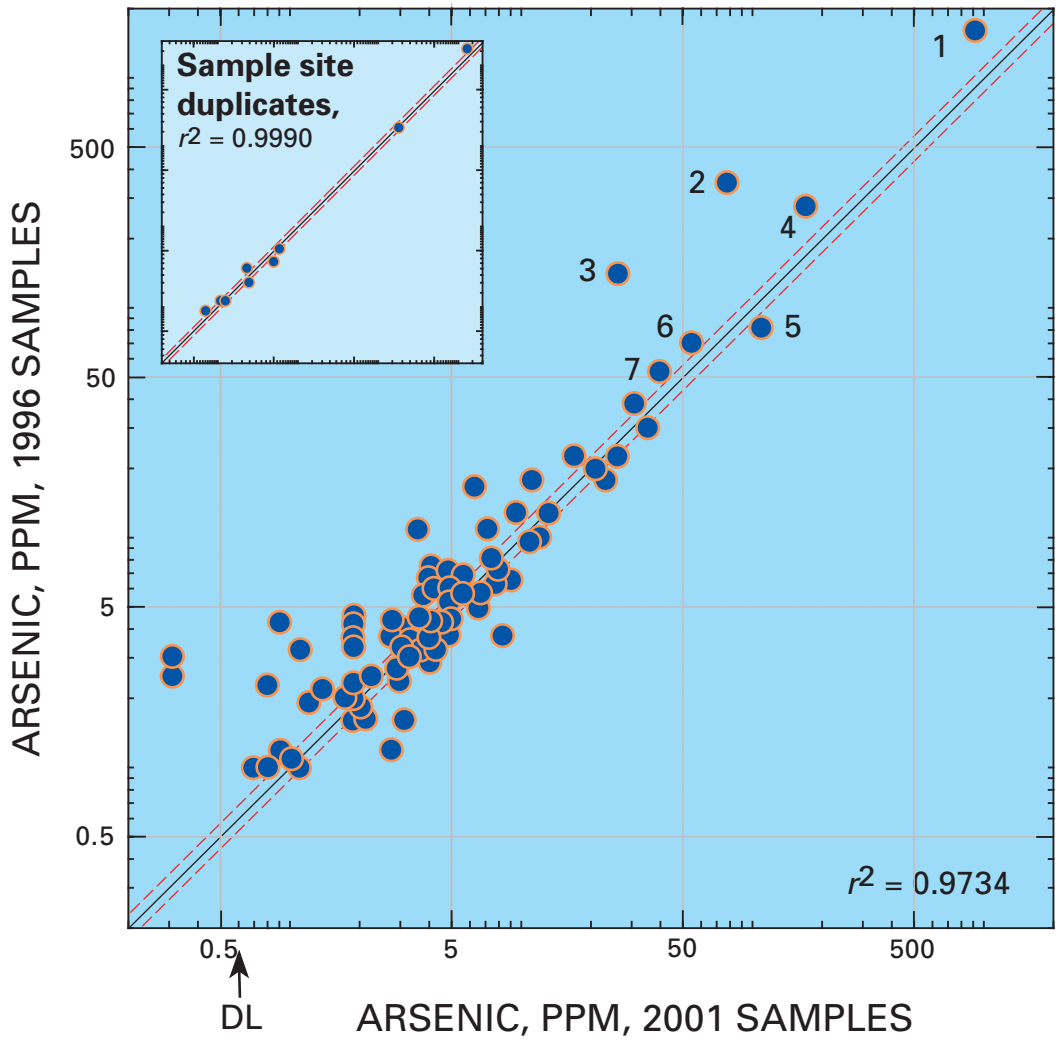

Figure 31. Arsenic in stream sediment, 1996 versus 2001 samples. Red dashed lines enclose ± 14 percent analytical error limits; ppm, parts per million; DL, analytical detection limit. 1, Blackbird Creek; 2, South Fork of Big Deer Creek; 3, Big Deer Creek at mouth; 4, Panther Creek upstream of Deep Creek; 5, Panther Creek upstream of Big Deer Creek; 6, Panther Creek upstream of Beaver Creek; 7, Panther Creek at mouth.

40 percent. For example, at the mouth of Big Deer Creek, the 1996 arsenic concentration was 140 ppm, while the 2001 arsenic concentration was only 26 ppm, an 80 percent reduction. The Blackbird mine area is being remediated, and a water treatment plant to divert and treat mine drainage was installed between the 1996 and 2001 sampling periods. Lower arsenic concentrations in 2001 sediments appear to reflect the success of this treatment plant in reducing precipitation of arsenic-bearing iron oxyhydroxide precipitates in affected drainages.

Geochemical Signatures of Diverse Mineral Deposit Types in the Upper Salmon River Watershed, Central Idaho

By Bradley S. Van Gosen, Robert G. Eppinger, Jane M. Hammarstrom, Paul H. Briggs, and D.W. Peters[1]

The upper part of the Salmon River watershed, in Custer County, central Idaho (fig. 32), was selected for a pilot study concerning the geochemistry of ore, mine waste, host rock, altered rock, stream sediment, and water. This huge watershed provides a cross section of the geology and mineral deposits that characterize the central part of the Headwaters Province. This topical area extends from near Stanley on the west to Challis on the east and includes mainly public but also some private lands that lie north and south of the Salmon River (fig. 32).

The purpose of this investigation is to support studies of ecosystem structure and function by providing appropriate information about the geologic framework within which the ecosystem operates. Lithologic/lithochemical units and mineral deposit types, as influences on biological processes, can be linked with local water properties to forecast environmental conditions. Thus, physical and chemical analysis of the region's various rock types produces information that impacts (1) assessment of forest health and salmon habitat, (2) assessment of local water characteristics in terms of quality and natural element content, and (3) development of management decisions and practices.

Reconnaissance Geochemical Study

Fifty-six sites were sampled, including mines, mill and smelter sites, and prospects located along tributaries to the Salmon River. Sites away from known mineralized areas were also sampled. The selected area is ideally suited to serve as a pilot project concerning geoenvironmental signatures of mineral deposits because:

1. The upper Salmon River watershed contains a number of distinct mineral deposit types, hosted by a wide variety of rock types and geologic settings, within a relatively small region.

The geologic framework and mineral-resource potential of the watershed are well documented (Worl and others, 1989; Fisher and Johnson, 1995). The Stanley to Challis region includes more than 200 inactive mines and prospects as well as a few active and recently reclaimed mines, mill sites, and smelter sites (Mitchell and others, 1986). Eleven types of mineral deposit types are represented. The area includes both mined and unmined deposits that are hosted by a variety of different lithologies (table 8). Many of the deposit types contain pyrite and other metal-sulfide minerals that can create acid drainage. Host rocks include carbonates that can provide natural acid neutralization, as well as granites, argillites, sandstones, black shale, and silicic volcanic rocks that have little or no acid-neutralizing capacity. The types of mineral deposits and host lithologies in the upper Salmon River watershed are also present in many other parts of the Headwaters Province.

2. Tributaries of the upper Salmon River contain spawning grounds of the threatened chinook salmon and endangered sockeye salmon, as well as habitats of threatened steelhead (migratory rainbow trout) and bull trout.

Efforts are being made to protect and restore habitat for these fish species throughout the Salmon River. Data collected in this area address the following questions:

- Are the waters and sediments in the upper Salmon River watershed affected by past mining and (or) by natural erosion of mineral deposits (for example, elevated metal concentrations, acidity)?
- Do the metal concentrations exceed regulatory standards or habitat conditions that would impede the reintroduction of these fish?
- Do stream sediments contain elevated concentrations of elements that may affect the health of benthic organisms?

3. The upper Salmon watershed includes Federal lands that are used for a variety of purposes.

The Salmon River is a designated National Wild and Scenic River. The topical area borders the Salmon River in the Salmon-Challis and Sawtooth National Forests. Lands administered by the Bureau of Land Management (BLM) also occur within the watershed. The area is used for numerous recreational purposes, including hiking, camping, rafting, and fishing. To address human health or ecosystem issues, a number of mines in the study area have already been reclaimed by the FLMA working cooperatively with the State and the U.S. Environmental Protection Agency (EPA).

[1]Salmon-Challis National Forest
HC63, Box 1669
Challis, ID 83226.

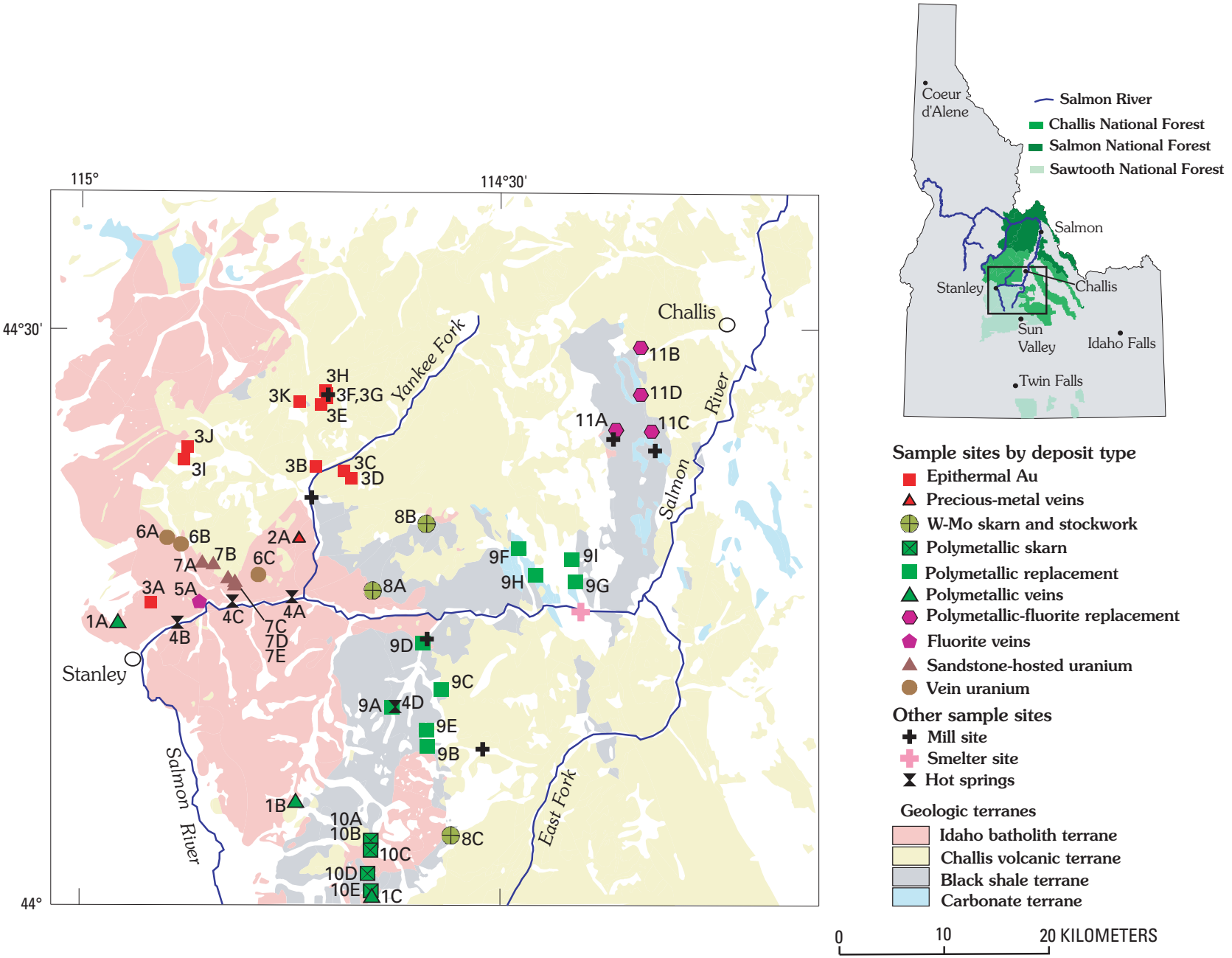

Figure 32. Upper Salmon River watershed and vicinity, showing sample sites, mineral deposit types, and generalized geology. See table 8 for key to numerical identities.

Study Methods

Representative examples of different types of mineral deposits were sampled throughout the watershed during the summers of 1999 through 2002 (table 8; fig. 32), including inactive mines and prospects, mineral occurrences, drainages, and unmineralized areas. Host rocks include granitoid igneous and volcanic rocks, metamorphosed rocks, and sedimentary rocks of several different ages and facies belts (Fisher and Johnson, 1995). A variety of different mineral deposit types, including those rich in precious metals (gold and silver), base metals (lead, copper, zinc), tungsten and molybdenum, uranium, or fluorite, or some combination of these elements (table 8; figs. 32, 33), were sampled at multiple sites.

At each site, samples of mineralized rock, altered rock, host rock, secondary minerals, mine waste, tailings (if present), and any available mine or seep discharges were collected (Van Gosen and others, 2000; Hammarstrom and others, 2002). A number of "background" sites, including active hot springs, streams upgradient from past and present mining activity, and representative outcrops of particular lithologies (not listed in table 8), were sampled to characterize natural conditions away from known mineralized areas. True "background" conditions are difficult to establish in developed areas; our data are actually "baseline" data because they represent the geochemistry at a particular time.

Previous studies demonstrate a number of geologic controls on the composition of natural water and mine water that drain mineral deposits in other geologic settings (Plumlee and others, 1999). By collecting geochemical data for multiple sample media, multiple mineral deposit types, and multiple examples of each deposit type in the same watershed and same climatic setting, we have been able to evaluate geologic controls of diverse types of mineral deposits and host rock on the water in the upper Salmon River watershed. Chemical composition of solid samples (mineralized rock, altered rock, host rock, secondary minerals, mine waste, tailings) provides a link to the interpretation of water samples collected at or near the same sites. For example, the presence of elevated cadmium and lead concentrations in water downstream from a mine may be explained by conditions originating at the mine site. If these metals are absent in solid samples of ore and mine or mill waste, then elevated cadmium and lead abundances may be related to some other source, such as discarded batteries or equipment. Water concentration may exceed standards because of elevated natural background concentrations or because of contamination from mining or other human activities. Similarly, both natural and disturbed streambed sediment may be inhospitable to benthic organisms, thereby having an adverse impact on the food supply for fish and other species.

Water Samples

Water was sampled at adit drainages, streams, ponds, springs, and seeps. Water directly related to mined deposits was collected, as well as background water samples. All water sampling was conducted in August, when stream and river discharges approach low-flow conditions following peak discharge in June. At each sample site, a filtered (0.45 μm disposable filter), acidified (HNO_3) sample and an unfiltered (raw), acidified (HNO_3) sample were collected and analyzed for comparison of dissolved versus suspended chemical constituents. Water parameters measured in the field at each site included pH, conductivity, field alkalinity, turbidity, dissolved oxygen, acidity, flow (estimate), color, and odor. Cations were determined by inductively coupled plasma–atomic emission spectrometry (ICP-AES) and inductively coupled plasma–mass spectrometry (ICP-MS); anions were measured by ion chromatography (Taggart, 2002).

Solid Samples

The solid media collected in this study included

1. Composite samples of fine (<2 mm diameter) material from the upper 5 cm of mine-waste, mill-tailings, and flotation-tailings piles
2. Stream sediments upstream and downstream of mined deposits and occurrences
3. Ore- to sub-ore-grade rocks from mine dumps, ore piles, and adits
4. Wallrocks found adjacent to the ore zones, containing the alteration minerals that border the ore bodies
5. Unaltered examples of the rock types that host the mineral deposits
6. Soils in mineralized and unmineralized (background) settings in mined areas, and
7. Secondary minerals, coatings, and crusts.

Solid samples were analyzed for 40 major, minor, and trace elements by ICP-AES. In addition, arsenic, antimony, selenium, tellurium, thallium, gold, mercury, total carbon, carbonate carbon, and total sulfur were analyzed by element-specific techniques. Composite mine-waste materials were subjected to a passive leach procedure (Hageman and Briggs, 2000; Hageman, 2000) to simulate the potential chemical composition of initial rainwater runoff from the surfaces of mine-waste and mill-tailings piles.

Results

All of the analytical data and site observations from this study were compiled in a digital database, which can be used to create customized views of the geochemical landscape at a variety of scales. The database provides a tool for land managers, ecologists, biologists, geoscientists, and consultants to evaluate relationships between the geochemical signature of the topical area and other spatial parameters.

The following site-specific reports were prepared for areas of particular interest to the USDA Forest Service and BLM:

Table 8. Types of mineral deposits sampled by this study within the upper Salmon River watershed.

No. in fig. 33[1]	Deposit type	Mineral deposit description	Host-rock type	Examples sampled in the project area[2]
1	Polymetallic veins	Pb-Cu-Zn-Ag-Au quartz veins within shear zones.	granitic rocks	Bronco mine (1A), Aztec mine (1B).
2	Precious-metal veins	Au-Ag-bearing quartz veins	granitic rocks	Prospect along Rankin Creek (2A).
3	Epithermal Au	Au-bearing rhyolite porphyry dike	granitic rocks	Iron Crown mine (3A).
4	Hot spring	Active hot springs	variable	Sunbeam (4A), Elkhorn (4B), Basin Creek (4C), Slate Creek (4D) hot springs.
5	Fluorite veins	F-quartz veins filling fault zones	granitic rocks	Hideout group (5A).
6	Vein U	U concentrations in fracture zones	granitic rocks	Baker claims (6A), Lightning No. 2 mine (6B), Alta mine (6C).
7	Sandstone-hosted U	U minerals in fluvial rocks	arkosic conglomerate, arkosic sandstone, siltstone.	Shorty Pit (7A), East Basin No. 1 (7B), Coal Creek No. 1 (7C), and Deer Strike mines (7D); Little Joe prospects (7E).
3	Epithermal Au	Au-Ag-base-metal (Cu-Pb-Zn)-bearing veins.	volcanic rocks	Charles Dickens (3B), General Custer (3C), Lucky Boy (3D), Montana (3E), McFadden (3F), Golden Gate (3G), and Tonto (3H) mines.
3	Epithermal Au	Thin veins with low Au values	rhyolitic volcanics	Hindman and Jumbo claims (3I); several prospects in the Red Mountain area (3J).
3	Epithermal Au	Disseminated and vein Au-Ag deposits.	volcanic and volcaniclastic rocks.	Grouse Creek mine (3K).
8	W-Mo skarn and stockwork.	W-Mo deposits	contact-metamorphosed argillite and quartzite.	Peach Creek W claims (8A), Thompson Creek W mine (8B), Baker Lake molybdenum prospect (8C).
9	Polymetallic replacement.	Zn-Pb-Cd-Ag deposits	argillite-limestone-quartzite-marble-hornfels breccia.	Hoodoo mine (9A).
1	Polymetallic veins	Pb-Zn-W-Ag in quartz veins within shear zones.	granitic rock	Reconstruction vein (1C).
10	Polymetallic skarn	Zn-Pb-Ag (±W±Au) deposits	contact-metamorphosed argillite and sheared argillite.	Confidence property (10A), Deer Trail mine (10B), Rupert mine (10C), Meadow View property (10D), Empire Vein (10E).
9	Polymetallic replacement	Zn-Pb-Ag-Cu deposits along faults.	sheared argillite	Livingston mine (9B), Cal-Ida mine (9C), Silver Bell group (9D), Hermit mine (9E).
9	Polymetallic replacement	Pb-Zn-Ag deposits	calcareous argillite	Redbird mine (9F).
9	Polymetallic replacement	Ag-Pb-Zn deposits	dolomite and quartzite	Clayton mine (9G), South Butte mine (9H), unnamed prospect (9I).
11	Polymetallic-fluorite replacement.	Fluorite-rich Ag-Cu-Pb-Zn-veins in fault zones.	slate	Skylark mine (11A).
11	Polymetallic-fluorite replacement.	Massive fluorite and quartz	dolomite breccia in a paleokarst horizon.	Chalspar No. 1 claim (11B).
11	Polymetallic-fluorite replacement.	Fluorite-rich Ag-Pb-Zn-Cu deposits along fault zones.	dolomite	Pacific mine (11C).
11	Polymetallic-fluorite replacement.	Fluorite-rich Cu-Ag-Pb-Zn deposits	dolomite breccia in a paleokarst horizon.	Keystone mine (11D).

[1]Numbers refer to areas labeled in figure 33 (west to east).

[2]Number-letter combinations refer to sample sites in figure 32.

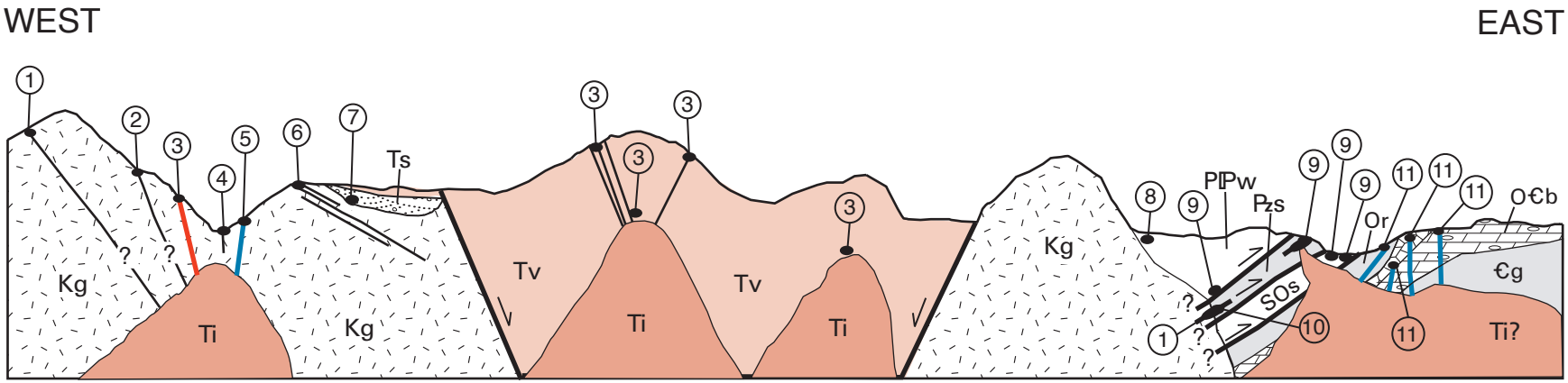

EXPLANATION

Tv	**Challis Volcanic Group (Eocene)**—Dominantly volcanic and volcaniclastic rocks
Ts	**Arkosic sandstone, conglomerate, and siltstone (Eocene?)**—Fluvial deposits at the base of the Challis Volcanic Group; deposited on the eroded surface of the Idaho batholith
Ti	**Intrusive rocks coeval with the Challis Volcanic Group (Eocene)**—Queried where inferred
Kg	**Plutonic granitoid rocks of the Idaho batholith (Cretaceous)**—Dominantly medium grained to coarse-grained quartz monzonite and granodiorite
PIPw	**Wood River Formation (Lower Permian to Middle Pennsylvanian)**—Sandstone, limestone, quartzite, argillite, siltstone, and local conglomerate
Pzs	**Salmon River assemblage (Paleozoic)**—Argillite, siltstone, sandstone, and local limestone
SOs	**Saturday Mountain Formation, Kinnikinic Quartzite, and Ella Dolostone (Lower Silurian to Ordovician)**—Dolomite, quartzite; locally abundant siltstone, shale
Or	**Ramshorn Slate (Ordovician)**—Mainly slate; minor sandstone, conglomerate
O€b	**Bayhorse Dolomite (Lower Ordovician and Upper Cambrian**—Dolomite, limestone
€g	**Garden Creek Phyllite (Middle? Cambrian)**—Phyllite; minor dolomite

Rhyolite dike

Fluorite-bearing fracture zone

Fracture zone—Queried where extent uncertain

Fault with large offset—Barb shows direction of relative movement; queried where extent uncertain

Figure 33. Schematic cross section displaying general geologic setting of mineral deposits in upper Salmon River watershed of central Idaho. Circled numbers refer to mineral deposit types listed in table 8. Diagram is not to scale and is designed for descriptive purposes only; precise relationships between mineral deposits, structures, and intrusions should not be inferred from the diagram. Rock unit descriptions are provided in Fisher and others (1992), Hobbs and others (1991), and Hobbs (1985).

1. Results for the Thompson Creek tungsten mine (fig. 32, site 8B), a tungsten-molybdenum skarn deposit, are summarized in Van Gosen and others (2000).

2. Hammarstrom and others (2002) described the pre-reclamation environmental composition of waters and stream sediments at the Clayton silver mine (fig. 32, site 9G), a polymetallic replacement deposit.

3. Chemical and mineralogical data for massive slag from the Clayton Smelter (fig. 32), which processed ore from many of the deposits in the watershed, are included in Piatak and others (2003).

Highlights

Acid-Rock Drainage

Acid-rock drainage is the water-quality hazard produced by the oxidation of pyrite in an aqueous environment. Acid water that drains waste rock, tailings, open pits, and adits typically has low pH values (2–4) and elevated concentrations of potentially toxic metals (Nordstrom and Alpers, 1999). Mine-related acid-rock drainage is referred to as acid mine drainage. Mine-related water in the watershed topical area falls into two groups: (1) acidic water with pH in the range from 3 to 4 and dissolved base-metal concentrations >100 ppb (parts per billion, equal to μg/L, micrograms per liter); and (2) near-neutral water (pH 5.5–8.5) with highly variable dissolved base-metal concentrations (fig. 34). Group 1 water samples are associated with epithermal gold deposits, such as the Grouse Creek mine. These deposits are pyrite rich and are hosted by silica-rich volcanic rocks that have little to no acid-neutralizing capacity. Group 2 water samples include those draining carbonate-hosted deposits (polymetallic skarn and replacement deposits). Zinc is the principal dissolved base metal. Fourteen mine-related water samples and 1 stream sample (collected 0.8 km downstream from a mine site) contained dissolved zinc concentrations that exceed the EPA's recommendation for the maximum concentration for zinc in surface water that is safe for aquatic life, which they established as 120 μg/L of zinc (U.S. Environmental Protection Agency, 2002, p. 13). An aquatic community exposed to these high concentrations of zinc (>120 μg/L), even briefly, is expected to result in an "unacceptable effect" on the aquatic life. Background stream waters sampled upstream of mines in the topical area are all near-neutral and contain <3 μg/L dissolved zinc. The natural hot springs sampled had elevated pH (8.8–9.5) and very low dissolved base metals. Natural cold-water springs in unmineralized or weakly mineralized areas have near-neutral pH and dissolved base-metal contents of <50 μg/L. One spring flowing from beneath a talus pile in an area of altered volcanic rock had a pH of 4.2. Although pyrite was present in many of the mineral deposits in the watershed, this study shows that significant acid mine drainage was not present at most of the mine sites. However, natural acid-rock drainage is associated with hydrothermally altered rocks of the Challis volcanic terrain in the western part of the study area.

Lithologic Controls on Water Quality

Acidity and alkalinity are useful parameters for comparison of water from diverse sources. Acidity of a water sample is its quantitative capacity to neutralize a strong base. Acidity is calculated by measuring the volume of strong base that must be added to the water sample in order to reach a designated pH (pH of 8.3 for total acidity). Alkalinity is similarly calculated, and is the capacity of water to neutralize a strong acid to a pH of 4.5 (Ficklin and Mosier, 1999). Acidity and alkalinity reflect the pH and buffering capacity of the water being studied. Mine drainage associated with the mineral deposits in the topical area that are hosted by rhyolitic (quartz-rich) volcanic rocks has high acidity (fig. 35; table 8). The streams sampled across the pilot area had alkalinity ranging from 22 to 110 ppm $CaCO_3$, indicating that the streams have at least some acid-neutralizing capacity.

Arsenic

Elevated arsenic abundances are common to a variety of mineral deposit types within the upper Salmon River watershed. Consequently, arsenic abundances are elevated in a variety of sample media collected from a variety of different types of deposits in the watershed. For example, uranium ore in the Stanley area contains up to 8,600 ppm (parts per million) arsenic (fig. 32, sites 7A–7E). Ore from many polymetallic skarn, vein, and replacement deposits, as well as ore from epithermal gold deposits, contains more than 1,000 ppm arsenic. Approximately 40 percent of the mine-waste piles and mill tailings sampled contain arsenic in soil-size material in excess of the EPA preliminary remediation goal for arsenic in industrial soils (260 ppm As). About 30 percent of our stream-sediment samples exceeded the consensus-based probable effects concentration (PEC) guideline for arsenic (>33 ppm As) in sediments associated with fresh-water aquatic ecosystems. PEC is defined as the concentration above which adverse toxic effects are likely to occur (MacDonald and others, 2000). These data provide a screening tool to define areas where site-specific toxicity studies may be warranted.

The enforceable Maximum Contaminant Level (MCL) for arsenic allowed in drinking water was previously 50 ppb (equal to 0.05 mg/L), as set by the EPA. On January 23, 2006, the MCL for arsenic in drinking water was lowered to 10 ppb (U.S. Environmental Protection Agency, 2001). All the background water samples collected in the upper Salmon River watershed contained <10 ppb dissolved arsenic (fig. 36). However, some mine-related water contains dissolved arsenic concentrations in excess of the previous and the revised drinking water standards. A natural spring discharging from mineralized bedrock near the General Custer mine

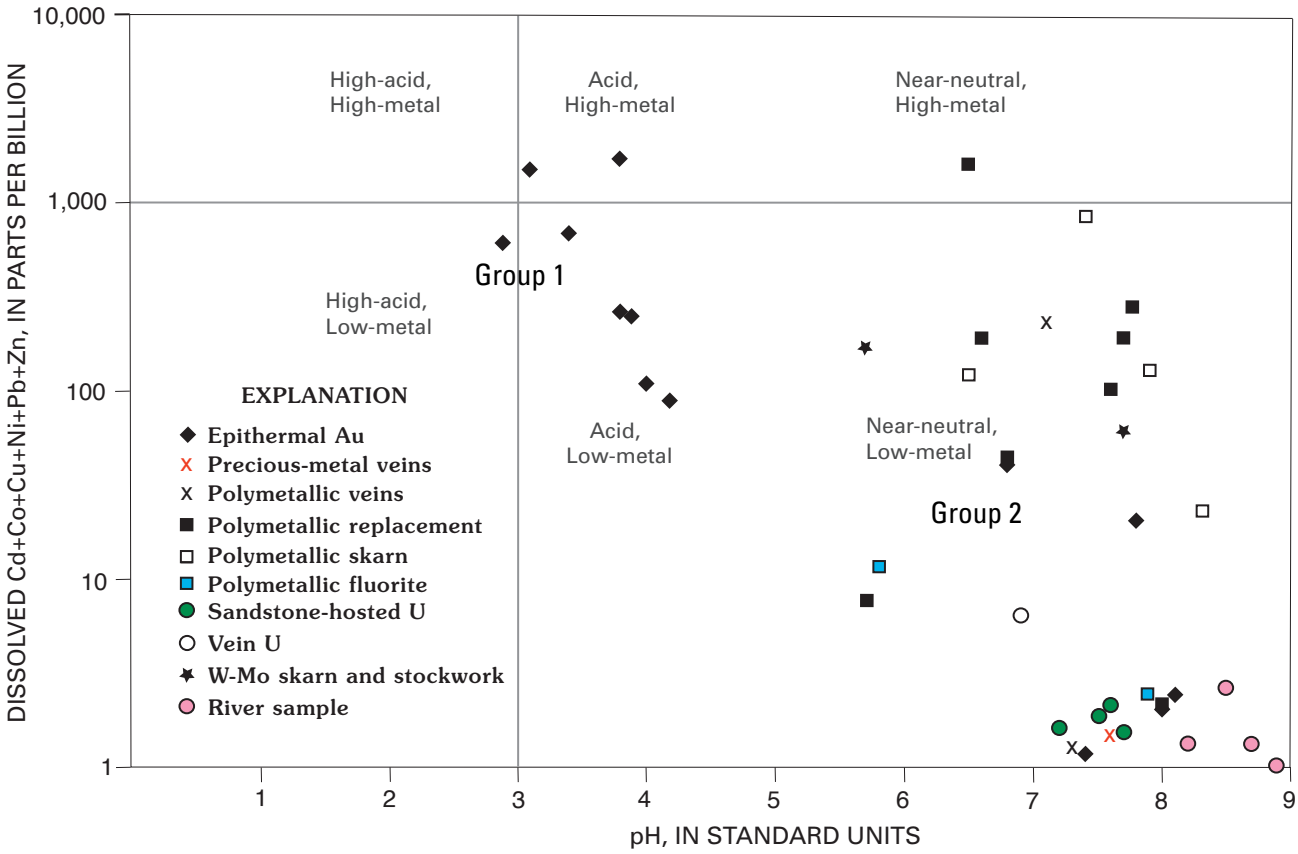

Figure 34. Ficklin diagram showing sum of dissolved base-metal concentrations in mine water (adit drainage, springs or seeps in mined areas, and open pit water) and river water as a function of pH. Mine-related water in the watershed falls into two broad groups: (1) Group 1 water is acidic (pH 3 to 4) with dissolved base-metal concentrations >100 ppb, and (2) Group 2 water is near-neutral (pH 5.5 to 8.5) with variable dissolved base-metal concentrations. Boundaries and names of fields are from Plumlee and others (1999). Parts per billion (ppb) and micrograms per liter (μg/L) are equivalent concentration units.

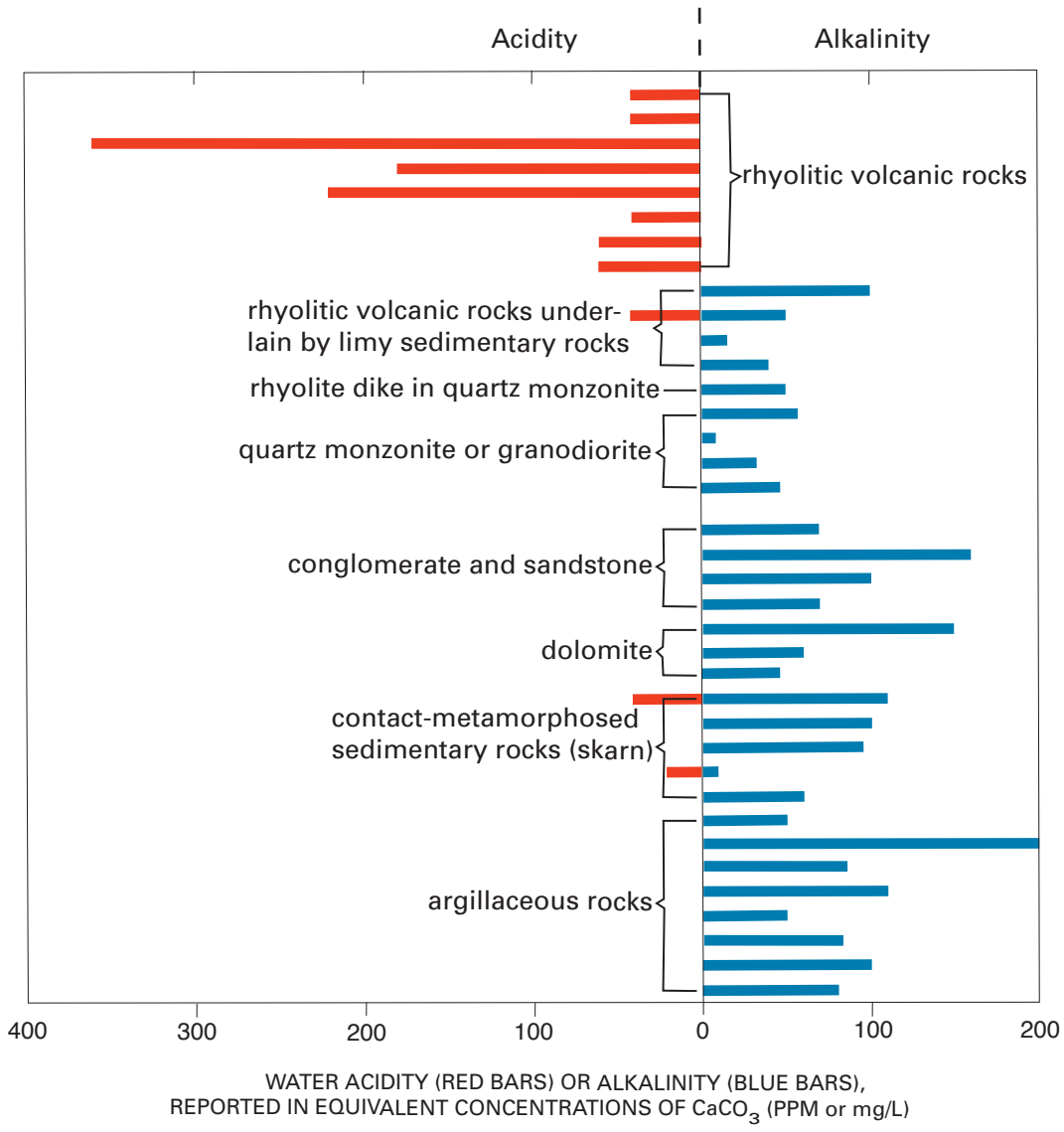

Figure 35. Graphical display of acidity and alkalinity measured in 37 mine water samples from upper Salmon River watershed. These samples, also plotted in figure 34, include adit drainage and pond, spring, and seep water from within mined areas. Labels indicate primary host rock type at each mineral deposit. Acidity and alkalinity defined by Ficklin and Mosier (1999).

(fig. 32, site 3C) contained 110 ppb dissolved arsenic. Some adit water and water in a pond that fills an open pit contained dissolved arsenic concentrations in excess of current (2003) EPA fresh-water chronic and acute contaminant criteria (150 and 340 ppb, respectively).

Wildlife such as deer and elk are known to drink arsenic-rich mine water in the area, which may affect their health. However, relationships between mine-water chemistry and wildlife health have not been studied in this region. New domestic water wells are likely to be developed in the watershed as more homes are built. Further, water supplies in public campgrounds may be unsuitable for drinking as indicated by new water-quality standards. Thus, in central Idaho, management issues of natural and anthropogenically modified water and (or) sediment include an evaluation of concerns related to arsenic abundances when plans are prepared or modified.

Environmentally Significant Metals in Mine Wastes, Mill Tailings, and Stream Sediments

Many metals, including arsenic, cadmium, chromium, mercury, nickel, lead, zinc, and a number of others (Kelly, 1999; Goyer and Clarkson, 2001; Sullivan and Krieger, 2001), can act as toxins to humans and biota. Several metals that potentially pose significant environmental risk are concentrated in mine-waste piles and mill tailings that are scattered throughout the pilot area and the greater watershed area. The metals occur in a variety of concentrations and mineral forms, each of which can react at different rates via an array of dynamic processes throughout the ecosystem.

High metal concentrations do not necessarily indicate an environmental hazard. Many factors influence metal hazard potential, including solubility, physical and chemical mobility, exposure setting, and biologic availability of the metal (Krieger and others, 1999). Analyses of solid media, considered relative to water-quality data, are useful in evaluating the chemical characteristics of (1) specific sites of interest and (2) groups of deposits sharing similar attributes (deposit types).

Analyses of fine (<2 mm diameter) material on the surfaces of mine-waste and mill-tailings piles show that most polymetallic skarn, polymetallic replacement, and polymetallic-fluorite replacement deposits in the watershed (table 8) contain the highest concentrations of metals; especially enriched are antimony, lead, and zinc. For example, surfaces of about three-fourths of the waste piles associated with polymetallic deposits have lead concentrations that exceed the EPA's preliminary goal for lead in industrial soils (1,200 ppm Pb). About one-fourth of the same mine and mill piles contain antimony in excess of the EPA remediation goal of 410 ppm Sb. High zinc concentrations are common in mine and mill piles associated with polymetallic deposits—more than three-fourths of the surficial samples from polymetallic dumps contain at least 0.1 weight percent Zn. Additionally, as noted previously, a majority of the deposit types and their waste piles contain arsenic concentrations that exceed the EPA's preliminary goal for industrial soils (260 ppm As).

Many of the stream-sediment samples that were collected downstream from former mining operations reveal metal concentrations that exceed PEC guidelines (MacDonald and others, 2000) for sediment in fresh-water aquatic ecosystems. Many stream-sediment samples collected downstream of polymetallic skarn deposits exceed the PEC guidelines for arsenic, cadmium, chromium, nickel, and zinc. Concentrations of these metals, plus lead, typically exceed the PEC in sediment downstream of developed polymetallic replacement deposits. Chromium and nickel concentrations exceed the PEC in sediment collected downstream from tungsten-molybdenum skarn and stockwork deposits.

Metal abundances in stream sediment downstream from mined deposits should be compared to background sediment collected from the same or similar geologic setting. For example, some background sediment samples were collected upstream from mines and mill sites, yet contain abundances of cadmium and chromium that exceed the PEC guideline values. Cadmium and chromium enrichments of this sort were most common where the stream segments crossed dark, carbonaceous, fissile sedimentary rocks (argillite or black shale or slate). Thus, surrounding host rocks can naturally contribute metals to the streambed through erosion; as examples, cadmium and chromium are dispersed from black shale and arsenic from volcanic rocks in this fashion.

Conclusions

Mine-related water in the upper region of the Salmon River watershed is an expression of varied mineral deposit types and their host geologic environments. Water samples were collected during periods (in August of three successive years) when stream and river discharges were approaching base flow. Results suggest that acid mine drainage is not a widespread problem in the area. However, natural acid-rock drainage occurs locally in mineralized areas of the volcanic terrain. Additionally, mineral deposit types and geologic terrains not associated with volcanic rocks (fig. 32) typically yield neutral to alkaline natural water that exhibits a variety of different metal concentrations (fig. 34).

A number of potentially toxic metals are concentrated in abandoned mine waste piles and mill tailings in the upper Salmon River watershed. Polymetallic skarn, polymetallic replacement, and polymetallic-fluorite replacement deposits contain the highest concentrations of metals; these deposit types are especially enriched in antimony, lead, and zinc. Most deposits in the watershed contain elevated concentrations of arsenic.

To fully evaluate the significance of the metal anomalies requires comparison to background values obtained from the same drainage or similar geologic environment. Metal hazard analyses also consider the solubility, physical and chemical

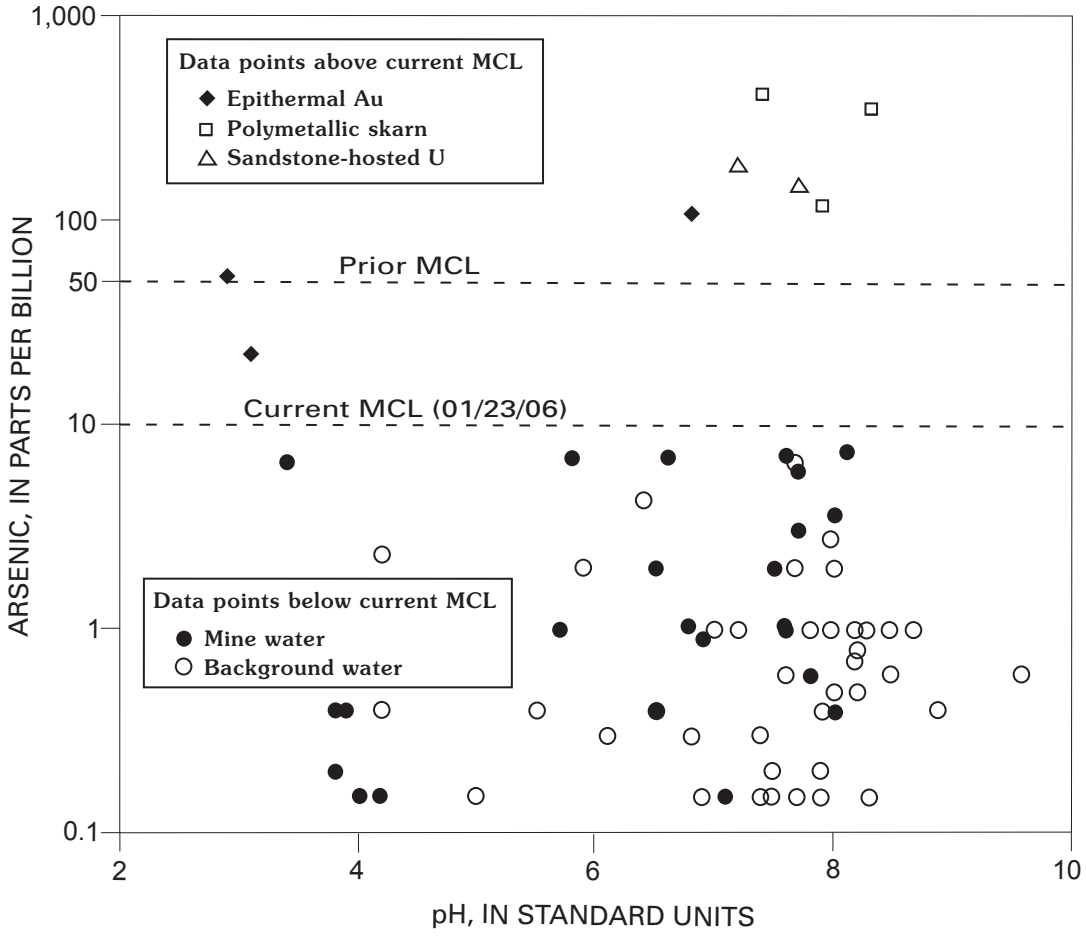

Figure 36. Dissolved arsenic concentrations versus pH in natural waters collected in the upper Salmon River watershed. Samples include: mine water, which includes adit drainage and ponds, seeps, and springs in mined areas; and background water, such as creeks, ponds, and springs that lie upgradient of mined areas. Dashed lines, prior and current (January 23, 2006) Maximum Contaminant Level (MCL) standard for arsenic in drinking water, as set by the EPA (U.S. Environmental Protection Agency, 2001). Deposit type is shown for water samples with arsenic above the MCL.

mobility, exposure setting, and biologic availability of potentially toxic metals.

Applications of the Study

Geochemical data for different sample media provide a snapshot of prevailing conditions in the upper region of the Salmon River watershed and can be used to

- Prioritize inactive and abandoned mine site cleanup and develop cost-effective remediation strategies
- Anticipate environmental effects of future mine development for similar deposit types
- Identify the geochemical signature of solid materials and water that may affect biota
- Extrapolate to geologically similar settings elsewhere in the Headwaters Province to predict the likelihood of adverse environmental effects of mining
- Increase our understanding of the geoenvironmental signature for a number of mineral deposit types within a relatively dry ecoregion: the Middle Rocky Mountain Steppe–Coniferous Forest–Alpine Meadow Province ecoregion (Bailey, 1995).

Summary

The quantity and quality of geologic data and of geologic understanding of the Headwaters Province, part of the geologically least well known area in the continental United States, are significantly enhanced through the research activities of this project. Improved geologic mapping, newly acquired digital geologic map data sets, and standardization of digital data sets enhance future availability and use of geoscience data at a variety of scales for assessments of mineral resource potential, interpretation of geology, and interpretation of geophysical and geochemical data sets. Geochemical data, initially available for the project area from the NURE and RASS databases, were compromised by the presence of artificial anomalies along quadrangle and project boundaries that resulted from variable determination limits and levels of accuracy and precision. Normalization of these data using standardized concentrations fostered creation of geochemical surface models that can be combined with diverse data sets in future evaluations. As a consequence of data synthesis and conversion activities conducted by the Headwaters Province project, complete province-wide digital data sets are now more easily accessible, scalable, available in standardized formats, and adaptable for local and regional uses; they are consequently readily applicable to land-use planning decisions.

New interpretations of aeromagnetic maps for the Headwaters Province were combined with limited new geologic observations of mostly covered basement to develop a comprehensive basement framework; the resulting synthesis integrates topical and regional studies that are applicable to local as well as global mineral resource assessments. Although the Great Falls tectonic zone was previously identified as a zone of concentrated mineralization, the overwhelming influence on metal endowment exerted by the Paleoproterozoic suture in the center of the zone is now demonstrated in findings of the Headwaters Province project. Results of the project identify the fundamental impact of endowed basement composition and of deep-seated structural flaws related to basement architecture as the features critical to localizing much younger hydrothermal mineralization across the Headwaters Province. Development of these concepts has resulted from accumulation and evaluation of region-wide deposit data sets, study of the composition, age, and origin of the many plutonic systems that host mineral deposits, and investigation (in four dimensions) of magmatism and hydrothermal mineralization associated with the Boulder batholith.

Reevaluation of basement tectonics in the context of the stratigraphic and structural setting of Mesoproterozoic strata is applied in formulating region-wide models that document how tectonic setting and basin evolution influenced the location of sediment-hosted mineral deposits. Crosscutting northwest-trending Mesoproterozoic structures are now seen to have clearly exerted fundamental controls on development of Proterozoic sedimentary basins (the Belt, east-central Idaho, and Windermere). These structures were also probably important in localizing sediment-hosted deposits and later in channeling basement metal endowments through associated fractures, resulting in crustal metal recycling during later orogenesis and resulting mineralization episodes. The geochemical signature of these structurally controlled facies belts in the upper region of the Salmon River watershed is now well established, as a consequence of baseline multi-media sampling and analysis completed as part of the Headwaters Province project. Host-rock and mineral deposit compositional characteristics are available for extrapolation to assessments of the impacts of geologic factors on endangered habitats, province-wide. The Headwaters Province project has significantly enhanced the potential efficacy of future regional, national, and global mineral resource and geoenvironmental assessments by providing comprehensive data, readily accessible to future use by all interested parties.

References Cited

Anderson, A.L., 1947, Cobalt mineralization in the Blackbird district, Lemhi County, Idaho: Economic Geology, v. 42, p. 22–46.

Anderson, A.L., 1961, Geology and mineral resources of the Lemhi quadrangle, Lemhi County, Idaho: Idaho Bureau of Mines and Geology Pamphlet 124, 111 p.

Anderson, H.E., and Davis, D.W., 1995, U-Pb geochronology of the Moyie sills, Purcell Supergroup, southeastern British Columbia—Implications for the Mesoproterozoic geological history of the Purcell (Belt) basin: Canadian Journal of Earth Sciences, v. 32, p. 1180–1193.

Armstrong, R.L., 1975, Precambrian (1,500 m.y. old) rocks of central Idaho—The Salmon River Arch and its role in Cordilleran sedimentation and tectonics: American Journal of Science, v. 275–A, p. 437–467.

Armstrong, R.L., Hollister, V.F., and Harakel, J., 1978, K-Ar dates for mineralization in the White Cloud–Cannivan porphyry molybdenum belt of Idaho and Montana: Economic Geology, v. 73, p. 94–108.

Armstrong, R.L., Taubeneck, W.H., and Hales, P.L., 1977, Rb/Sr and K/Ar geochronometry of Mesozoic granitic rocks and their Sr isotopic composition, Oregon, Washington, and Idaho: Geological Society of America Bulletin, v. 88, p. 397–411.

Arth, J.G., Zen, E-an, Sellers, G., and Hammarstrom, J.M., 1986, High initial Sr isotopic ratios and evidence for magma mixing in the Pioneer batholith of southwest Montana: Journal of Geology, v. 94, p. 419–430.

Bailey, R.G., 1995, Descriptions of the ecoregions of the United States: U.S. Department of Agriculture Forest Service Miscellaneous Publication 1391, 108 p.

Bankey, Viki, and Kleinkopf, M.D., 1988, Bouguer gravity anomaly map and four derivative maps of Idaho: U.S. Geological Survey Geophysical Investigations Map GP–978, scale 1:1,000,000.

Becraft, G.E., Pinckney, D.M., and Rosenblum, Sam, 1963, Geology and mineral resources of the Jefferson City quadrangle, Jefferson and Lewis and Clark Counties, Montana: U.S. Geological Survey Professional Paper 428, 101 p.

Bennett, E.H., 1977, Reconnaissance geology and geochemistry of the Blackbird Mountain–Panther Creek region, Lemhi County, Idaho: Idaho Bureau of Mines and Geology Pamphlet 167, 108 p.

Berg, R.B., and Lonn, J.D., 1996, Preliminary geologic map of the Nez Perce Pass 30- by 60-minute quadrangle, Montana: Montana Bureau of Mines and Geology Open-File Report MBMG 339, 7 p., 1 plate, scale 1:100,000.

Berg, R.B., Lonn, J.D., and Locke, W.W., 1999, Geologic map of the Gardiner 30′×60′ quadrangle, south-central Montana: Montana Bureau of Mines and Geology Open-File Report MBMG 387, 2 plates, scale 1:100,000.

Berg, R.B., Lopez, D.A., and Lonn, J.D., 2000, Geologic map of the Livingston 30′×60′ quadrangle, south-central Montana: Montana Bureau of Mines and Geology Open-File Report MBMG 406, scale 1:100,000.

Bond, G.C., and Kominz, M.A., 1984, Construction of tectonic subsidence curves for the early Paleozoic miogeocline, southern Canadian Rocky Mountains—Implications for subsidence mechanisms, age of break up and crustal thinning: Geological Society of America Bulletin, v. 95, p. 155–173.

Brady, J.B., Burger, H.R., Cheney, J.T., and Harms, T.A., eds., 2004, Precambrian geology of the Tobacco Root Mountains, Montana: Geological Society of America Special Paper 377, 256 p.

Briggs, P.H., 1990, Elemental analysis of geologic materials by inductively coupled plasma–atomic emission spectrometry, *in* Arbogast, B.F., Quality assurance manual for the Branch of Geochemistry: U.S. Geological Survey Open-File Report 90-668, p. 83–91.

Brimhall, G.H., Jr., 1973, Mineralogy, texture, and chemistry of early wall rock alteration in the deep underground mines and Continental area, Butte district, Montana, *in* Miller, R.N., ed., Guidebook for the Butte field meeting of Society of Economic Geologists, 1973: Butte, Mont., Society of Economic Geologists, p. H1–H5.

Brimhall, G.H., Jr., Cunningham, A.B., and Stoffregen, R., 1984, Zoning in precious metal distribution within base metal sulfides—A new lithologic approach using generalized inverse methods: Economic Geology, v. 79, p. 209–226.

Cater, F.W., Pinckney, D.M., Hamilton, W.B., Parker, R.L., Weldin, R.D., Close, T.J., and Zilka, N.T., 1973, Mineral resources of the Idaho Primitive Area and vicinity, Idaho, *with a section on* The Thunder Mountain district, by B.F. Leonard, *and a section on* Aeromagnetic interpretation, by W.E. Davis: U.S. Geological Survey Bulletin 1304, 431 p., plates in pocket.

Cater, F.W., Pinckney, D.M., and Stotelmeyer, R.B., 1975, Mineral resources of the Clear Creek–Upper Big Deer Creek Study Area, contiguous to the Idaho Primitive Area, Lemhi County, Idaho: U.S. Geological Survey Bulletin 1391–C, 41 p.

Christie-Blick, N., and Levy, M., 1989, Concepts of sequence stratigraphy, with examples from strata of Late Proterozoic and Cambrian age in the western United States, *in* Christie-Blick, N., and Levy, M., eds., Late Proterozoic and Cambrian tectonics, sedimentation, and record of metazoan radiation in the Western United States: Washington, D.C., American Geophysical Union, 28th International Geological Congress, Field Trip Guidebook T331, p. 23–38.

Colpron, M., Logan, J.M., and Mortensen, J.K., 2002, U-Pb zircon age constraint for late Neoproterozoic rifting and initiation of the lower Paleozoic passive margin of western Laurentia: Canadian Journal of Earth Sciences, v. 39, p. 133–143.

Connor, J.J., 1990, Geochemical stratigraphy of the Yellowjacket Formation (Middle Proterozoic) in the area of the Idaho cobalt belt, Lemhi County, Idaho, Part A, Discussion; Part B, Geochemical data: U.S. Geological Survey Open-File Report 90-0234, 30 p.

Connor, J.J., and Evans, K.V., 1986, Geologic map of the Leesburg quadrangle, Idaho: U.S. Geological Survey Miscellaneous Field Studies Map MF–1880, scale 1:62,500.

Cook, F.A., 1995, Lithospheric processes and products in the southern Canadian Cordillera, a Lithoprobe perspective: Canadian Journal of Earth Sciences, v. 32, p. 1803–1824.

Cox, D.P., 1992, Descriptive model of distal disseminated Ag-Au, *in* Bliss, J.D., Developments in mineral deposit modeling: U.S. Geological Survey Bulletin 2004, p. 19–20.

Crittenden, M.D., Jr., Stewart, J.H., and Wallace, C.A., 1972, Regional correlation of Upper Precambrian strata in western North America: 24th International Geological Congress, 1972, Section 1, p. 334–341.

Crittenden, M.D., Jr., and Wallace, C.A., 1973, Possible equivalent of the Belt Supergroup in Utah, *in* Belt Symposium 1973, Volume 1: Moscow, Idaho, Idaho Bureau of Mines and Geology, p. 116–138.

Crock, J.G., Lichte, F.E., and Briggs, P.H., 1983, Determination of elements in National Bureau of Standards' geological reference materials SRM 278 obsidian and SRM 688 basalt by inductively coupled argon plasma–atomic emission spectrometry: Geostandards Newsletter, v. 7, no. 2, p. 335–340.

Dehler, C.M., Elrick, M., Karlstrom, K.E., Smith, G.A., Crossey, L.J., and Timmons, J.M., 2001, Neoproterozoic Chuar Group (≈800–742 Ma), Grand Canyon—A record of cyclic marine deposition during global cooling and supercontinent rifting: Sedimentary Geology, v. 141–142, p. 465–499.

Del Rio, S.M., 1960, Mineral resources of Colorado First Sequel: Denver, Colo., State of Colorado Mineral Resources Board, 764 p.

Derkey, P.D., Johnson, B.R., Lackaff, B.B., and Derkey, R.E., 1998, Digital geologic map of the Rosalia 1:100,000 quadrangle, Washington and Idaho; a digital database for the 1990 S.Z. Waggoner map: U.S. Geological Survey Open-File Report 98-357, 27 p., scale 1:100,000.

Doughty, P.T., and Chamberlain, K.R., 1996, Salmon River Arch revisited—New evidence for 1370 Ma rifting near the end of deposition in the Middle Proterozoic Belt basin: Canadian Journal of Earth Science, v. 33, p. 1037–1052.

Doughty, P.T., Price, R.A., and Parrish, R.R., 1998, Geology and U-Pb geochronology of Archean basement and Proterozoic cover in the Priest River complex, northwestern United States, and their implications for Cordilleran structure and Precambrian continent constructions: Canadian Journal of Earth Sciences, v. 33, p. 1037–1052.

du Bray, E.A., 1995, Geologic map showing distribution of Cretaceous intrusive rocks in the central Big Belt Mountains, Broadwater and Meagher Counties, Montana: U.S. Geological Survey Miscellaneous Field Studies Map MF–2291, scale 1:50,000.

Earhart, R.L., 1986, Descriptive model of Blackbird Co-Cu, *in* Cox, D.P., and Singer, D.A., Mineral deposit models: U.S. Geological Survey Bulletin 1693, p. 142.

Ekren, E.B., 1988, Stratigraphic and structural relations of the Hoodoo Quartzite and Yellowjacket Formation of Middle Proterozoic age from Hoodoo Creek eastward to Mount Taylor, central Idaho: U.S. Geological Survey Bulletin 1570, 17 p.

Eppinger, R.G., 2002, Pre-fire baseline stream-sediment and stream-water geochemical data from a recently burned area in central Idaho, and suggestions for application of geochemical data to wildfire science [abs], *in* Coffelt, L.L., and Livingston, R.K., Second U.S. Geological Survey wildland fire science workshop, Los Alamos, New Mexico, Oct. 31–Nov. 3, 2000: U.S. Geological Survey Open-File Report 02-11, p. 51. Accessed 1/24/2007 at URL http://pubs.er.usgs.gov/usgspubs/ofr/ofr0211/.

Eppinger, R.G., 2003, Geochemical comparison of pre- and post-wildfire stream sediment and water samples from drainages impacted by large wildfires of 2000, central Idaho, U.S.A. [abs.]: Geological Society of America special meeting, Wildland fire impacts on watersheds; understanding, planning, and response, October 21–23, 2003, Denver, Colo., Program and Proceedings, Poster Abstracts section, p. 3.

Eppinger, R.G., Briggs, P.H., Brown, Zoe Ann, Crock, J.G., Meier, Allen, Theodorakos, P.M., and Wilson, S.A., 2001, Baseline geochemical data for stream sediment and surface water samples from Panther Creek, the Middle Fork of the Salmon River, and the Salmon River from North Fork to Corn Creek, collected prior to the severe wildfires of 2000 in central Idaho: U.S. Geological Survey Open-File Report 01-0161. Accessed 1/24/2007 at URL http://pubs.usgs.gov/of/2001/ofr-01-0161/.

Eppinger, R.G., Briggs, P.H., Rieffenberger, Betsy, and Van Dorn, Carol, 2004, Comparing pre- and post-wildfire stream sediment and water geochemistry from drainages impacted by the Clear Creek and Wilderness Complex wildfires of 2000, central Idaho [abs], *in* Livingston, R.K., Third U.S. Geological Survey wildland fire-science workshop, Denver, Colorado, Nov. 12–15, 2002: U.S. Geological Survey Scientific Investigations Report 2004-5005, p. 23, CD-ROM. Accessed 1/24/2007 at URL http://pubs.er.usgs.gov/usgspubs/sir/sir20045005/.

Eppinger, R.G., Briggs, P.H., Rieffenberger, Betsy, and Van Dorn, Carol, 2003, Comparing pre- and post-wildfire stream sediment and water geochemistry from drainages impacted by large wildfires of 2000, Central Idaho, U.S.A.: Sixth International Symposium on Environmental Geochemistry, Sept. 7–11, 2003, final programme and book of abstracts, University of Edinburgh, p. 201.

Eppinger, R.G., Briggs, P.H., Rieffenberger, Betsy, Van Dorn, Carol, Brown, Zoe Ann, Crock, J.G., Hageman, P.L., Meier, Allen, Sutley, S.J., Theodorakos, P.M., and Wilson, S.A., 2003, Geochemical data for stream sediment and surface water samples from Panther Creek, the Middle Fork of the Salmon River, and the Salmon River, collected before and after the Clear Creek, Little Pistol, and Shellrock wildfires of 2000 in central Idaho: U.S. Geological Survey Open-File Report 03-152. Available on CD-ROM; accessed 2/13/2006 at URL http://pubs.usgs.gov/of/2003/152/.

Evans, K.V., 1998, The Yellowjacket Formation of east-central Idaho, *in* Berg, R.B., ed., Belt Symposium III: Montana Bureau of Mines and Geology Special Publication 112, p. 17–30.

Evans, K.V., Aleinikoff, J.N., Obradovich, J.D., and Fanning, C.M., 2000, SHRIMP U-Pb geochronology of volcanic rocks, Belt Supergroup, western Montana—Evidence for rapid deposition of sedimentary strata: Canadian Journal of Earth Sciences, v. 37, p. 1287–1300.

Evans, K.V., and Connor, J.J., 1993, Geologic map of the Blackbird Mountain 15-minute quadrangle, Lemhi County, Idaho: U.S. Geological Survey Miscellaneous Field Studies Map MF–2234, scale 1:62,500.

Evans, K.V., and Green, G.N., compilers, 2003, Geologic map of Salmon National Forest and vicinity, east-central Idaho: U.S. Geological Survey Geologic Investigations Series Map I–2765, scale 1:100,000. Accessed 5/18/2004 at URL http://pubs.usgs.gov/imap/i-2765/.

Evans, K.V., and Zartman, R.E., 1990, U-Th-Pb and Rb-Sr geochronology of middle Proterozoic granite and augen gneiss, Salmon River Mountains, east-central Idaho: Geological Society of America Bulletin, v. 102, p. 63–73.

Faure, G., 1986, Principles of isotope geology: New York, John Wiley, 589 p.

Ferri, R., Rees, C., Nelson, J., and Legun, A., 1999, Geology and mineral deposits of the northern Kechika Trough between Gataga River and the 60th parallel: British Columbia Ministry of Energy and Mines Bulletin 107, 122 p.

Ficklin, W.H., and Mosier, E.L., 1999, Field methods for sampling and analysis of environmental samples for unstable and selected stable constituents, Chapter 12 *in* Plumlee, G.S., and Logsdon, M.J., eds., The environmental geochemistry of mineral deposits—Part A, Processes, techniques, and health issues: Society of Economic Geologists, Inc., Reviews in Economic Geology, v. 6A, p. 249–264.

Fisher, F.S., and Johnson, K.M., eds., 1995, Geology and mineral resource assessment of the Challis 1°×2° quadrangle, Idaho: U.S. Geological Survey Professional Paper 1525, 204 p. plus appendixes, 23 plates.

Fisher, F.S., McIntyre, D.H., and Johnson, K.M., 1992, Geologic map of the Challis 1°×2° quadrangle, Idaho: U.S. Geological Survey Miscellaneous Investigations Series Map I–1819, scale 1:250,000, 39 p. pamphlet. Accessed 5/18/2004 at URL http://pubs.usgs.gov/imap/i-1819/.

Fortescue, J.A.C., 1992, Landscape geochemistry; retrospect and prospect—1990: Applied Geochemistry, v. 7, p. 1–54.

Gabrielse, H., 1972, Younger Precambrian of the Canadian Cordillera: American Journal of Science, v. 272, p. 521–536.

Gorman, A.R., and 12 others, 2002, Deep Probe—Imaging the roots of western North America: Canadian Journal of Earth Sciences, v. 39, p. 375–398.

Goyer, R.A., and Clarkson, T.W., 2001, Toxic effects of metals, Chapter 23 *in* Klaassen, C.D., ed., Casarett and Doull's toxicology—The basic science of poisons: New York, McGraw-Hill, p. 811–867.

Green, G.N., and Tysdal, R.G., 1996, Digital maps and figures on CD-ROM for mineral and energy resource assessment of the Helena National Forest, west-central Montana: U.S. Geological Survey Open-File Report 96-683-B, CD-ROM, scale 1:126,720.

Gunn, S.H., 1991, Isotopic constraints on the crustal evolution of southwest Montana: Santa Cruz, Calif., University of California at Santa Cruz Ph. D. dissertation, 190 p.

Hageman, P.L., 2000, A simple field leach test for rapid screening and qualitative characterization of mine waste dump material on abandoned mine lands: U.S. Geological Survey Open-File Report 00-015, 13 p.

Hageman, P.L., and Briggs, P.H., 2000, A simple field leach test for rapid screening and qualitative characterization of mine waste dump material on abandoned mine lands, *in* ICARD 2000, Proceedings of the Fifth International Conference on Acid Rock Drainage, Volume 2: Society for Mining, Metallurgy, and Exploration, Inc., p. 1463–1475.

Hahn, G.A., and Hughes, G.J., Jr., 1984, Sedimentation, tectonism, and associated magmatism of the Yellowjacket Formation in the Idaho Cobalt Belt, Lemhi County, Idaho, *in* Hobbs, S.W., ed., The Belt: Montana Bureau of Mines and Geology Special Publication 90, p. 65–67.

Hambrey, M.J., and Harland, W.B., 1985, The Late Proterozoic glacial era: Palaeogeography, Palaeoclimatology, Palaeoecology, v. 51, p. 255–272.

Hammarstrom, J.M., Eppinger, R.G., Van Gosen, B.S., Briggs, P.H., and Meier, A.L., 2002, Case study of the environmental signature of a recently abandoned, carbonate-hosted replacement deposit—The Clayton mine, Idaho: U.S. Geological Survey Open-File Report 02-10, 44 p. Available at URL http://pubs.usgs.gov/of/of02-010/.

Hammarstrom, J.M., Tomascak, P., and Krogstad, E.J., 1993, Old crustal Nd signature for the Pioneer Batholith: American Geophysical Union 1993 Spring Meeting abstracts, Eos Supplement, April 20, 1993, p. 335.

Harrison, J.E., Cressman, E.R., and Whipple, J.W., 1992, Geologic and structure maps of the Kalispell 1°×2° quadrangle, Montana, and Alberta and British Columbia: U.S. Geological Survey Miscellaneous Investigations Map I–2267, scale 1:250,000.

Harrison, J.E., Griggs, A.B., Wells, J.D., Kelley, W.N., Derkey, P.D., and EROS Data Center, 2000, Geologic and structure maps of the Wallace 1°×2° quadrangle, Montana and Idaho—A digital database: U.S. Geological Survey Miscellaneous Investigations Series Map I–1509–A, version 1.0, 21 p., scale 1:250,000.

Harrison, J.E., Whipple, J.W., and Lidke, D.J., 1998, Geologic map of the western part of the Cut Bank 1°×2° quadrangle, Montana: U.S. Geological Survey Geologic Investigations Series Map I–2593, 1 sheet, scale 1:250,000.

Helsel, D.R., and Hirsch, R.M., 2002, Statistical methods in water resources: U.S. Geological Survey Techniques of Water Resources Investigations, Book 4, Chapter A3, 510 p. Only available online at URL http://water.usgs.gov/pubs/twri/twri/twri4a3/.

Hobbs, S.W., 1985, Structural and stratigraphic controls of ore deposits in the Bayhorse area, Idaho, Chapter K *in* McIntyre, D.H., ed., Symposium on the geology and mineral deposits of the Challis 1°×2° quadrangle, Idaho: U.S. Geological Survey Bulletin 1658–A–S, p. 133–140.

Hobbs, S.W., Hays, W.H., and McIntyre, D.H., 1991, Geologic map of the Bayhorse area, central Custer County, Idaho: U.S. Geological Survey Miscellaneous Investigations Series Map I–1882, scale 1:62,500, 14 p. pamphlet.

Hoffman, P.F., 1999, The break-up of Rodinia, birth of Gondwana, true polar wander and the snowball Earth: Journal of African Earth Sciences, v. 28, p. 17–33.

Hoffman, P.F., Kaufman, A.J., Halverson, G.P., and Schrag, D.P., 1998, A Neoproterozoic snowball earth: Science, v. 281, p. 1342–1346.

Hughes, G.J., Jr., 1983, Basinal setting of the Idaho Cobalt Belt, Blackbird mining district, Lemhi County, Idaho, *in* The genesis of Rocky Mountain ore deposits—Changes with time and tectonics: Denver Region Exploration Geologists Society, p. 21–27.

Idaho Geological Survey, 1996a, Digital geology of the Riggins 1:100,000-scale quadrangle, Idaho, *in* Digital geologic map compilation for the Nez Perce and Clearwater National Forests: Idaho Geological Survey CD-ROM, produced under contract to USDA Forest Service [unpublished], scale 1:100,000.

Idaho Geological Survey, 1996b, Digital geology of the Grangeville 1:100,000-scale quadrangle, Idaho, *in* Digital geologic map compilation for the Nez Perce and Clearwater National Forests: Idaho Geological Survey CD-ROM, produced under contract to USDA Forest Service [unpublished], scale 1:100,000.

Idaho Geological Survey, 1996c, Digital geology of the Headquarters 1:100,000-scale quadrangle, Idaho, *in* Digital geologic map compilation for the Nez Perce and Clearwater National Forests: Idaho Geological Survey CD-ROM, produced under contract to USDA Forest Service [unpublished], scale 1:100,000.

Janecke, S.U., Vandenburg, C.J., and Blankenau, J.J., 1998, Geometry, mechanisms and significance of extensional folds from examples in the Rocky Mountain Basin and Range province, U.S.A.: Journal of Structural Geology, v. 20, p. 841–856.

Jefferson, C.W., and Parrish, R.R., 1989, Late Proterozoic stratigraphy, U-Pb zircon ages, and rift tectonics, Mackenzie Mountains, northwestern Canada: Canadian Journal of Earth Sciences, v. 26, p. 1784–1801.

Johnson, B.R., and Derkey, P.D., 1998, Digital geologic map of the Spokane 1:100,000 quadrangle, Washington and Idaho; a digital database for the 1990 N.L. Joseph map: U.S. Geological Survey Open-File Report 98-115, 13 p. and 1 digital plate, scale 1:100,000.

Kalakey, T.J., John, B.E., and Lageson, D.R., 2001, Fault-controlled emplacement in the Sevier fold-and-thrust belt of southwest Montana, U.S.A.: Journal of Structural Geology, v. 23, p. 1151–1165.

Karlstrom, K.E., Bowring, S.A., Dehler, C.M., Knoll, A.H., Porter, S.M., Des Marais, D.J., Weil, A.B., Sharp, Z.D., Geissman, J.W., Elrick, M.B., Timmons, J.M., Crossey, L.J., and Davidek, K.L., 2000, Chuar Group of the Grand Canyon—Record of breakup of Rodinia, associated change in the global carbon cycle, and ecosystem expansion by 740 Ma: Geology, v. 28, p. 619–622.

Kayser, H.Z., 2001, Digital geologic map of the east half of the Pullman 1°×2° quadrangle, Idaho; a digital database for the 1979 Rember and Bennett map: U.S. Geological Survey Open-File Report 01-262, 29 p., 1 sheet, scale 1:250,000.

Kellogg, K.S., and Williams, V.S., 2000, Geologic map of the Ennis 30′×60′ quadrangle, Madison and Gallatin Counties, Montana, and Park County, Wyoming: U.S. Geological Survey Geologic Investigations Series I–2690, scale 1:100,000.

Kelly, M.G., 1999, Effects of heavy metals on the aquatic biota, Chapter 18 *in* Plumlee, G.S., and Logsdon, M.J., eds., The environmental geochemistry of mineral deposits—Part A, Processes, techniques, and health issues: Society of Economic Geologists, Inc., Reviews in Economic Geology, v. 6A, p. 363–371.

Kesler, S.E., 1994, Mineral resources, economics and the environment: New York, Macmillan College Publishing Company, Inc., 391 p.

Kiilsgaard, T.H., and Bennett, E.H., 1995, Eocene plutonic terrane, *in* Fisher, F.S., and Johnson, K.M., Geology and mineral resource assessment of the Challis 1°×2° quadrangle, Idaho: U.S. Geological Survey Professional Paper 1525, p. 44–47.

Kiilsgaard, T.H., and Hall, W.E., 1995, Radioactive black-sand placer deposits, *in* Fisher, F.S., and Johnson, K.M., Geology and mineral resource assessment of the Challis 1°×2° quadrangle, Idaho: U.S. Geological Survey Professional Paper 1525, p. 183–189.

Kiilsgaard, T.H., Stanford, L.R., and Lewis, R.S., 2001, Geologic map of the Idaho City 30×60 minute quadrangle, Idaho: Idaho Geological Survey Geologic Map Series 29, scale 1:100,000.

Klein, T.L., 2004, Mineral deposit data for epigenetic base- and precious-metal and uranium-thorium deposits in south-central and southwestern Montana and southern and central Idaho: U.S. Geological Survey Open-File Report 2004-1005, 16 p. Accessed 5/18/2004 at URL http://pubs.usgs.gov/of/2004/1005/.

Krieger, G.R., Hattemer-Frey, H.A., and Kester, J.E., 1999, Bioavailability of metals in the environment—Implications for health risk assessment, Chapter 17 *in* Plumlee, G.S., and Logsdon, M.J., eds., The environmental geochemistry of mineral deposits—Part A, Processes, techniques, and health issues: Society of Economic Geologists, Inc., Reviews in Economic Geology, v. 6A, p. 357–361.

Lang, J.R., Baker, T., Hart, C.J.R., and Mortensen, J.K., 2000, An exploration model for intrusion-related gold systems: Society of Economic Geologists Newsletter 40, p. 1–15.

Larsen, E.S., Jr., 1940, Petrographic province of central Montana: Geological Society of America Bulletin, v. 51, p. 887–948.

Levinson, A.A., 1980, Introduction to exploration geochemistry, Second Edition: Wilmette, Ill., Applied Publishing, 924 p.

Lewis, R.S., 1998a, Geologic map of the Butte 1°×2° quadrangle, Montana: Montana Bureau of Mines and Geology Open-File Report MBMG 363, 16 p., 1 plate, scale 1:250,000.

Lewis, R.S., 1998b, Geologic map of the Montana part of the Missoula West 30- by 60-minute quadrangle: Montana Bureau of Mines and Geology Open-File Report MBMG 373, 20 p., 2 plates, scale 1:100,000.

Lewis, R.S., Burmester, R.F., Kauffman, J.D., and Frost, T.P., 2000, Geologic map of the St. Maries 30×60 minute quadrangle, Idaho: Idaho Geological Survey Digital Geologic Map DGM–1, scale 1:100,000.

Lewis, R.S., Burmester, R.F., McFadden, M.D., Derkey, P.D., and Oblad, J.R., 1999, Digital geologic map of the Wallace quadrangle, Idaho: U.S. Geological Survey Open-File Report 99-390, 46 p., scale 1:100,000.

Lewis, R.S., and Derkey, P.D., 1999, Digital geologic map of part of the Thompson Falls 1:100,000 quadrangle, Idaho: U.S. Geological Survey Open-File Report 99-438, 32 p., 1 digital plate.

Lewis, R.S., and Stanford, L.R., 2002a, Digital geologic map of the Elk City 30×60 minute quadrangle, Idaho: Idaho Geological Survey Digital Geologic Map Series DGM–05, 1 CD-ROM, scale 1:100,000.

Lewis, R.S., and Stanford, L.R., 2002b, Digital geologic map of the Kooskia 30×60 minute quadrangle, Idaho: Idaho Geological Survey Digital Geologic Map Series DGM–06, 1 CD-ROM, scale 1:100,000.

Lewis, R.S., and Stanford, L.R., 2002c, Digital geologic map of the Hamilton 30×60 minute quadrangle, Idaho: Idaho Geological Survey Digital Geologic Map Series DGM–03, 1 CD-ROM, scale 1:100,000.

Lewis, R.S., and Stanford, L.R., 2002d, Digital geologic map of the Missoula West 30×60 minute quadrangle, Idaho: Idaho Geological Survey Digital Geologic Map Series DGM–02, 1 CD-ROM, scale 1:100,000.

Lewis, R.S., and Stanford, L.R., 2002e, Digital geologic map of the Nez Perce Pass 30×60 minute quadrangle, Idaho: Idaho Geological Survey Digital Geologic Map Series DGM–04, 1 CD-ROM, scale 1:100,000.

Lindgren, Waldemar, 1904, A geological reconnaissance across the Bitterroot Range and Clearwater Mountains in Montana and Idaho: U.S. Geological Survey Professional Paper 27, 123 p.

Link, P.K., Christie-Blick, N., Devlin, W.J., Elston, D.P., Horodyski, R.J., Levy, M., Miller, J.M.G., Pearson, R.C., Prave, A., Stewart, J.H., Winston, D., Wright, L.A., and Wrucke, C.T., 1993, Middle and Late Proterozoic stratified rocks of the western U.S. Cordillera, Colorado Plateau, and Basin and Range province, *in* Reed, J.C., Jr., Bickford, M.E., Houston, R.S., Link, P.K., Rankin, D.W., Sims, P.K., and Van Schmus, W.R., eds., Decade of North American Geology, Precambrian—Conterminous U.S.: Geological Society of America, The Geology of North America, v. C–2, p. 463–595.

Link, P.K., Mahoney, J.B., Bruner, D.J., Batatian, L.D., Wilson, Eric, and Williams, F.J.C., 1995, Geologic map of outcrop areas of sedimentary units in the eastern part of the Hailey 1°×2° quadrangle and the southern part of the Challis 1°×2° quadrangle, south-central Idaho: U.S. Geological Survey Bulletin 2064–C, plate 1, scale 1:100,000.

Link, P.K., Winston, D., and Boyack, D., 2003, Stratigraphy of the Mesoproterozoic Belt Supergroup, Salmon River Mountains, Lemhi County, Idaho: Northwest Geology, v. 32, p. 107–123.

Long, K.R., DeYoung, J.H., and Ludington, S.D., 1998, Database of significant deposits of gold, silver, copper, lead, and zinc in the United States—Part B, Digital data: U.S. Geological Survey Open-File Report 98-206–B.

Lonn, J.D., and Berg, R.B., 1996, Preliminary geologic map of the Hamilton 30- by 60-minute quadrangle, Montana: Montana Bureau of Mines and Geology Open-File Report MBMG 340, 9 p., 1 plate, scale 1:100,000.

Lonn, J.D., and McFaddan, M.D., 1999, Geologic map of the Montana part of the Wallace 30- by 60-minute quadrangle: Montana Bureau of Mines and Geology Open-File Report MBMG 388, 15 p., 2 plates, scale 1:100,000.

Lonn, J.D., Skipp, Betty, Ruppel, E.T., Janecke, S.U., Perry, W.J., Jr., Sears, J.W., Bartholomew, M.J., Stickney, M.C., Fritz, W.J., Hurlow, H.A., and Thomas, R.C., 2000, Geologic map of the Lima quadrangle, southwest Montana: Montana Bureau of Mines and Geology Open-File Report MBMG 408, 3 sheets, parts A, B, and C, scale 1:100,000.

Lopez, D.A., 1981, Stratigraphy of the Yellowjacket Formation of east-central Idaho: U.S. Geological Survey Open-File Report 81-1088, 218 p.

Lopez, D.A., 2000, Geologic map of the Big Timber 30′×60′ quadrangle, south-central Montana: Montana Bureau of Mines and Geology Open-File Report MBMG 405, scale 1:100,000.

Lopez, D.A., 2001, Preliminary geologic map of the Red Lodge 30′×60′ quadrangle, south-central Montana: Montana Bureau of Mines and Geology Open-File Report MBMG 423, 1 plate, scale 1:100,000.

Lund, Karen, 2004, Geology of the Payette National Forest, Valley, Idaho, Washington, and Adams Counties, west-central Idaho: U.S. Geological Survey Professional Paper 1666, 86 p., 2 plates.

Lund, Karen, Aleinikoff, J.N., Evans, K.V., and Fanning, C.M., 2003, SHRIMP U-Pb geochronology of Neoproterozoic Windermere Supergroup, central Idaho—Implications for rifting of western Laurentia and synchroneity of Sturtian glacial deposits: Geological Society of America Bulletin, v. 115, p. 349–372.

Lund, Karen, Aleinikoff, J.N., Kunk, M.J., Unruh, D.M., Zeihen, G.D., Hodges, W.C., du Bray, E.A., and O'Neill, J.M., 2002, SHRIMP U-Pb and $^{40}Ar/^{39}Ar$ age constraints for relating plutonism and mineralization in the Boulder batholith region, Montana: Economic Geology, v. 97, p. 241–267.

Lund, Karen, Derkey, P.D., Brandt, T.R., and Oblad, Jon, 1999, Digital geologic map database of the Payette National Forest and vicinity, Idaho: U.S. Geological Survey Open-File Report 98-219–B, 45 p., scale 1:100,000.

Lund, Karen, Evans, K.V., and Esparza, L.E., 1983, Mineral resource potential map of the Special Mining Management Zone—Clear Creek, Idaho: U.S. Geological Survey Miscellaneous Field Studies MF–1576–A.

Lund, Karen, Tysdal, R.G., Evans, K.V., and Winkler, G.R., 2003, Geologic map of the west half of the Salmon National Forest, *in* Evans, K.V., and Green, G.N., compilers, Geologic map of the Salmon National Forest and vicinity, east-central Idaho: U.S. Geological Survey Miscellaneous Investigations Map I–2765.

Lund, K.I., and Tysdal, R.G., 2007, Stratigraphic and structural setting of the sediment-hosted Blackbird cobalt-copper deposits, east-central Idaho, U.S.A., *in* Link, P.K., and Lewis, R.S. eds., Proterozoic geology of western North America and Siberia: Society for Sedimentary Geology Special Publication 86, p. 129–147.

MacDonald, D.D., Ingersoll, C.G., and Berger, T.A., 2000, Development and evaluation of consensus-based sediment quality guidelines for freshwater ecosystems: Archives of Environmental Contamination and Toxicology, v. 39, p. 20–31.

Martin, M.W., Dilles, J.H., and Proffett, J.M., 1999, U-Pb geochronologic constraints for the Butte porphyry system: Geological Society of America Abstracts with Programs, v. 31, p. 380.

McCafferty, A.E., Bankey, Viki, and Brenner, K.C., 1998, Montana aeromagnetic and gravity maps and data: U.S. Geological Survey Open-File Report 98-333.

McFaul, E.J., Mason, G.T., Ferguson, W.B., and Lipin, B.R., 2000, U.S. Geological Survey Mineral Databases—MRDS and MAS/MILS: U.S. Geological Survey Digital Data Series DDS-52, CD-ROM.

Meyer, C., Shea, E.P., Goddard, C.C., Jr., Zeihen, L.G., Guilbert, J.M., Miller, R.N., McAleer, J.F., Brox, G.B., Ingersoll, R.G., Jr., Burns, G.J., and Wigal, T., 1968, Ore deposits at Butte, Montana, *in* Ridge, J.D., ed., Ore deposits of the United States, 1933–1967, The Graton-Sales Volume II: American Institute of Mining and Metallurgical Engineers, p. 1373–1416.

Miller, F.K., Burmester, R.F., Miller, D.M., Powell, R.E., and Derkey, P.D., 1998, Digital geologic map of the Sandpoint 1°×2° quadrangle, Washington, Idaho, and Montana: U.S. Geological Survey Open-File Report 99-144, 72 p., 1 digital plate, scale 1:250,000.

Miller, F.K., McKee, E.H., and Yates, R.G., 1973, Age and correlation of the Windermere Group in northeastern Washington: Geological Society of America Bulletin, v. 84, p. 3723–3730.

Miller, R.N., 1973, Production history of the Butte district and geological function, past and present, *in* Miller, R.N., ed., Guidebook for the Butte field meeting of Society of Economic Geologists, 1973: Butte, Mont., Society of Economic Geologists, p. F1–F10.

Mitchell, V.E., Strowd, W.B., Hustedde, G.S., and Bennett, E.H., 1986, Mines and prospects of the Challis quadrangle, Idaho, Second Edition: Idaho Geological Survey Mines and Prospects Map Series, 56 p., 1 plate, scale 1:250,000.

Motooka, J.M., 1988, An exploration geochemical technique for the determination of preconcentrated organometallic halides by ICP-AES: Applied Spectroscopy, v. 42, p. 1293–1296.

Moye, F.J., ed., 1990, Geology and ore deposits of the Trans-Challis fault system/Great Falls tectonic zone: Tobacco Root Geological Society, Fifteenth Annual Field Conference Guidebook, 121 p.

Mudge, M.R., Earhart, R.L., Whipple, J.W., and Harrison, J.E., 1982, Geologic and structure map of the Choteau 1°×2° quadrangle, western Montana: U.S. Geological Survey Miscellaneous Investigations Series Map I–1300, 2 sheets, scale 1:250,000.

Mueller, P., Shuster, R., D'Arcy, K., Heatherington, A., Hutman, A., and Williams, I., 1995, Source of the northeastern Idaho batholith—Evidence for a Paleoproterozoic terrane in the northwestern U.S.: Journal of Geology, v. 103, p. 63–72.

Mueller, P.A., Heatherington, A.L., Kelly, D.M., Wooden, J.A., and Mogk, D.W., 2002, Paleoproterozoic crust within the Great Falls tectonic zone—Implications for the assembly of southern Laurentia: Geology, v. 30, p. 127–130.

Munts, S.R., 2000, Digital geologic map of the Coeur d'Alene 1:100,000 quadrangle, Idaho and Montana: U.S. Geological Survey Open-File Report 00-135, version 1.0, 30 p., 1 digital plate, scale 1:100,000.

NAMAG, 2002, Magnetic anomaly map of North America: Compiled by North America Magnetic Anomaly Group (available from U.S. Geological Survey).

Nash, J.T., and Connor, J.J., 1993, Iron and chlorine as guides to stratiform Cu-Co-Au deposits, Idaho cobalt belt, U.S.A.: Mineralium Deposita, v. 28, p. 99–106.

Nash, J.T., and Hahn, G.A., 1986, Volcanogenic character of sediment-hosted Co-Cu deposits in the Blackbird mining district, Lemhi County, Idaho; an interim report: U.S. Geological Survey Open-File Report, 29 p.

Nash, J.T., and Hahn, G.A., 1989, Stratabound Co-Cu deposits and mafic volcaniclastic rocks in the Blackbird mining district, Lemhi County, Idaho, *in* Boyle, R.W., Brown, A.C., Jefferson, C.W., Jowett, E.C., and Kirkham, R.V., eds., Sediment-hosted stratiform copper deposits: Geological Association of Canada Special Paper 36, p. 339–356.

Nold, J.L., 1990, The Idaho cobalt belt, northwestern United States—A metamorphosed Proterozoic exhalative ore district: Mineralium Deposita, v. 25, p. 163–168.

Nordstrom, D.K., and Alpers, C.N., 1999, Geochemistry of acid mine waters, *in* Plumlee, G.S., and Logsdon, M.J., eds., The environmental geochemistry of mineral deposits—Part A, Processes, techniques, and health issues: Society of Economic Geologists, Inc., Reviews in Economic Geology, v. 6A, p. 133–160.

Obradovich, J.D., and Peterman, Z.E., 1968, Geochronology of the Belt Series, Montana: Canadian Journal of Earth Sciences, v. 5, p. 737–747.

O'Leary, R.M., and Meier, A.L., 1986, Analytical methods used in geochemical exploration, 1984: U.S. Geological Survey Circular 948, 48 p.

O'Neill, J.M., 1999, An Early Proterozoic collisional orogen beneath and south of the Belt Basin, *in* Berg, R.B., ed., Belt Symposium III: Montana Bureau of Mines and Geology Special Publication 111, p. 227–234.

O'Neill, J.M., and Christiansen, R.L., 2002, Geologic map of the Hebgen Lake quadrangle, Beaverhead, Madison, and Gallatin Counties, Montana, Park and Teton Counties, Wyoming, and Clark and Fremont Counties, Idaho: Montana Bureau of Mines and Geology Open-File Report MBMG 464, 1 plate, scale 1:100,000.

O'Neill, J.M., and Lopez, D.A., 1985, The Great Falls tectonic zone—Its character and regional significance: American Association of Petroleum Geologists Bulletin, v. 69, p. 437–447.

Piatak, N.M., Seal, R.R., II, Hammarstrom, J.M., Meier, A.L., and Briggs, P.H., 2003, Geochemical characterization of slags, other mine waste, and their leachate from the Elizabeth and Ely mines (Vermont), the Ducktown mining district (Tennessee), and the Clayton smelter site (Idaho): U.S. Geological Survey Open-File Report 03-260, 53 p. Available at URL http://pubs.usgs.gov/of/2003/of03-260/.

Plumlee, G.S., Smith, K.S., Montour, M.R., Ficklin, W.H., and Mosier, E.L., 1999, Geologic controls on the composition of natural waters and mine waters draining diverse mineral-deposit types, Chapter 19 *in* Filipek, L.H., and Plumlee, G.S., eds., The environmental geochemistry of mineral deposits—Part B, Case studies and research topics: Society of Economic Geologists, Inc., Reviews in Economic Geology, v. 6B, p. 373–432.

Prave, A.R., 1999, Two diamictites, two cap carbonates, two D13C excursions, two rifts; The Neoproterozoic Kingston Peak Formation, Death Valley, California: Geology, v. 27, p. 339–342.

Rehn, W.M., 1983, Petrology and geochemistry of the Blue Joint area, southwestern Montana: Golden, Colo., Colorado School of Mines M.S. thesis, 203 p.

Rehn, W.M., and Lund, Karen, 1981, Eocene extensional plutonism in the Idaho batholith region: Geological Society of America Abstracts with Programs, v. 13, no. 7, p. 536.

Rhodes, B.P., and Hyndman, D.W., 1988, Regional metamorphism, structure, and tectonics of northeastern Washington and northern Idaho, *in* Ernst, W.G., ed., Metamorphism and crustal evolution of the western United States (Rubey volume 7): Englewood Cliffs, N.J., Prentice-Hall, p. 272–295.

Roberts, S.A., 1973, Pervasive early alteration in the Butte district, Montana, *in* Miller, R.N., ed., Guidebook for the Butte field meeting of Society of Economic Geologists, 1973: Butte, Mont., Society of Economic Geologists, p. HH1–HH8.

Roots, C.F., and Parrish, R.R., 1988, Age of the Mount Harper volcanic complex, southern Ogilvie Mountains, Yukon, *in* Radiogenic age and isotopic studies, Report 2: Geological Survey of Canada Paper 88-2, p. 29–35.

Rose, A.W., Hawkes, H.E., and Webb, J.S., 1979, Geochemistry in mineral exploration, Second Edition: London, Academic Press, 657 p.

Ross, C.P., 1925, The copper deposits near Salmon, Idaho: U.S. Geological Survey Bulletin 774, 44 p.

Ross, C.P., 1934a, Some lode deposits in the northwestern part of the Boise Basin, Idaho: U.S. Geological Survey Bulletin 846–D, p. 279–285.

Ross, C.P., 1934b, Geology and ore deposits of the Casto quadrangle, Idaho: U.S. Geological Survey Bulletin 854, 135 p.

Ross, C.P., 1947, Geology of the Borah Peak quadrangle, Idaho: Geological Society of America Bulletin, v. 58, p. 1085–1160.

Ross, G.M., McMechan, M.E., and Hein, F.J., 1989, Proterozoic history—The birth of the miogeocline, *in* Ricketts, B.D., ed., Western Canada sedimentary basin; A case history: Calgary, Alta., Canadian Society of Petroleum Geologists, p. 79–104.

Ross, G.M., ed., 2002, The lithoprobe Alberta basement transect: Canadian Journal of Earth Sciences, v. 39, no. 3, 437 p.

Rostad, O.H., 1978, K-Ar dates for mineralization in the White Cloud–Cannivan porphyry molybdenum belt of Idaho and Montana—A discussion: Economic Geology, v. 73, p. 1366–1368.

Rudnick, R.L., and Gao, S., 2004, Composition of the continental crust, *in* Rudnick, R.L., ed., The crust; Holland, H.D., and Turekian, K.K., executive eds., Treatise on geochemistry, Volume 3: Amsterdam, Elsevier, p. 1–64.

Ruppel, E.T., 1963, Geology of the Basin quadrangle, Jefferson, Lewis and Clark, and Powell Counties, Montana: U.S. Geological Survey Bulletin 1151, 121 p.

Ruppel, E.T., 1975, Precambrian Y sedimentary rocks in east-central Idaho: U.S. Geological Survey Professional Paper 889–A, 23 p.

Ruppel, E.T., 1978, Medicine Lodge thrust system, east-central Idaho and southwest Montana: U.S. Geological Survey Professional Paper 1031, 23 p.

Ruppel, E.T., 1998, Geologic map of the eastern part of the Leadore 30′×60′ quadrangle, Montana and Idaho: Montana Bureau of Mines and Geology Open-File Report MBMG 372, scale 1:100,000.

Ruppel, E.T., and Lopez, D.A., 1988, Regional geology and mineral deposits in and near the central part of the Lemhi Range, Lemhi County, Idaho: U.S. Geological Survey Professional Paper 1480, 122 p.

Ruppel, E.T., O'Neill, J.M., and Lopez, D.A., 1993, Geologic map of the Dillon 1°×2° quadrangle, Idaho and Montana: U.S. Geological Survey Miscellaneous Investigations Series Map I–1803–H, scale 1:250,000.

Sales, R.H., and Meyer, C., 1948, Wall-rock alteration, Butte, Montana: Transactions of the American Institute of Mining Engineers, v. 178, p. 9–35.

Sharp, B.J., and Cavender, W.S., 1962, Geology and thorium-bearing deposits of the Lemhi Pass area, Lemhi County, Idaho, and Beaverhead County, Montana: U.S. Geological Survey Bulletin 1126, 76 p.

Sims, P.K., Bankey, Viki, and Finn, C.A., 2001, Preliminary Precambrian basement map of Colorado—A geologic interpretation of an aeromagnetic anomaly map: U.S. Geological Survey Open-File Report 01-0364, scale 1:1,000,000.

Sims, P.K., Finn, C.A., and Rystrom, V.L., 2001, Preliminary Precambrian basement map showing geologic-geophysical domains, Wyoming: U.S. Geological Survey Open-File Report 01-199, scale 1:1,000,000.

Sims, P.K., Lund, Karen, and Anderson, E.M., 2005, Precambrian crystalline basement map of Idaho—An interpretation of aeromagnetic anomalies: U.S. Geological Survey Scientific Investigations Map 2884, scale 1:1,000,000.

Sims, P.K., O'Neill, J.M., Bankey, Viki, and Anderson, E.M., 2004, Precambrian basement geologic map of Montana—An interpretation of aeromagnetic anomalies: U.S. Geological Survey Scientific Investigations Map 2829, scale 1:1,000,000.

Sims, P.K., Stein, H.J., and Finn, C.A., 2002, New Mexico structural zone—An analogue of the Colorado Mineral Belt: Ore Geology Reviews, v. 21, p. 211–225.

Skipp, Betty, 1987, Basement thrust sheets in the Clearwater orogenic zone, central Idaho and western Montana: Geology, v. 15, p. 220–224.

Smedes, H.W., Klepper, M.R., and Tilling, R.I., 1973, The Boulder batholith, Montana (A summary), *in* Miller, R.N., ed., Guidebook for the Butte Field Meeting of the Society of Economic Geologists: Butte, Mont., The Anaconda Company, p. E1–E3.

Sobel, L.S., 1982, Sedimentology of the Blackbird mining district, Lemhi County, Idaho: Cincinnati, Ohio, University of Cincinnati M.S. thesis, 235 p.

Spanski, G.T., 2004, Inventory of significant deposit occurrences in the Headwaters area in western Montana, Idaho, and extreme eastern Oregon and Washington: U.S. Geological Survey Open-File Report 2004-1038.

Stein, H.J., and Cathles, L.M., 1997, The timing and duration of hydrothermal events: Economic Geology, v. 92, p. 763–765.

Stewart, J.H., 1972, Initial deposits in the Cordilleran geosyncline; evidence of a Late Precambrian (<850 m.y.) continental separation: Geological Society of America Bulletin, v. 83, p. 1345–1360.

Stewart, J.H., 1991, Latest Proterozoic and Cambrian rocks of the western United States—An overview, *in* Cooper, J.D., and Stevens, C.H., eds., Paleozoic paleogeography of the Western United States—II: Pacific Section, Society of Economic Paleontologists and Mineralogists, v. 1, p. 13–38.

Sullivan, J.B., Jr., and Krieger, G.R., eds., 2001, Clinical environmental health and toxic exposures, Third Edition: Philadelphia, Pa., Lippincott Williams and Wilkins, 1,323 p.

Taggart, J.E., Jr., ed., 2002, Analytical methods for chemical analysis of geologic and other materials, U.S. Geological Survey: U.S. Geological Survey Open-File Report 02-223. Available at URL http://pubs.usgs.gov/of/ofr-02-0223/.

Taylor, C.D., Winick, J.A., Unruh, D.M., and Kunk, M.J., 2004, Geochronology and geochemistry of the Idaho-Montana porphyry belt: Geological Society of America Abstracts with Programs, v. 36, no. 4, p. 4.

Tietbohl, D.R., 1981, Structure and stratigraphy of the Hayden Creek area, Lemhi Range, east-central Idaho: University Park, Pa., The Pennsylvania State University M.S. thesis, 121 p.

Tietbohl, D.R., 1986, Proterozoic diamictite beds in the Lemhi Range, east-central Idaho, *in* Roberts, S.M., ed., Belt Supergroup: Montana Bureau of Mines and Geology Special Publication 94, p. 197–207.

Tweto, Ogden, and Sims, P.K., 1963, Precambrian ancestry of the Colorado mineral belt: Geological Society of America Bulletin, v. 74, p. 991–1014.

Tysdal, R.G., 1996a, Geologic map of adjacent parts of the Hayden Creek and Mogg Mountain quadrangles, Lemhi County, Idaho: U.S. Geological Survey Miscellaneous Investigations Series Map I–2563, scale 1:24,000.

Tysdal, R.G., 1996b, Geologic map of the Lem Peak quadrangle, Lemhi County, Idaho: U.S. Geological Survey Geologic Quadrangle Map GQ–1777, scale 1:24,000.

Tysdal, R.G., 2000a, Stratigraphy and sedimentology of Middle Proterozoic rocks in northern part of Lemhi Range, Lemhi County, Idaho: U.S. Geological Survey Professional Paper 1600, 40 p.

Tysdal, R.G., 2000b, Revision of Middle Proterozoic Yellowjacket Formation, central Idaho: U.S. Geological Survey Professional Paper 1601–A, 13 p.

Tysdal, R.G., 2002, Structural geology of western part of Lemhi Range, east-central Idaho: U.S. Geological Survey Professional Paper 1659, 33 p.

Tysdal, R.G., and Desborough, G.A., 1997, Scapolitic metaevaporite and carbonate rocks of Proterozoic Yellowjacket Formation, Moyer Creek, Salmon River Mountains, central Idaho: U.S. Geological Survey Open-File Report 97-268, 26 p.

Tysdal, R.G., and Moye, Falma, 1996, Geologic map of the Allison Creek quadrangle, Lemhi County, Idaho: U.S. Geological Survey Geologic Quadrangle Map GQ–1778, scale 1:24,000.

Tysdal, R.G., Lund, Karen, and Evans, K.V., 2003, Geologic map of the west half of the Salmon National Forest, *in* Evans, K.V., and Green, G.N., compilers, Geologic map of the Salmon National Forest and vicinity, east central Idaho: U.S. Geological Survey Miscellaneous Investigations Map I–2765.

Umpleby, J.B., 1913, Geology and ore deposits of Lemhi County, Idaho: U.S. Geological Survey Bulletin 528, 182 p.

U.S. Environmental Protection Agency, 2001, 40 CFR Parts 9, 141 and 142—National primary drinking water regulations; Arsenic and clarifications to compliance and new source contaminants monitoring: Federal Register, v. 66, no. 14 [Monday, January 22, 2001], p. 6976–7066.

U.S. Environmental Protection Agency, 2002, National recommended water quality criteria—2002: U.S. Environmental Protection Agency Report EPA-822-R-02-047, 33 p.

Vanderwilt, J.W., 1947, Mineral resources of Colorado: Mineral Resource Board, Colorado Geological Survey, 547 p.

Van Gosen, B.S., Eppinger, R.G., Hammarstrom, J.M., Briggs, P.H., Crock, J.G., Gent, Carol, Meier, A.L., Sutley, S.J., and Theodorakos, P.M., 2000, Analytical data for reconnaissance geochemical samples from mine dumps, stream sediments, and waters at the Thompson Creek tungsten mine, Custer County, Montana: U.S. Geological Survey Open-File Report 00-0239, 28 p. of text, 5 data files. Available at URL http://pubs.usgs.gov/of/2000/ofr-00-0239/.

Van Gosen, B.S., Wilson, A.B., Hammarstrom, J.M., and Kulik, D.M., 1996, Mineral resource assessment of the Custer National Forest in the Pryor Mountains, Carbon County, south-central Montana: U.S. Geological Survey Open-File Report 96-256, scale 1:126,720.

Vhay, J.S., 1948, Cobalt-copper deposits of the Blackbird district, Lemhi County, Idaho: U.S. Geological Survey Strategic Minerals Investigation Preliminary Report 3-219, 26 p.

Vuke, S.M., Berg, R.B., Lonn, J.D., and Kellogg, K.S., 1995, Geologic map of the Bozeman 30′×60′ quadrangle, Montana: Montana Bureau of Mines and Geology Open-File Report MBMG 334, scale 1:100,000.

Welsch, E.P., Crock, J.G., and Sanzolone, Richard, 1990, Trace-level determination of arsenic and selenium using continuous-flow hydride generation atomic absorption spectrophotometry, *in* Arbogast, B.F., Quality assurance manual for the Branch of Geochemistry: U.S. Geological Survey Open-File Report 90-668, p. 38–45.

Wilson, A.B., and Elliott, J.E., 1997, Geologic maps of western and northern parts of Gallatin National Forest, south-central Montana: U.S. Geological Survey Geologic Investigation Series I–2584, scale 1:126,720.

Wilson, A.B., and Skipp, Betty, 1994, Geologic map of the eastern part of the Challis National Forest and vicinity, Idaho: U.S. Geological Survey Miscellaneous Investigations Series Map I–2395, scale 1:250,000.

Winston, D., and Link, P.K., 1993, Middle Proterozoic rocks of Montana, Idaho, and eastern Washington—The Belt Supergroup, *in* Reed, J.C., Jr., Bickford, M.E., Houston, R.S., Link, P.K., Rankin, D.W., Sims, P.K., and Van Schmus, W.R., eds., Decade of North American geology, Precambrian—Conterminous U.S.: Geological Society of America, The Geology of North America, v. C–2, p. 487–517.

Woakes, M., 1960, Potassium-argon dates on the mineralization at Butte, Montana: Berkeley, Calif., University of California M.S. thesis, 42 p.

Worl, R.G., and Johnson, K.M., 1995, Map showing geologic terranes of the Hailey 1°×2° quadrangle and the western part of the Idaho Falls 1°×2° quadrangle, south-central Idaho: U.S. Geological Survey Bulletin 2064–A, plate 1, scale 1:250,000.

Worl, R.G., Wilson, A.B., Smith, C.L., and Kleinkopf, M.D., 1989, Mineral resource potential and geology of the Challis National Forest, Idaho: U.S. Geological Survey Bulletin 1873, 101 p., 4 plates.

Young, G.M., 1995, Are Neoproterozoic glacial deposits preserved on the margins of Laurentia related to the fragmentation of two supercontinents?: Geology, v. 23, p. 153–156.

Zen, E-an, Marvin, R.F., and Mehnert, H.H., 1975, Preliminary petrographic, chemical, and age data, on some intrusive and associated contact metamorphic rocks, Pioneer Mountains, southwestern Montana: Geological Society of America Bulletin, v. 86, p. 367–370.